Author Manuscript

Author Manuscript

Author Manuscript

Author Manuscript

HHS Public Access

Author manuscript

Chem Soc Rev. Author manuscript; available in PMC 2018 March 29.

Published in final edited form as:

Chem Soc Rev. 2012 April 07; 41(7): 2740–2779. doi:10.1039/c1cs15237h.

The golden age: gold nanoparticles for biomedicine†

Erik C. Dreaden[a], **Alaaldin M. Alkilany**[b], **Xiaohua Huang**[c], **Catherine J. Murphy**[*,d], and **Mostafa A. El-Sayed**[*,a]

[a]Laser Dynamics Laboratory, Department of Chemistry and Biochemistry, Georgia Institute of Technology, Atlanta, GA 30332-0400, USA

[b]Department of Pharmacology and Toxicology, Georgia Health Sciences University, 1459 Laney Walker Blvd., Augusta, GA 30912, USA

[c]Department of Chemistry, University of Memphis, 213 Smith Chemistry Bldg, Memphis, TN 38152-3550, USA

[d]Department of Chemistry, University of Illinois at Urbana-Champaign, 600 South Mathews Avenue, Urbana, IL 61801, USA. E-mail: murphycj@illinois.edu; Fax: +1 217 244 3186; Tel: +1 217 333 7680

Abstract

Gold nanoparticles have been used in biomedical applications since their first colloidal syntheses more than three centuries ago. However, over the past two decades, their beautiful colors and unique electronic properties have also attracted tremendous attention due to their historical applications in art and ancient medicine and current applications in enhanced optoelectronics and photovoltaics. In spite of their modest alchemical beginnings, gold nanoparticles exhibit physical properties that are truly different from both small molecules and bulk materials, as well as from other nanoscale particles. Their unique combination of properties is just beginning to be fully realized in range of medical diagnostic and therapeutic applications. This *critical review* will provide insights into the design, synthesis, functionalization, and applications of these artificial molecules in biomedicine and discuss their tailored interactions with biological systems to achieve improved patient health. Further, we provide a survey of the rapidly expanding body of literature on this topic and argue that gold nanotechnology-enabled biomedicine is not simply an act of ‘gilding the (nanomedicinal) lily’, but that a new ‘Golden Age’ of biomedical nanotechnology is truly upon us. Moving forward, the most challenging nanoscience ahead of us will be to find new chemical and physical methods of functionalizing gold nanoparticles with compounds that can promote efficient binding, clearance, and biocompatibility and to assess their safety to other biological systems and their long-term term effects on human health and reproduction (472 references).

†Part of the nanomedicine themed issue.

* melsayed@gatech.edu; Fax: +1 404 894 4066; Tel: +1 404 894 0292.

Author Manuscript Author Manuscript Author Manuscript Author Manuscript

I. Introduction

Gold is the quintessential noble element. By nature, it is highly unreactive and as such, historical artifacts made of gold are able to retain their brilliant luster for thousands of years without tarnishing (*i.e.* chemical oxidation) or deterioration (Fig. 1). In its bulk form, gold's uses in jewelry, coinage, and electronics are well known. Gold thin films commonly present in office windows (only 20 nm thick) are able to transmit large amounts of visible light while efficiently reflecting infrared light ($\lambda > 800$ nm), keeping heat inside in the winter and warm air outside in the summer months.[1] In its molecular form, gold compounds can serve in diverse roles ranging from catalysts[2–4] to anti-arthritic medications.[5] *Chemical Society Reviews* has even devoted an entire issue to gold (year 2008, volume 37), containing two dozen articles that showcased the state of the art at that time, from fundamental reactivity to applications in many areas.

The word *nano*, derived from the Greek *nanos*, meaning dwarf, is used to describe any material or property which occurs with dimensions on the nanometre scale (1–100 nm). Unlike bulk- or molecular-scale gold, nanoscale gold can exhibit vivid colors (Fig. 2) which have made them hugely popular objects of study for chemists, physicists, and now biomedical practitioners (see Fig. 3 and Table 1). But beyond their beauty, gold nanoparticles exhibit properties which are fundamentally different from all others.[6] Due to their size, these particles preferentially accumulate at sites of tumor growth/inflammation and enter cells by mechanisms very different and much more rapid than those of small molecules. Their intense photophysical properties allow for their use in biodiagnostic assays that are as simple to interpret as a pregnancy test (many of use may have already used one such test marketed under First Response® in the 1990's). Because of their facile surface chemistry, gold nanoparticles can act as artificial antibodies whose binding affinity can be precisely tuned by varying the density of binding ligands on their surfaces. The efficient conversion of light into heat by gold nanoparticles can allow for the highly specific thermal ablation of diseased or infected tissues. Their ability to absorb copious amounts of X-ray radiation can be used to enhance cancer radiation therapy or increase imaging contrast in diagnostic CT scans (computed tomography). Because of their multivalency, gold nanoparticles can shield unstable drugs or poorly soluble imaging contrast agents and facilitate their efficient delivery to otherwise inaccessible regions of the body. Due to their comparable size relative to proteins, gold nanoparticles can selectively perturb and modify cellular processes in ways that small molecules and proteins cannot, allowing them to act as intrinsic drug agents. Most importantly, all of the previously discussed benefits of gold nanotechnology-enabled biomedicine can be combined in a single construct, allowing simultaneous targeting, diagnostic, and therapeutic functionality which can be chemically tailored for a particular patient or disease.[6]

II. Size, shape and surface chemistry of gold nanocrystals

A. Synthesis

While the first syntheses of colloidal gold pre-date much of the peer-reviewed literature, the first scientific report describing the production of colloidal gold nanoparticles came in 1857 when Michael Faraday found that the "fine particles" formed from the aqueous reduction of

Author Manuscript Author Manuscript Author Manuscript Author Manuscript

gold chloride by phosphorus could be stabilized by the addition of carbon disulfide, resulting in a “beautiful ruby fluid”.[9] Today, most colloidal synthetic methods for obtaining gold nanoparticles (Fig. 4a) follow a similar strategy (Table 2), whereby solvated gold salt is reduced in the presence of surface capping ligands which prevent aggregation of the particles by electrostatic and/or physical repulsion. Particle size is adjusted by varying the gold ion : reducing agent or gold ion : stabilizer ratio, with larger (and typically less monodisperse) sizes obtained from larger ratios.

Using theoretical electrodynamics set forth by Maxwell in 1865,[10] Mie showed in 1908 that the intense colors from Faraday’s gold solutions arose from the absorption and scattering of light by spherical gold nanoparticles which they contained.[12] Following the advent of the electron microscope by Knoll and Ruska in 1932,[13] Turkevich *et al.* provided the first structural studies of gold nanoparticles formed under varying synthetic conditions in 1951[14] and in 1973, Frens performed systematic studies of Turkevich’s citrate-mediated growth method, producing monodisperse spherical gold nanoparticles 16–150 nm in diameter.[15] Until recently, the mechanism by which these particles form was presumed to proceed *via* spontaneous nucleation and isotropic growth (*i.e.* LaMer growth);[16] however studies by Pong *et al.* indicate that the small (*ca.* 5 nm diameter) nuclei formed by citrate-mediated thermal reduction of chloroauric acid initially self-assemble into a network of interconnected chains.[17] As these chains grow in diameter with increasing Au deposition, spherical particles break off from these structures, forming the nanosphere product typically observed from this synthesis. This “necklace-breaking” mechanism is fundamentally distinct from other multiparticle mechanisms such as classic Ostwald ripening (in which smaller particles are consumed by larger particles) or oriented attachment (in which small crystalline particles fuse with one another along a crystalline face). Related approaches have been used to obtain monodisperse gold nanospheres as large as 430 nm (Fig. 4b).[18]

In 1981, Schmid *et al.* showed that much smaller (1.4 ± 0.4 nm diameter) phosphine-stabilized gold particles could be produced from the reduction of PPh_3AuCl by diborane in benzene, yielding $Au_{55}(PPh_3)_{12}Cl_6$.[19] This cluster is a true molecule with a well-defined formula weight, unlike the colloidal gold solutions discussed in the previous paragraph. Hutchison later reported that gold clusters 1.4–10 nm in diameter could be obtained *via* ligand exchange and that these particles could be similarly produced under ambient conditions and without the need for diborane gas.[20] In 1994, Brust *et al.* investigated the synthesis of thiol-stabilized gold clusters using a two-phase system in which gold chloride was solvated in toluene by way of a phase-transfer reagent (tetraoctylammonium bromide).[21] Here, dodecanethiol was used as a stabilizer for gold clusters formed in the organic phase as reducing sodium borohydride was added to the aqueous phase. These and similar clusters[22] have attracted much attention due to their molecule-like properties and facile conjugation, however due to their reported toxicity,[23,24] biomedical applications are somewhat limited, including uses in immunolabeling,[25,26] and as contrast agents for X-ray imaging[27] and radiation therapy.[28]

Interest in the shape-controlled synthesis of gold nanostructures began to take hold in the early 1990’s, when Masuda *et al.*[29] and Martin[30] developed techniques to prepare gold nanorods by electrochemical reduction into nanoporous aluminium oxide membranes. These

Author Manuscript Author Manuscript Author Manuscript Author Manuscript

methods produced relatively monodisperse structures, but due to the low yield and somewhat large diameter (>100 nm), the optical response from these nanorods was, at the time, difficult to discern and largely dominated by multipolar plasmon resonance modes due to phase retardation of the incident field, resulting in non-symmetric plasmon field density distribution.[44,45] Wang and coworkers later demonstrated the synthesis of much smaller gold nanorods (*ca.* 10 nm in diameter) by electrochemical oxidation of a gold plate electrode in the presence of cationic, quaternary ammonium surfactants (cetyltrimethylammonium bromide, or CTAB, and tetraoctylammonium bromide, or TOAB) and under ultrasonication.[46] The resulting nanorods solutions exhibited plasmon resonance modes for their short (transverse) and long (longitudinal) axis polarizations, verifying for the first time with gold nanorods the optical theory proposed by Gans 1912 for the scattering and absorption of spheroidal plasmonic nanoparticles.[47]

Murphy *et al.*[48] and Nikoobakht and El-Sayed[49] later demonstrated a colloidal growth method to produce monodisperse gold nanorods in high yield based on seeded growth (Fig. 4c). In this method, small (*ca.* 1.5 nm diameter) single-crystal seed particles, produced from the reduction of chloroauric acid by borohydride in the presence of CTAB, are aliquoted into Au(I) growth solution prepared from the mild reduction of chloroauric acid by ascorbate and the addition of $AgNO_3$ and CTAB. Using this method, gold nanorods *ca.* 10–20 nm in diameter and up to 300 nm in length can be obtained in relatively high yield, allowing for their subsequent use in a number of biomedical applications.[31] Nanorod aspect ratio can be controlled by the seed/gold salt ratio or by the relative concentration of additive impurity ions. For some time, the precise mechanism and purported reproducibility of nanorod growth has remained a hotly debated topic, confounded by the fact that some nanorod preparations contained additive impurity ions such as silver and others did not.[50] Proposed contributions include underpotential deposition, halide adsorption, surface packing density, and alloy formation among others. Electron microscopy indicated that the nanorods grow along the [001] direction with less stable crystalline facets along the sides of the rods and more stable crystalline facets at its tips.[32] A more recent re-analysis of these same gold nanorods suggest that the side faces are much higher-index facets than previously believed.[33] Pure gold nanorods made in the absence of silver ions show a pentatetrahedral twinned structure, again with the most stable bulk gold facets at the ends of the nanorods.[51] Vibrational spectroscopy and thermogravimetric analysis showed that the cationic surfactant forms a bilayer about the nanorods with the charged head groups facing outward.[31,52] More recently, Mirkin and coworkers have shown that the concentration of iodine contaminants present in various commercially-available CTAB stocks plays a critical role in determining the subsequent morphology and explain the apparent lack of reproducibility reported among nanorod preparations employed by various research groups. The authors proposed that preferential iodine adsorption on {111} facets at the nanorod tips prevent CTAB binding and thus promote longitudinal growth. Surprisingly, the roles of silver and halide ion adsorption in directing anisotropic growth remains a point of contention.[53] Khanal and Zubarev have further studied the CTAB/gold nanorod system and shown that the length and width of these nanorods can be amplified by addition of excess Au(I) and that their lengths can be selectively etched by the addition of Au(III), allowing the size and optical properties of these structures to bet tailored *via* the disproportionation reaction of Au(I) to produce Au(III) and

Author Manuscript Author Manuscript Author Manuscript Author Manuscript

Au(0).[54] Liz-Marzán and coworkers also showed that spherically-capped colloidal gold nanorods could be reshaped to form single-crystal octahedra, using poly(vinylpyrrolidone) (PVP) functionalized gold nanorods as seeds for the ultrasound-induced reduction of chloroauric acid by *N*,*N*-dimethylformamide (DMF) in the presence of PVP.[33] The authors showed that by increasing the ratio of gold salt to nanorod seeds, the subsequent morphology varies from sharpened (octagonal) rods to tetragons to octahedra (Fig. 4d). The authors attribute this transformation to differing Au growth rates on various crystallographic facets of the nanorods (*i.e.* {111} < {110} < {100}) and variations in surface energy due to the adsorption of ions and/capping agent(s).

Silica-gold core–shell nanoparticles, or gold nanoshells (Fig. 4e), have recently attracted much attention due to their interesting optical properties and numerous biomedical applications. Aden and Kerker predicted in 1951[55] that concentric spherical particle could exhibit tunable plasmon resonance which varies as a function of the ratio of shell thickness to core radius. Halas and coworkers showed in 1998 that near-infrared absorbing gold nanoshells could be prepared by electrostatically adsorbing small gold nanoparticles to the surfaces of silica nanoparticles and subsequently reducing additional gold onto the structures to form a conformal shell.[34] In a typical synthesis, silica nanoparticle cores are synthesized by the base-catalyzed condensation of orthosilicate[56] (*i.e.* Stöber hydrolysis) and functionalized with an amine-terminal silane. Small, anionic gold nanoparticles synthesized from the aqueous reduction of chloroauric acid by tetrakis(hydroxymethyl)phosphonium chloride (THPC) are electrostatically adsorbed onto the surfaces of the silica cores and added to a solution of mildly reduced chloroauric acid. When formaldehyde is added to the solution, the adsorbed gold particles serve as nucleation sites for the further reduction of gold around the silica core, subsequently forming a conformal nanoshell. In later reports, reduction with carbon monoxide (rather than formaldehyde) was shown to produce thinner and more uniform nanoshells.[57] Other related structures with novel optical properties such as asymmetric “nanoeggs” and quadruply concentric “nanomatryushkas” have also been developed.[58]

Gold nanocages and nanoframes recently developed by Xia and coworkers (Fig. 4f) also show promise in a variety of biomedical applications due to their desirable optical properties and potentially cargo-holding hollow structures.[59,60] The synthesis of these structures is based on a phenomenon known as galvanic replacement, whereby more noble metal ions (*e.g.* Au, Pt) spontaneously oxidize the surface atoms of a less noble metal (*e.g.* Ag, Cu) with concomitant reduction of the more noble metal.[60] In this case, gold nanocages/frames are produced by reacting Au(III) with silver nanocubes produced from the polyol reduction of silver nitrate. Because the reduction of one Au(III) ion requires surface oxidation to three Ag(I) ions, the density of the resulting structure is significantly decreased: in the case of a single-crystal cube, initially forming hollow Au/Ag alloy “nanoboxes” which further react to form porous Au nanocages and eventually faceless Au “nanoframes”.[35]

Near-infrared absorbing (spherical) hollow gold nanoparticles (Fig. 4g) have also been recently developed for use in drug loading/delivery and photothermal therapy applications. Caruso and coworkers obtained hollow gold nanospheres by calcination or dissolution of polystyrene–gold core–shell nanoparticles.[61] Here, polystyrene nanospheres were coated in

Author Manuscript Author Manuscript Author Manuscript Author Manuscript

polyelectrolyte multilayer films and small, 4-(dimethylamino)pyridine (DMAP) stabilized gold nanospheres (6 nm diameter) were electrostatically adsorbed to the polyelectrolyte surface. Hydroxylamine was then used to further reduce chloroauric acid onto the seed-coated polystyrene spheres, forming a nearly conformal gold shell. The polystyrene cores were then removed by dissolution in tetrahydrofuran (THF) or calcination at 310 °C to obtain hollow gold spheres *ca.* 650 nm in diameter. Liang *et al.* later showed that similar structures could be obtained by galvanic replacement with citrate-stabilized cobalt nanospheres synthesized from the reduction of $CoCl_2$ by borohydride under anaerobic conditions.[36] Subsequent addition of the cobalt nanospheres to chloroauric acid gave hollow gold nanoshells (*ca.* 60 nm diameter) in high yield. Wall thicknesses could be tuned by adjusting the ratio of gold salt to Co nanoparticles.

In 2004, Yang and coworkers showed that more geometrically complex gold nanostructures (100–300 nm in size) could be synthesized by a modified polyol process (Fig. 4h).[37] Using ethylene glycol as a solvent/reducing agent and PVP as a particle stabilizer, tetrahedra, cubes, octahedra, and icosahedra were obtained in high yield with good monodispersity. The authors found that the subsequent nanoparticle morphology was highly dependent on the concentration of gold present in the reaction solution, with tetrahedra formed at high concentrations and icosahedra (as well as a small number of octahedra) at lower concentrations. By adding a small quantity of silver nitrate during the reaction process, gold nanocubes were also obtained. Here, the authors suggested that crystallographically preferential adsorption of PVP resulted in enhanced [100] growth and suppressed [111] growth, yielding {111}-dominant tetrahedra and icosahedra. They also hypothesized that preferential adsorption of silver ions to {111} facets could lead to the formation of {100}-dominant cubes. Murphy and Sau later demonstrated the high-yield synthesis of similarly complex gold nanostructures *via* seed-mediated growth methods closely related to that used to produce colloidal nanorods.[62] By varying the concentrations of Au(III), ascorbic acid, and silver nitrate present in the growth solution, as well as the quantity of added seeds, rectangular, hexagonal, cubic, triangular, and star-like nanoparticles were obtained. In 2006, Song and coworkers developed an analogous seed-less, modified polyol synthesis.[63,64] Briefly, chloroauric acid was reduced in/by 1,5-pentanediol in the presence of PVP stabilizer. As the concentration of $AgNO_3$ was increased during the reaction, the subsequent morphology ranged from Au octahedra, truncated octahedra, cuboctahedra, cubes, to higher polygons. As previously hypothesized by Yang and coworkers, the authors attributed this control to the suppression of [100] growth and/or enhanced [111] growth. Niu *et al.* later showed that other complex gold nanostructures could be produced in high yield (>96%) by a related seeded growth method.[38] Here, CTAB-capped gold nanorods were amplified in a Au(III)/CTAB solution and functionalized with cetylpyridinium chloride (CPC) to serve as single-crystalline seeds (*ca.* 40 nm diameter) for the subsequent growth of rhombic dodecahedral, octahedral, and cubic gold nanocrystals from Au(I). Interestingly, the authors found that the CPC surfactant preferentially stabilized {100} > {110} > {111} facets, in contrast to their typically observed surface free energies (*i.e.* {110} > {100} > {111}). A rhombic dodecahedral morphology (Fig. 4i) was observed when CPC-Au{100} (and to a lesser extent, −Au{110}) association was dominant and octahedral geometries (Fig. 4j) were observed when CPC-Au{111} association was found to dominate. Cubic gold nanoparticles

Author Manuscript Author Manuscript Author Manuscript Author Manuscript

were found to form upon the addition of Br^- ions which the authors attributed to increasing stabilization of {100} facets by Br^- adsorption and subsequent electrostatic association of CP^+.

Recently, Mirkin and coworkers have also developed a method to produce monodisperse gold nanocubes in high yield (Fig. 4k) by a seeded growth technique analogous to that used to produce nanorods, except in this case, using the chloride analog of CTAB: cetyltrimethylammonium chloride, CTAC.[39] The authors found that nanocube size could be adjusted by simply varying the amount of seeds added to the growth solution, obtaining cubes with edge lengths ranging from 38 ± 7 nm to 269 ± 18 nm with and as high as 95% yield. Due to the concavity of their faces, the nanocubes exhibited a surface plasmon resonance *ca.* 80 nm red-shifted from their {100}-faced counterparts and are expected to exhibit novel catalytic properties. The authors hypothesized that the formation of high-index {720} facets could be due to surface-bound Ag formed by underpotential deposition (UPD) and its increasing stabilization by a Cl^- adlayer. Ming *et al.* previously obtained structurally-related, near-infrared absorbing tetrahexahedral gold nanoparticles enclosed by 24 {037} facets using a similar synthetic approach involving CTAB (>95% yield) (Fig. 4l).[40] Personick *et al.* showed that rhombic dodecahedra (Fig. 4m) and obtuse triangular bipyramids (Fig. 4n) could be obtained by a seeded (7 nm diameter) growth involving CTAC and dilute Ag^+ concentrations, obtaining the only {110}-faceted bipyrimidal gold nanostructures reported to date (31 ± 5 nm and 270 ± 26 nm edge length, respectively).[41] Crystallographic analysis found that the rhombic dodecahedra contained 12 identical {110} facets while the near-infrared absorbing triangular bipyrimads contained 2 triangular prisms separated by bridging (111) planes. Further analysis indicated that these structural differences arose from the use of a mixture of seeds containing both single-crystals and twin-defected particles and that their product particles could be easily isolated by size-selective filtration. Interestingly, they also found that as the Au(III) : seed ratio was increased that deposition increasingly favored growth on twinned bipyramidal particles, an effect they hypothesized resulted from the low(er) binding affinity of Cl^- for Au which allowed Ag UPD growth-directing effects to dominate. Even more exotic structures such as gold trisoctahedra have been obtained in by a simple aqueous reduction of chloroauric acid (Fig. 4o).[42] Zheng and coworkers showed that these nanostructures, 100–200 nm in diameter and enclosed by 24 {221} facets, are formed by the ascorbic acid reduction of chloroauric acid in the presence of CTAC (*ca.* 85% yield). While the precise mechanism for their formation is yet to be fully determined, the authors also found that CTA^+ and Cl^- were necessary for the formation of trisoctahedra and suggested that ascorbic acid or its oxidation products may stabilize high-energy concave faces.

Triangular, or prismatic, nanoparticles have been obtained by a number of methods including photoreduction, seed-mediated growth, plasmon-driven synthesis, and biosynthesis. Sastry and coworkers first obtained gold nanoprismatic structures in fair yield (*ca.* 200–500 nm in size, 45% yield) from the aqueous reduction of chloroauric acid by lemongrass extract.[65] The authors attributed this transformation to the reducing capacity of aldose sugars present in the plant extract, with shape-directing formation due to the crystallographically preferential adsorption of aldehydes/ketones present in the extract. Schatz *et al.* later showed that similar gold nanoprisms (144 ± 30 nm edge length) could be

Author Manuscript Author Manuscript Author Manuscript Author Manuscript

synthesized in high yield using a seeded growth method (Fig. 4p).[43] In a typical synthesis, borohydride-reduced, citrate-capped spherical seeds (5.2 ± 0.6 nm diameter) are synthesized from chloroauric acid and sequentially amplified in a solution of chloroauric acid, sodium hydroxide, ascorbic acid, and CTAB. The nanoprisms were isolated by filtration using a commercially-available aluminium oxide membrane (100 nm nominal pore size) and analyzed using optical spectroscopic and computational methods.

To the novice nano-synthetic chemist, all of the above methods sound alarmingly similar. Most include gold seed particles bearing ionic groups, the addition of metal ions with a reducing agent, and other additives which promote the formation of one shape or another. This similarity highlights both the power and frustration of colloidal nanoparticle synthesis: that small changes in reaction conditions can lead to very different reaction products, suggesting overall that these nanoparticles are the result of kinetic, as opposed to thermodynamic, stabilization effects. Viable thermodynamic arguments can also be made, usually with the idea that the additives bind to particular facets of the gold and lower the surface energy of that facet; however, because the stability of hydrated, nanoscale metal crystalline facets is difficult to predict and control in the presence of ions, many groups have adopted the use of a “hard template” approach to control nanoparticle shape.

Since its first demonstration in the early 1990s, template-based electrochemical deposition of gold nanostructures has found subsequent use in a variety of biomedical and bioanalytical applications. Keating *et al.* have shown that multisegmented, template-deposited nanorod structures can be employed in a multiplexed bioanalytical detection scheme (*i.e.* nanobarcode, NBC, assay).[66] By electrodepositing metallic segments of varying length, surface chemistry, and composition (*e.g.* Au, Ag, Pt, Ni, Co, Cu), large nanorods (600 nm × *ca.* 10 microns or more) with striped features can be prepared.[57] Subsequent chemistry to attach proteins and/or DNA to these multisegmented nanorods has led to detection of biomolecules with high sensitivity by fluorescence readout (*e.g.* sandwich-assay based configurations). Because the nanobarcodes and their segment patterns can be easily distinguished by optical microscopy, biomolecule detection schemes can be highly multiplexed: that is, the detection of the unique optical signature corresponding to each type of nanorod can indicate the presence of a specific biomolecule which it recognizes. Mirkin and coworkers later showed that by incorporating short segments of a selectively-etchable material (*e.g.* Ag, Ni) that discrete structures separated by sub-diffraction limited distances could be synthesized in high yield with good monodispersity (on-wire lithography, OWL).[67] In a typical synthesis, gold and silver segments are electrodeposited into the cylindrical pores of aluminium oxide membrane template by sequential addition and removal of metal salt solutions. The membrane template is then etched by hydroxide and the multisegmented nanorods are deposited onto a substrate. A thin layer of gold or glass is then deposited to cover one side of the nanorod, providing structural support across length of the multisegmented nanorod and allowing distances between gold segments to be maintained following removal and etching (*e.g.* nitric acid dissolution of Ag or Ni). The technique has been applied in a variety of applications including surface-enhanced Raman spectroscopic detection and molecular electronics.

Author Manuscript Author Manuscript Author Manuscript Author Manuscript

Apart from colloidal nanostructures with well-defined geometry, branched gold nanostars[68–71] have also proven to be useful in a number of biomedical applications: (i) due to their intense scattering properties, amenable to microscopic labeling-based applications,[69] (ii) their high spectral sensitivity to changes in the local dielectric environment, useful in bimolecular sensing applications,[69,71] and (iii) their high near-infrared absorption which can be leveraged in laser photothermal therapy approaches or for electromagnetic enhancement of *in vivo*, *in vitro*,[72] and *in situ*[73] surface enhanced Raman spectroscopy (SERS).[74,75] Hafner and coworkers have obtained gold nanostars by replacing the small (1–2 nm diameter) gold seeds used in a typical gold nanorod synthesis with commercially-available (10 nm diameter) gold nanospheres capped by citrate.[69] Liz-Marzán and coworkers have developed a method to produce gold nanostars with high yield and reproducibility using a method similar to that used to produce gold decahedra and octahedra.[76] Briefly, an aqueous solution of chloroauric acid (Au^{3+}) is gently reduced (Au^{+}) by DMF in the presence of PVP (10 kDa), followed by further reduction by borohydride. The seeds are aged for 24 h and an aliquot is added to a solution of chloroauric acid which has also been mildly reduced by DMF in the presence of PVP. Monodispersity was found to be improved upon pre-reduction of Au^{3+} to Au^{+} by DMF and the morphology/resonance wavelength was found to be controlled by the gold salt : seed ratio. Final nanostar dimensions were determined from the size of the seeds and increasingly sharp structures relevant to SERS- and sensing-based applications were formed at ambient temperatures. For a comprehensive survey of the synthesis, properties, and applications of gold nanostars, interested readers are directed to ref. 70.

While biomedical applications of gold nanoparticles typically involve so-called “bottom-up” synthetic approaches, a number of diagnostic and bioanalytical applications can make use of the high uniformity and precise spatial arrangement(s) afforded by top-down fabrication methods. For example, in the late 1990’s Van Duyne and coworkers developed a template-based synthesis in which gold nanoparticle arrays could be deposited using a shadow-mask approach (Fig. 5a).[77,78] Here, two-dimensional close-packed arrays of polymer nanospheres were self-assembled onto flat substrates and gold was vapor deposited into the pyramidal voids formed at their intersections (termed nanosphere lithography, NSL). Following removal of the polymer spheres (*e.g.* in organic solvent), ordered arrays of plasmon resonant nanoparticles were obtained over large areas in high yield.[78] Moerner *et al.*,[79] and El-Sayed *et al.*[80] have employed electron-beam lithographic methods to obtain arrays of gold nanostructures with precise control over the structural morphology and interparticle spacing (Fig. 5b). Whitesides and coworkers have shown that gold nanostructures (*ca.* ≥ 30 nm) can be fabricated by a so-called “nanoskiving” method whereby gold deposited onto flat or structured polymeric substrates (typically epoxy) are sectioned *via* ultramicrotome and released (*e.g.* by oxygen plasma etching) (Fig. 5c–e).[81] Mirkin and coworkers have developed a lithographic method based on atomic force microscopy (AFM) in which chemical resists consisting of self-assembled monolayers are patterned onto gold thin films which are subsequently etched to reveal precise, large-area patterned arrays of gold nanostructures (dip-pen lithography, DPL) (Fig. 5f–i).[82,87] In a more recent report, Aizenberg and coworkers have shown that directional vapor deposition of gold and combined electrochemical deposition of conducting polymers onto PDMS-molded

Author Manuscript Author Manuscript Author Manuscript Author Manuscript

substrates can be used to fabricate gold nanostructured particle arrays with tapered, anisotropic, and overhanging features (structural transformation by electrodeposition on patterned substrates, STEPS) (Fig. 5j–l).[83]

While many of the aforementioned “top-down” synthetic approaches often yield substrate-supported/bound gold nanostructures, these methods can also be used to produce freestanding gold nanoparticles amenable to colloidal dispersion and a variety of biomedical applications. Lee and coworkers have recently explored the use of three-dimensional, crescent-shaped hollow gold nanostructures (nanocrescent moons) obtained *via* shadow mask Au vapor deposition onto sacrificial template nanoparticles (Fig. 5m–o).[84,88] In a typical synthesis, commercially-available polystyrene nanospheres are deposited onto a glass substrate coated with an acetone-soluble polymer (photoresist). The planar sample is then rotated as gold is directionally (*i.e.* electron-beam) deposited onto the polystyrene spheres, leaving a shadow-masked cavity at the sphere–substrate interface. Depending on the angle between the substrate and the incident flux of gold, as well as the size of the sacrificial templates, the geometry and thus, the optical properties of the nanocrescent structures can be easily tuned throughout the visible and near-infrared spectral regions. The template-bound nanocrescents are subsequently released from the substrate *via* acetone lift-off and the polystyrene templates are then removed *via* dissolution in toluene. The free nanocrescents can be functionalized with a variety of colloidal stabilizers and linker molecules for a range of biomedical diagnostic and therapeutic applications. Because of their sharp surface features and intraparticle plasmon coupling effects, these particles have proven to be highly useful as substrates for surface enhanced Raman scattering (SERS)[84,88] and can be synthesized in a hierarchical manner to incorporate other functional materials such as magnetic segments[88] which can facilitate *ex vivo* manipulation or enhanced contrast in magnetic resonance imaging (MRI).

Odom and coworkers have shown that free-standing, hollow, pyramidal gold nanostructures of varying geometry can be obtained in a related approach utilizing nanopatterned silicon and vapor-phase metal deposition (Fig. 5p–s).[85,89] Here, the authors first fabricate an array of cylindrical posts (*ca.* 250 nm diameter) on a Si substrate *via* phase-shift photolithography using a positive-tone photoresist. A thin (*ca.* 20 nm) film of Cr is next deposited onto the array and the photoresist is removed by lift-off in acetone. The exposed array of Si nanofeatures is then chemically etched by KOH/isopropyl alcohol (IPA) to yield an array of negative nanopyramidal pits. A thin (*ca.* 20–60 nm) film of gold (or another type/combination of metal/material) is then vapor deposited onto the array and the Cr template layer is removed using a commercial chemical etchant to reveal an array of substrate-bound, hollow gold nanopyramids. The nanopyramids are subsequently released *via* KOH/IPA Si etching and can be similarly functionalized with a variety of colloidal stabilizers or linker groups for the attachment of biomolecules. Like the hollow gold nanocrescents, because gold nanopyramids exhibit sharp surface features and intense intraparticle near-field coupling, these structures exhibit both near-infrared absorption for photothermal contrast and high electromagnetic SERS enhancement.[90] One particularly attractive feature of these structures is the ability to differentially functionalize the inner and outer surfaces of the nanopyramids by doing so before/after release from the Si support.[86] Tipless, or truncated, nanopyramidal structures can also be fabricated[91] by rotating the planar template array at

Author Manuscript Author Manuscript Author Manuscript Author Manuscript

some angle with respect to incident flux of collimated (electron-beam deposited) gold vapor, allowing for further SERS enhancement and an increase in multipolar plasmon contributions which can contribute to novel nonlinear optical phenomena such as Fano[92,93] resonance. Photothermal conversion from these structures in solution[94] ($\Delta T \leq 18$ °C) has been shown to be comparable to those obtainable with more conventional nanorod, nanoshell, nanocage, and hollow gold nanostructures *in vivo*, well above those minimally required for therapeutic hyperthermia[95] ($\Delta T \approx 3$–6 °C).

B. Functionalization

Chemical tuning of the nanoparticle surface is necessary to impart biological compatibility and specificity to gold nanoparticles. The synthetic reagent CTAB, for example, which is so crucial in a number of preparations of gold nanorods and other shapes, is toxic to cells at micromolar concentrations on its own.[96] We do note, however, that in terms of delivery of nanoparticles to cancerous tumors, the “leaky vasculature” of tumor tissue itself favors (passive) nanoparticle localization there, without the need for (active) chemical functionalization.[97–100] We also note that the binding of a “toxic” agent such as CTAB to a nanoparticle surface makes it far less bioavailable than it would be if it were free in solution, and therefore the tolerable dose of a nanoparticle bearing a given molecule might be quite different than that of the molecule alone.[96]

Functionalization of gold nanoparticles for biomedical applications follows largely on work initially conducted by Nuzzo and Whitesides on the formation of self-assembled monolayers (SAMs) of molecules on planar gold[101,102] and later by Bard[103,104] and Murray[105–107] in studying the dynamics and conformations of these assemblies by electrochemical, scanning probe, and mass spectrometric methods. A rich variety of functional molecular linkers and passivating agents are currently employed in the conjugation of gold nanoparticles used in biomedical applications; however, the anchoring groups utilized for attachment of these molecules to the gold surface generally include: thiolate,[21,108,109] dithiolate,[110] dithiocarbamate,[111] amine,[112] carboxylate,[112] selenide,[113] isothiocyanate,[108,112] or phosphine[19,109] moieties. Recent evidence suggests that direct Au–C bond formation may be achieved by way of a trimethyl tin leaving group; however its use in biomedical- or nanoparticle-based applications has yet to be tested.[114] The choice of particular molecular anchor typically varies depending on the desired lability of the molecule for a specific application, with trends in bonding strength generally following Pearson’s hard–soft acid–base (HSAB) theory for a soft Au(I) surface. Non-labile applications most often employ thiol-based anchoring groups while labile applications often make use of amine or carboxylate surface anchors. Burda and coworkers, for example have shown that therapeutic outcomes following gold nanoparticle-mediated delivery of photodynamic therapy agents drastically benefits from the use of more labile amino linkers *versus* stronger thiol groups due to vesicular sequestration of particle-bound drug molecules.[115,116]

In the case of common alkanethiols, room temperature surface adsorption is spontaneous, occurring over milliseconds to minutes.[102] Packing/reordering of the monolayer can occur over several hours, however in practice, overnight particle-ligand incubation with additional sonication or gentle heating is often sufficient to achieve optimal results. Murray place

Author Manuscript Author Manuscript Author Manuscript Author Manuscript

exchange[105–107] of the nanoparticle-bound SAMs can also be performed to functionalize gold nanoparticles with mixed or fully exchanged monolayers with coverages as high as 1.5 × 10^{15} molecules cm^{-2}. Typical alkanethiol coverages however, are typically on the order of 1.5 × 10^{14} molecules cm^{-2}.[103]

Although the bond strength between anchoring groups and the gold surface plays a critical role in determining the subsequent functionality, packing density and surface energetics make equally important contributions. While dithiolates are often viewed as preferable to their mono-thiolate counterparts due to multivalent binding avidity, these molecules are actually more prone to oxidative desorption due to inefficient packing (Fig. 6).[110] Cima *et al.* have found that thiolates, most commonly employed for attachment to gold nanoparticles in non-labile biomedical applications, can remain stably adsorbed for up to 35 days under physiologic conditions.[117] This suggests that thiolates may be a preferred functional group for attachment of biological molecules to gold surfaces in many biomedical applications.

Common among most applications of gold nanoparticles in biomedicine is the need for adequate stabilization in biological environments containing high serum concentrations and high ionic strengths. Thiolated poly(ethylene glycol), PEG–SH, is by far the most commonly employed surface ligand used with biomedical gold nanoparticles. Its well-documented hydrophilicity permits the aqueous dispersion of gold nanoparticles conjugated with a wide range of lipophilic molecules[118] and increases circulatory half life[119] by blocking adsorption of serum proteins and opsonins which facilitate uptake and clearance by the reticuloendothelial system (RES).[120–123] Recent studies by Dai and coworkers indicate that carbon nanotubes (far more hydrophobic than gold nanoparticles) functionalized with branched PEG ligands exhibit superior pharmacokinetics and minimal RES uptake compared with PEG ligands of the same molecular weight.[124] Circulating gold nanoparticles can be expected to benefit from similar functionalization strategies. Recent evidence from Jordan and coworkers also suggest that polyoxazoline (PO*x*) stabilizers may serve as suitable alternatives and/or superior ligands to PEG.[125–127]

Cationic surfactants, so important to gold nanoparticle shape control (*e.g.* CTAB, CPC, CTAC, *etc.*), appear to adsorb by a different mechanism: as a bilayer on the nanoparticle surface.[31,52] Here, the quaternary ammonium groups face the solvent, with a postulated chemisorbed bromide at the gold surface; mass spectrometry[128] and vibrational spectroscopy[129–131] data suggest that Au–Br is indeed present at the surface. Subsequent conjugation of biomolecules, then, rests on either replacement or overcoating of this surfactant bilayer (*vide infra*).

Gold nanoparticles can be conjugated with a variety of biofunctional molecules by simple physical methods such as hydrophobic–hydrophobic interaction (Fig. 7a) and charge-pairing (Fig. 7b). Rotello and coworkers have shown that highly hydrophobic molecules (*e.g.* chemotherapeutics such as paclitaxel and doxorubicin) can be labily bound to biomedical gold nanoparticle conjugates *via* the use of amphiphilic ligands.[132] By creating a hydrophobic corona inside of a hydrophilic ligand shell, they were able to demonstrate the entrapment and efficient release of hydrophobic fluorescent molecules *via* “membrane-mediated diffusion”.[132] Classical cross coupling reagents can also be employed for the non-

Author Manuscript Author Manuscript Author Manuscript Author Manuscript

labile conjugation of a wide range of biofunctional targeting, therapeutic, and imaging contrast agents (Fig. 7c). Most applications involving amine-containing molecules/proteins employ classical carbodiimide cross coupling (carboxylate + amine → amide) with a number of commercial chemical manufacturers producing ready-made *N*-hydroxysuccinimide (NHS)-activated heterobifunctional polymers and ligands.[133,134] Linkage to sulfhydryl groups can be similarly achieved by way of maleimide-terminal ligands, also widely commercially available.[135] Huisgen cycloaddition (click, or azide–alkyne coupling) has been similarly employed in a number of gold nanoparticle conjugation strategies.[134]

Inorganic complexes such as cisplatin or its prodrug forms can also be datively bound to gold nanoparticle ligands by way of appropriate ligands (Fig. 8a).[136] Lippard and coworkers have shown that a Pt(IV) prodrug form of cisplatin can be coordinated by carboxylate-terminal ligands on gold nanoparticles which facilitate intracellular transport and subsequent activation of the prodrug. Mirkin and coworkers have pioneered the use oligonucleotide-functionalized gold nanoparticles, employing thiolated ssDNA as surface linkers to which targeting ligand-, biomolecule-, and/or imaging contrast agent-tethered complementary ssDNA can be hybridized (Fig. 8b).[137,138] Recently, Rotello and coworkers have demonstrated the synthesis, gold nanoparticle conjugation, and photo-triggered release of the cytotoxic thymidylate synthase inhibitor 5-fluorouracil (5-FU) by way of a photocleavable, *o*-nitrobenzyl PEG–SH linker, demonstrating significant toxicity following UV exposure and dramatically diminished cytotoxicity in its absence (Fig. 8c).[139]

Other strategies for the functionalization of gold nanoparticle conjugates employ core–shell type geometries where the nanoparticle or other molecules are entrapped within a polymer or dielectric shell which can be further conjugated. Gittins and Caruso showed that gold nanospheres could be encapsulated *via* consecutive adsorption of charge-paired polyelectrolyte films, also known as layer-by-layer (LbL) assemblies.[140] Gold nanospheres were coated with alternating layers of anionic sodium poly(styrenesulfonate) (PSS) (15.2 kDa) and cationic poly(diallyldimethylammonium chloride) (PDADMAC) (20 kDa) with the adsorption of each layer following centrifugal purification. The resulting nanoparticles exhibited tunable surface charge and allowed for the electrostatic adsorption of proteins (see Fig. 7b) over a wide range of isoelectric points and solvent pH values. The same LbL concept works for coating gold nanorods, enabling switching of the effective surface charge from positive to negative, and overcoating the surfactant bilayer to present ammonium, sulfate, or other charged groups to the solvent.[141,142] Stable, hollow polymeric nanocapsules can be obtained by CN^- etching of both polymer-coated gold nanospheres[140,143] and nanorods.[144] Due to their hierarchical assembly and controllable interlayer diffusion, Hammond and coworkers have found LbL assemblies useful in a number of multidrug and gene delivery applications.[145–149]

In the mid 1990's, Liz-Marzán *et al.*[150] showed that gold nanoparticles could be fully encapsulated by silica (glass) shells[151] (Fig. 9a) by vitreophobic surface conjugation and facile silane chemistry (Fig. 9b).[152] This prospect is particularly attractive for use with gold nanorods, where compelling evidence showing complete removal/displacement of CTAB molecules from the sides of the rods has yet to be demonstrated. Natan *et al.*[153] and Nie *et*

Author Manuscript Author Manuscript Author Manuscript Author Manuscript

al.[154] have further explored this concept, fabricating gold–silica core–shell nanoconjugates containing entrapped Raman reporter molecules (Fig. 9d). Because the enhanced optical properties afforded by resonant excitation of the gold core's surface plasmon resonance (surface enhanced Raman scattering, SERS), highly multiplexed *in vivo* SERS has been demonstrated.[155]

Functionalization of gold nanoparticles can be qualitatively verified by a number of means including vibrational spectroscopy (*e.g.* IR or Raman), plasmon resonance shift, thermogravimetric analysis (TGA),[133] and/or hydrodynamic diameter or zeta potential change (*via* dynamic light scattering, DLS). In practice however, quantitative measures such as absorption/fluorescence assay,[118,156] mass spectrometry (inductively-coupled plasma, ICP,[157,158] or matrix-assisted laser desorption ionization, MALDI),[159] X-ray photoelectron spectroscopy (XPS),[160,161] and/or cyclic voltammetry are preferred.

III. Gold nanocrystals for *in vitro* diagnostics

A valuable review of gold nanoparticles for *in vitro* diagnostics by Rosi and Mirkin is recommended as supplemental reading.[162]

A. SERS-based assays

Surface-enhanced Raman scattering (SERS)[163,164] is the enhancement of Raman-active vibrations associated with proximity to a nanoscale metal surface (*e.g.* a surface covered with plasmonic nanoparticles). SERS typically requires that the molecule be within the electromagnetic near-field of the localized surface plasmon (roughly the particle diameter) and is attributed predominantly to electromagnetic[165] enhancement mechanisms, but also chemical[166] (charge-transfer) contributions. In the electromagnetic SERS mechanism, the surface plasmon field enhances both the incident (exciting) photons, as well as the inelastically scattered Raman-shifted photons. For maximum enhancement, it is recommended that the surface plasmon band be broad enough to encompass both the incident field excitation wavelength range, as well as the Stokes- or anti-Stokes-shifted Raman scattered photons. In this case, the intensity of the Raman scattered photons is enhanced roughly proportional to $E^2_{\text{laser}} \times E^2_{\text{laser}\pm\text{Raman}}$ where E is the local electromagnetic field around the molecule. For this reason, and the fact that plasmonic field is greatly enhanced at the junctions between nanoparticles (where these fields couple and overlap), aggregated silver nanoparticles having broad plasmon spectra have been used in a number of SERS studies. Silver nanoparticles also exhibit stronger plasmon fields than gold nanoparticles of the same size and shape due to the fact that their plasmon band does not partially overlap with interband electronic transitions observed with gold nanoparticles ($\lambda <$ 500 nm) and silver nanoparticles (<300 nm). This overlap decreases the degree of coherence of the motion of the free electrons that produce the surface plasmon field. Electromagnetic enhancement can increase the intensity of Raman scattered photons from nearby molecules by several orders of magnitude. Chemical enhancement proposes that chemisorption of molecules to the nanoparticle surface increases their polarizability and thus increases the Raman signals *via* charge-transfer. This mechanism, if present, makes a much smaller enhancement contribution compared with that of the electromagnetic mechanism.

Author Manuscript Author Manuscript Author Manuscript Author Manuscript

Because Raman spectroscopy is a vibrational technique like infrared spectroscopy, signals can be used as fingerprints to identify molecules. Since its discovery in the 1970s,[163,165] SERS has been widely used in chemical and biological analysis in the research laboratory; commercial applications have been slow in coming due largely due to reproducibility issues in quantitative analytical applications (possible due to irreproducibility in substrate nanoscale morphology, or in accurate assessment of the number of molecules bound to the nanoparticle surface, or both).[168] Although silver is known to give higher field enhancements and thus stronger SERS activity, gold nanoparticles are popular substrates for SERS-based biomedical detection because they are easy to prepare, show excellent biocompatibility, are significantly more stable (*i.e.* not easily oxidized).[169,170]

SERS-based assays can be categorized in two ways: label-free assays and Raman reporter assays. In the first approach, molecules are directly adsorbed onto the nanoparticles and thus are recognized by their enhanced Raman signals; no external label needs to be attached to the analyte of interest. Detection can be achieved with the use of individual gold nanoparticles, especially with diameters of 60 to 80 nm, but good SERS signals frequently rely on nanoparticle aggregation due to increased local electromagnetic fields and therefore much stronger Raman enhancement than individual particles.[171–176] Huang *et al.* showed that head and neck cancer cells can be differentiated from normal cells by the assembly of immunogold nanorods on the surfaces of cancer cells.[172] This assembly was found to result in sharp, highly polarized, and well-resolved Raman signals of the capping materials on the nanorods (Fig. 10). This label-free method is simple and can give molecular information about the target cell, but signals can often be complicated heterogeneity in the surrounding cellular matrix or impurities surrounding the particles whose Raman signals could also be enhanced. Liz-Marzán and coworkers have shown that gold nanostars can be used to detect a wide variety of chemisorbing and non-chemisorbing analytes (biomarkers) at zeptomolar detection limits ($E^4 \approx 10^{10}$) by sandwiching a drop-cast thin film of the analyte solution between a gold film and a subsequently drop-cast film of gold nanostars.[74,177]

In Raman reporter assays, molecules with large Raman cross sections (*e.g.*, organic dye molecules with highly-delocalized p electrons) are adsorbed or covalently conjugated to nanoparticles, thereby giving a strong SERS spectrum specific to the embedded/attached molecule. This specific SERS spectrum is used as the signal readout when the particles are subsequently functionalized with surface coatings, biomolecules, *etc.* that are farther out from the nanoparticle surface (and thus give no Raman signal). This Raman reporter method is highly specific because it avoids signal interference from competing species in proximity. Enhancement can be as high as 10^{14} and, thus, these Raman reporter particles can provide readouts in ultrasensitive assays.[178,179]

In the last decade, gold Raman reporter particles have been widely used to detect biomarkers in cancer[180–185] and other diseases,[186–189] as well as viral[190–192] and bacterial[181,193–196] microorganisms. The use of nanoparticle aggregation to strongly enhance Raman signals has been used to form “molecular beacons” with signal amplifications, about 40–200 fold higher than traditional molecular beacons that are based on quenching or fluorescence resonance energy transfer (FRET).[181] Due to their high sensitivity, Raman reporter particles were recently found to be a promising tool for detection of rare cells such as circulating tumor

Author Manuscript Author Manuscript Author Manuscript Author Manuscript

cells (CTCs).[197,198] Wang *et al.* reported that epidermal growth factor-conjugated, peptide-SERS-encoded gold nanoparticles can detect CTCs in mouse and human blood samples (Fig. 11). Their Raman reporters showed high specificity to head and neck cancer cells in a sea of white blood cells with a sensitivity threshold of 5–50 cells per mL blood.[198] Brust and coworkers have recently shown that silica-encapsulated, branched gold nanostar Raman reporters may provide increasing SERS enhancement over similar spherical reporters for non-invasive and multiplexed *in vivo* imaging applications.[72] Compared to fluorescence detection, this SERS approach is advantageous because readout signals are sharp, distinct from complex biological fluids, and minimize effects from biological background fluorescence. Multiplexed detection can also be achieved by using different reporter molecules without changing the size or shape of the nanoparticles or their excitation wavelength.[199–203]

B. LSPR shift assay (refractive index sensing)

Localized surface plasmon resonance (LSPR) assays are based on shifting of the LSPR wavelength in response to changes in the local refractive index that surrounds a plasmonic nanoparticle or surface.[12,204–206] The spherical plasmon resonance condition[207] $\varepsilon_r = -2\varepsilon_m$, where ε_r is the dielectric function of the metal, and ε_m is the dielectric function of the medium at a given wavelength, shows that an increase in ε_m requires an increase in the value of the ε_r in order to satisfy the resonance condition for LSPR. For an increasing refractive index n {where $\varepsilon_m = \varepsilon'_m + {}_i\,\varepsilon''_m = (n + ik)^2$}, such as that observed when a protein ($n \approx 1.35$–1.6) is adsorbed to the surface of a nanoparticle dispersed in aqueous solution ($n \approx 1.333$), a red shift of the plasmon resonance wavelength is observed.[208,209] Thus, by monitoring the wavelength of the LSPR band (either absorption or scattering), changes in the local chemical and biochemical environment can be detected. If the surface of the metal nanoparticle is appropriately functionalized, these shifts can be chemically specific. LSPR assays, offer a simple, selective and label-free way for molecular detection. Their performance is characterized *via* the so-called sensitivity factor (SF) (*i.e.* plasmon wavelength shift per unit change in the effective refractive index of the surrounding medium, nm RIU^{-1}), which depends on the nanoparticle size, shape and composition. Theoretical studies by Lee and El-Sayed showed that nanorods give higher LSPR sensitivity than nanospheres, that larger nanoparticles are more sensitive than smaller ones, and that silver nanoparticles give better scattering quantum yield (the ratio of the scattered efficiency to the total extinction at each resonance maximum) than gold.[209] Very recently, Mahmoud and El-Sayed showed both experimentally and theoretically that the high sensitivity factor observed from hollow nanoparticles (*i.e.* nanocages and nanoframes) results from coupling between plasmon fields of their inner and outer surfaces.[210] Willets and Van Duyne have demonstrated extensively that arrays of silver triangular nanoparticles prepared by nanosphere lithography (NSL) are highly effective for quantitative detection of a variety of chemicals and biochemicals.[211] Gold nanoparticles 30 nm in diameter have a sensitivity of ~70 nm RIU^{-1},[212] which is modest compared to silver nanoparticles. LSPR shift from 40 nm gold colloids were reported to be sufficient to probe association and dissociation kinetics of antibody–antigen interactions.[213] NSL-derived gold substrates have higher sensitivity than randomly deposited substrates from colloidal Au,[214–216] suggesting that pre-organization of metal nanoparticles

Author Manuscript Author Manuscript Author Manuscript Author Manuscript

on the nanoscale have significant advantages for sensor applications. Somewhat in contrast to this notion is that single nanoparticles can be more sensitive in LSPR assays than ensemble average measurements, with the capability to detect spectra shifts of only a few meV.[217] This suggests that some particles may be "hot" for LSPR detection, and if it was possible to identify them and produce them in higher yield, the overall sensor capability might be improved. Gold nanorods,[218,219] nanostars,[68,69,220] and nanoprisms[80] appear to be excellent single particle LSPR sensors for a variety of biomolecules. With the use of dark field microspectroscopy system, Nusz *et al.* showed that biotin-conjugated gold nanorods can detect streptavidin with a sensitivity down to 1 nM (Fig. 12).[219] Depending on the system, nanomolar detection of protein in serum is possible.[221] Due to variations in LSPR peak widths associated with various nanoparticle sizes and shapes, researchers have become increasingly focused on the so-called dimensionless 'figure-of-merit' (FOM) as a measure of practical performance (*i.e.* sensitivity factor/LSPR peak width). We also note that a review article by Hafner and coworkers, entirely focused on LSPR sensors, has recently appeared; [222] we refer readers to that manuscript for more details of these types of sensors.

Another LSPR assay is based on the wavelength shift induced by changes of interparticle distance. This LSPR shift is due to the interparticle plasmon coupling (*i.e.* the electric field on one nanoparticle surface interacts with that of a neighboring particle).[223,224] As this "near-field" decays over a distance on the order of the size of the nanoparticles,[225] plasmon coupling depends largely on interparticle distance. LSPR shift decays near exponentially with interparticle separation[226] and decreasing interparticle distance, through nanoparticle assembly or aggregation, leads to an LSPR red shift, with larger shifts for shorter NP distances and larger assemblies or aggregate sizes.[227–230] Using the distance-dependence of plasmon coupling, Alivisatos and coworkers demonstrated a strategy to measure the distance between pairs of gold nanoparticles and were able to probe the dynamics of biomolecular binding.[231,232] The coupling-induced plasmonic shift is polarization dependent, red-shifting when the electric field vector of the light is parallel to the interparticle axis, and blue-shifting (to a lesser much lesser extent) when it is orthogonal to the interparticle axis.[233] Using these and other independently observed and calculated data from electron-beam fabricated nanoparticle pairs,[234] El-Sayed and coworkers have derived simple exponential relations to describe these distance-dependent wavelength shifts, independent of particle shape or composition.[235] For anisotropic nanoparticles, LSPR shift also depends on assembly orientation. While end-to-end assembly of gold nanorods results in a red-shift of the longitudinal LSPR band, side-by-side assembly results in a blue shift of the longitudinal plasmon band.[224]

Assembly-induced, or aggregation-based, LSPR shift has been widely used for the detection and sensing of nucleic acids, as first demonstrated and later extensively studied by Mirkin and coworkers.[162,227,228,230,236,237] In these experiments, two populations of gold nanospheres are functionalized with two non-complementary strands of oligonucleotides. When solution mixtures are exposed to target DNA that is complementary to both sequences of surface-bound DNA, the target DNA will bind to both nanoparticle populations *via* standard DNA hybridization and induce nanoparticle aggregation (Fig. 13).[162,227,228] Aggregation-induced LSPR red shift, as visualized by the overall solution color change from red to blue, offers the capability to detect low concentrations of nucleic acids using simple

Author Manuscript Author Manuscript Author Manuscript Author Manuscript

UV-Vis spectroscopy, or by spotting the solution on a silica support and simple lateral-flow (visual) detection. The melting profile of the nanoparticle-labeled DNA aggregates is much sharper than fluorophore-labeled or unlabelled DNA and has extensively been studied by Mirkin and coworkers.[137,138,156,162,167,227,228,230,236–243] Due to the extremely sharp melting transition, the method can differentiate DNA with single base-pair mismatch.[227,228] It is also a quick, easy, simple and inexpensive assay. The technique is amenable to other shapes such as gold nanorods which exhibit orientation-dependent assembly properties.[244,245] In a variation on this theme, Sato *et al.* demonstrated a new method for DNA detection, in which aggregation was induced by a reduction in the repulsive interactions between nanoparticles when target DNA bound to those on the surface of gold nanoparticles.[99] Another reported variation relies on DNA nonspecifically adsorbed to gold nanoparticles with subsequent binding with complementary target DNA, which induces dissociation of the probe DNA from the gold nanoparticles and thus promotes gold nanoparticle aggregation.[246]

C. Rapid test applications

In biodiagnostics, gold nanotechnologies are perhaps best known for their applications in lateral flow assay configurations. The over-the-counter First Response® pregnancy test (Carter–Wallace) is one such example, whereby the intense optical properties of gold nanoparticles are used as a chemically-stable, highly visible optical indicator.[247] In the "sandwich" later-flow immunoassay configuration, urine potentially containing the pregnancy biomarker, human chorionic gonadotropin (hCG), is sorbed onto a test strip and transported *via* capillary action to a upstream reservoir containing anti-hCG gold nanoparticle conjugates (18 nm diameter). If hCG is present, the gold nanoparticle–hCG complex travels upstream to a capture site containing immobilized polystyrene microparticles (0.3 μm diameter) conjugated with anti-hCG which binds hCG at a site distinct from that on the gold nanoparticles, resulting in the accumulation of an intense pink color at the capture/read site, indicating pregnancy.

Gold nanotechnologies can also play an important role in preventative medicine. For example, the rapid detection of food-borne pathogens is an increasing concern in today's global agricultural market and the use of gold nanoparticles in lateral flow assays for the detection of pathogenic toxins is a rapidly growing market. Enterohaemorrhagic Escherichia coli (EHEC), a rare strain of the common bacteria, is an example of one such pathogen, in 2011, responsible for 17 deaths, 1500 confirmed or suspected cases, and the loss of hundreds of millions of dollars following an outbreak of EHEC in northern Germany linked to contaminated sprouts grown in the region.[248] EHEC produces verotoxin (also known as Shiga-like toxin) which can result in kidney failure, hemolytic anemia, and a drop in blood platelet counts.[249] Although EHEC is often detected by a time-consuming culture analysis or PCR, Merck KGaA is currently marketing a lateral flow assay conceptually similar to the aforementioned pregnancy exam (Duopath[s]). In this case, the assay can assess the presence of verotoxin in just 20 minutes, with sensitivity and accuracy equal to that achievable by ELISA, culture analysis, and PCR.

Gold nanotechnology-enabled lateral-flow immunoassays can also be used for the diagnosis and monitoring of asthmatic and atopic patients. The ImmunoCAP® Rapid test (Phadia,

Author Manuscript Author Manuscript Author Manuscript Author Manuscript

Inc.) can detect immune responses (immunoglobulin E) associated with 10 prevalent allergens (8 inhalants, 2 foods) from blood samples in as little as 20 minutes, enabling accurate identification of atopy and allergen specificities in children.[250] While current applications of gold nanotechnologies in rapid test applications are currently limited to the detection of the previously mentioned proteins, a number of other targets are currently being investigated including nucleic acids (1.25 fM limit),[251] immunoglobulin G (IgG) to confirm anthrax vaccination,[252] sexually transmitted diseases (herpes simplex virus type 2),[253] bacterial drinking water contaminants,[254] psychotropic drug (benzodiazepin) metabolites,[255] and toxins produced by other food-borne pathogenic bacteria (*Staphylococcus aureus* B,[256] salmonella).[257] Assay configurations utilizing aptamer recognition have also been demonstrated with equal specificity and sensitivity to antibodies.[258]

IV. Gold nanocrystals for cellular and *in vivo* imaging

Plasmonic gold nanoparticles can also exhibit strongly enhanced radiative properties compared with bulk gold (*i.e.* light absorption, scattering, and fluorescence). While electromagnetic field enhancement has been widely used in SERS (*vide infra*), absorption, scattering and fluorescence enhancements make gold nanoparticles potential multimodal imaging agents.[6] Here we outline three main modalities in cellular and *in vivo* imaging, including light scattering imaging, two-photon fluorescence imaging, and photothermal/photoacoustic imaging.

Gold nanoparticles can strongly scatter light at their plasmon wavelengths, with the scattering cross-sections 10^5–10^6 times stronger than that of the emission from a fluorescent dye molecule.[259–261] LSPR scattering frequency and intensity depends on the size and shape of the nanoparticle.[162,262] Gold nanoparticles that are larger in size and nanorods with higher aspect ratios show stronger scattering efficiencies than their smaller counterparts, as demonstrated both theoretically and experimentally.[12,259–261,263–265] Gold nanoparticles with larger than 10 nm in diameter can be readily visualized under dark field scattering microscopy with a simple optical microscope.[266] In contrast to conventional fluorophores, the light-scattering nanoparticles are indefinitely photostable and do not blink. These features make gold-based nanoparticle probes very powerful for bioimaging. Observation of individual silver nanoparticles was first realized in dark field optical microscopy by Mock *et al.* in the early 2000's.[267] Later studies on gold nanoparticles by Sokolov *et al.*[268] showed that when 12 nm gold nanoparticles were conjugated to anti-epidermal growth factor receptor (anti-EGFR) antibodies, they specifically bound to EGFR proteins that are overexpressed on the surfaces of cervical cancer cells. Illumination of the nanoparticle-labeled cells with laser light from either a laser pointer or a confocal microscope lit up the gold nanoparticles, and thus, their associated cancer cells. Later, El-Sayed *et al.* used simple dark field optical microscopy to detect gold nanoparticle-labeled cancer cells.[269] The key advantages of dark field imaging is that nanoparticles are imaged in high-contrast with true color, making the technique amenable to multiplexed detection schemes by using gold nanoparticles of different size and shapes. As demonstrated in 2006 by Huang *et al.*,[270] gold nanorods scatter strongly in the near-infrared region, capable of detecting head and neck cancer cells under excitation at spectral wavelengths where biological tissues exhibit little attenuation (Fig. 14). Currently, dark field imaging based on the light-scattering properties

Author Manuscript Author Manuscript Author Manuscript Author Manuscript

of gold nanoparticles (spheres, rods, nanocages and nanoshells) is widely used for cancer imaging through functionalized nanoparticle–receptor binding on to cell surface biomarkers.[271–274]

In addition to molecular imaging for potential biodiagnostic applications, the light-scattering properties of gold nanoparticles have been useful in many other biomedicinal areas. For example, by functionalizing nanoparticles with both cytosolic-directing and targeting moieties, Kumar *et al.* reported the imaging of intracellular actin biomarkers in live cells.[275] Taton *et al.* demonstrated two-color detection of DNA sequences using 60 and 100 nm gold nanoparticles.[237] Oyelere *et al.* monitored nuclear targeting of nanoparticles to normal and malignant cells.[276] Qian *et al.* tracked cell cycle from birth through division with peptide-conjugated gold nanoparticles.[277] Murphy and coworkers have used gold nanorods as light-scattering markers to track local deformation fields (displacement and strains) in polymers.[263] These studies showcase the utility of gold nanoparticles as probes for mechanical studies in biological tissues. In later work, optical scattering patterns, in conjunction with digital image processing, was used to track local deformations between live cells.[278] Thus, the mechanical environment (compression, tension) that cells experience when assessing, adapting and rearranging their environment could be measured in real time. The use of gold nanoparticles for single particle tracking of bimolecular events in real time is also a topic of intense interest.[279–283]

Another modality in scattering-based imaging is optical coherence tomography (OCT). OCT uses a short coherence light source to provide optical cross-sectional imaging of tissues.[284,285] It can produce three dimensional images of a subject with micrometre resolution. Halas and coworkers demonstrated that systematically injected gold nanoshells strongly enhanced OCT image contrast from tumor tissues (Fig. 15).[286] Functionalized gold nanospheres, nanorods and nanocages have also been used for OCT imaging of cancer.[287–290]

Gold nanostructures can exhibit enhanced fluorescence properties, with quantum yields up to 0.001, which is weak in an absolute sense but still millions of times stronger than that of the bulk metal.[291,292] El-Sayed and coworkers have conducted experimental and computational studies on the fluorescence properties of gold nanorods and have found that the rods have emission 6–7 times stronger than that of bulk gold due to resonant enhancement of fluorescence emission by the longitudinal LSPR of the rods.[293,294] Quantum efficiency was found to increase with increasing aspect ratio. As demonstrated by Li *et al.*, the emission of long gold nanorods (length *ca.* 230 nm) at 740 nm is over 10 times stronger than that of short gold nanorods (length 30 nm).[295]

Gold nanocrystals, especially gold nanorods, exhibit enhanced two-photon luminescence (TPL), making them detectable at single particle levels under femtosecond NIR laser excitation.[292,296–299] In comparison to confocal fluorescence microscopy, TPL has the advantages of higher spatial resolution and reduced background signal;[300] however, deleterious photothermal effect can be induced due to plasmon excitation by continuous scanning with high intensity pulsed laser light. Nonetheless, TPL has been recently used for cancer imaging *in vitro* and *in vivo.* Durr *et al.* demonstrated the use of gold nanorods for

Author Manuscript Author Manuscript Author Manuscript Author Manuscript

TPL imaging of cancer cells embedded in collagen matrices with 75 μm spatial resolution.[301] The nanorod-enabled TPL intensity was 3 times stronger than that of two-photon autofluorescence. Tong *et al.* imaged nanoparticle absorption and uptake by cells *via* TPL of folate-conjugated gold nanorods (Fig. 16).[302] Single particle tracking using TPL was reported to study the mechanisms of cellular uptake of the targeted gold nanorods.[303] Cellular localization of the nanorods, could be clearly differentiated due to the high contrast associated with TPL imaging. For comparison, TPL imaging of an Au nanorod is 100 times stronger than the emission of single fluorescein isothiocyanate molecule.[304] Very recently, He *et al.* reported the novel detection of circulating tumor cells *in vivo* by using the TPL technique.[305] In this experiment, CTC-mimetic leukemia cells were injected into the blood stream of live mice, followed by injection of folate-conjugated gold nanorods to preferentially label the circulating cancer cells *in vivo*. TPL imaging with an intravital flow cytometer detected single cancer cells in the vasculature of the mouse ear. TPL was also used to study tumor and organ biodistribution of Au nano-shells[306–308] and systemic clearance and cellular level biodistribution of Au nanorods.[309] These latter studies underscore the importance of understanding the fate of these nanomaterials in living systems, and are a prerequisite for any experiments in which gold nanoparticles might be used in humans.

Photothermal (PT) and photoacoustic (PA) imaging are based on the use of laser-induced heating of materials, with the former relying on the direct detection of heat and latter on the detection of acoustic waves generated by the thermal expansion of air surrounding the materials. Gold nanocrystals are very promising contrast agents for PT and PA imaging due to their strong light absorption properties (extinction coefficients of ~10^9 M^{-1} cm^{-1}).[121] Because the optical absorption of a metal nanoparticle decreases as the third power of its diameter while scattering decreases as the six power of diameter, absorption prevails over scattering below a certain size. Thus, PT imaging is often best suited for small gold nanoparticles (down to 2 nm) while larger gold nanoparticles give stronger PA signals.[310–312] Compared to fluorescence-based approaches, PT imaging has the advantages of extended detection volume and temporal high stability of the photothermal signal. Gold nanoparticle-enhanced PT imaging techniques have been developed by Zharov and coworkers to image adherent cancer cells, as well as those circulating systemically.[311,313,314] Using gold-coated carbon nanotubes in combination with *in vivo* PT flow cytometry, these researchers imaged circulating stem cells[315] and lymphatic vessels *in vivo*.[316] Using the same laser sources, PT imaging can also be incorporated with PT therapy (*vide infra*) to monitor selective photothermolysis and to study the resulting pathophysiology.[317,318]

Compared to PT imaging, PA imaging is much more common in biomedicine.[319] This is because the PA technique combines the high contrast of optical imaging with the deep tissue penetration of ultrasound imaging. NIR-absorbing gold nanoparticles are optimal for PA imaging as tissue-penetrative NIR light is generally used for imaging deeper tissue in live animals. Widespread applications have been shown in recent years. One of these key areas is in tumor imaging. For example, Agarwal *et al.* used PT imaging to detect prostate cancer by using anti-HER2 conjugated gold nanorods.[320] This technique was also used by Li *et al.* to perform multiplexed imaging of different cancer cell receptors using Au nanorods of varying

Author Manuscript Author Manuscript Author Manuscript Author Manuscript

aspect ratio and with varying targeting molecules.[321] Zharov and coworkers have developed PT flow cytometry to image and detect circulating tumor cells *in vivo*.[315,322–324]

Gold nanoparticles have also shown great promise in PT imaging of lymphatic and blood vessels. In one report, 40 nm gold nanocages, stabilized with poly(ethylene) glycol (PEG), were intravenously injected into mouse animals and allowed to circulate. PA images acquired within 2 h after nanocage injection showed with great clarity and detail that the particles were present in the vasculature of the brain, allowing imaging of blood vessels as small as 100 μm which were not visible in the absence of contrast agents (Fig. 17).[325] Similarly, gold nanostars were reported to greatly enhance PA imaging contrast of the rat lymphatic system.[326] Other applications include detection of macrophages in atherosclerotic plaques,[327] imaging of early-stage inflammatory response,[328] and monitoring of antirheumatic drug delivery.[329]

Another imaging modality in which gold nanocrystals contrast agents excel is differential interference contrast (DIC) microscopy. DIC imaging is a widely-available approach to optical imaging which uses phase interference to produce high contrast image with a gray background. The method gives higher lateral resolution but shallower depth of field than dark field microscopy.[330] Many commercial fluorescence microscopes can be equipped for dark-field and DIC imaging. Fang and coworkers have conducted systematic studies on the behavior of gold nanorods in various biological environments,[331] studying behavior such as the dynamic rotational motion nanorods in live cells,[332] wavelength-dependent contrast properties,[333] and the applications of gold nanoparticle contrast agents in molecular multiplexed biomarker detection.[334]

In contrast to the above imaging modalities, the use of gold nanoparticles in X-ray computed tomography (CT), a standard medical imaging technique, is based purely on the atomic weight of gold relative to atoms present in biological tissues. Compared with clinical iodine CT contrast agents, gold nanorods have exhibited two-fold higher contrast in CT imaging of tumors.[123] Conventionally, CT is not an imaging technique that is capable of targeting molecular species; however, by conjugating gold nanoparticles with cancer-specific antibodies and other targeting ligands, Kopelman and coworkers were able to successfully demonstrate molecular CT imaging of tumors in live animals.[335] Gold nanoparticles have also been used to increase CT contrast in *in vivo* vascular imaging applications.[336]

V. Gold nanocrystals in medicine

Gold-based therapeutics have a long history in medicine;[6] as Higby stated, “it was natural that the exceptional properties of gold and the mystique surrounding the metal should induce man to seek medicinal application for it”.[280,337] Auranofin, an organogold drug with brand name Ridura®, is commonly used as antirheumatic agent.[338] Recently, gold-based molecular compounds have been found to significantly restrict the viral reservoir in primate AIDS models.[339] Radioactive gold seeds, microns in diameter, have also been implanted in tumors for internal radiation therapy (*i.e.* brachytherapy).[340]

Author Manuscript Author Manuscript Author Manuscript Author Manuscript

A. Gold nanoparticles as intrinsic drug agents

Gold nanoparticles of very small diameters (less than 2 nm) are able to penetrate cells and cellular compartments (such as the nucleus) and can be extremely toxic.[341] For example, it was found that gold nanoparticles (spheres, 1.4 nm in diameter) induce necrosis and mitochondrial damage to various cell lines *via* oxidative stress mechanisms which may be associated with its well-known catalytic activity at these sizes.[23] This approach can be useful in clinical therapies if these highly toxic nanoparticles are selectively targeted to malignant or diseased tissues. Interestingly, larger sizes of gold nanoparticles with the same surface capping agent, were found to be non-toxic under the same dosing conditions.[24] The molecular mechanisms underlying the effectiveness of these tiny nanoparticles to kill cancer cells were correlated with their ability to induce cellular oxidative stress, mitochondrial damage, and DNA interactions.[23,342] Recently, it was found that gold nanoparticles (5 nm in diameter) exhibit anti-angiogenic properties (inhibit the tumorigentic growth of new blood vessels) in both *in vitro* and *in vivo* studies.[343] The mechanisms associated with these novel effects were determined to lie in the ability of gold nanoparticles to selectively bind heparin-binding glycoproteins on the surfaces of endothelial cells and subsequent inhibition of their activity.[343]

Because of their comparable size relative to biomolecules and proteins, gold nanoparticles can also interact with and modify physiological processes when specifically localized within cells and tissues. Recently, El-Sayed and coworkers have explored the differential effects of cytoplasmic and perinuclear targeting on the growth and division of malignant cells.[344] By directing the accumulation of these particles *via* peptide sequences recognized by cell surface integrins (cytoplasmic delivery) and nuclear importins (perinuclear delivery) they were able to demonstrate pro-apoptotic effects (*via* DNA double-strand breaks) which were selective for malignant cells. Others have explored similar strategies whereby gold nanoparticles were found to selectively exert anti-proliferative and radiosensitization effects. We refer interested readers to Dreaden *et al.* for a more thorough discussion.[6]

B. Gold nanoparticles in photothermal therapy

Photothermal therapy is a central application of gold nanoparticles in medicine.[6,119,123,345–352] The ability of gold nanoparticles to absorb light and convert it to heat is a fascinating property and has been employed to destroy cancer cells, bacteria, and viruses (*vide infra*). Thus, laser-exposed gold nanoparticles could act as therapeutic agents by themselves and without the need for co-conjugated drugs. Gold nanoparticles absorb light with high efficiency (extinction coefficient ~10^9 M^{-1} cm^{-1})[262] in the near-infrared (NIR) region of the electromagnetic spectrum, where attenuation by biological fluids and tissues is minimal.[346,353,354] NIR exposure allows for high-depth photothermal therapy in the tissues due to the higher penetration of light at these wavelengths.[355] The differences between gold nanoparticles and classical photosensitizers in photodynamic therapy is that the former generates heat while the latter generates singlet oxygen upon irradiation, both destroying unwanted cells in the process.[345] Gold nanoparticles have the advantage of higher absorption cross section, higher solubility, efficient absorption at longer wavelengths, and facile conjugation with targeting molecules and drugs. These properties make gold nanoparticles promising candidates for photothermal therapy of cancer and various

Author Manuscript Author Manuscript Author Manuscript Author Manuscript

pathogenic diseases. Examples of the use of gold nanoparticles in photothermal therapy are abundant in the literature and we focus here on gold nanoparticles that absorb in the NIR regime of spectrum: nanorods, gold–silica nanoshells, nanocages, hollow gold nanoshells, and gold–gold sulfide nanoparticles.

Gold/silica nanoshells, as developed by Halas and coworkers, were some of the first to be applied in photothermal therapy.[271,349,352,356] Nanoshells are nanostructures with a silica core and a gold thin shell with tunable optical extinction in the vis-NIR, depending on the diameter of both the core and the shell. Upon NIR irradiation, nanoshells have been used to ablate various cancerous cell lines *in vitro* and have been successful in the *in vivo* treatment of cancer in animal models.[271,357–364] Despite the seeming ease of nanoshell synthesis and their desirable plasmonic properties, these particles are relatively large in size (~130 nm) compared with other NIR-absorbing gold nanoparticles. This size may decrease their accumulation in some cancerous tissues or impede their elimination from the body. Nonetheless, AuraLase[s], a product based on gold nanoshells, is being commercialized by Nanospectra Biosciences and is currently in the process of FDA-sanctioned human pilot studies.

Gold nanorods, as developed by Murphy and El-Sayed, are promising candidates in plasmonic photothera-peutics.[270,345–347,354,365,366] Gold nanorods enjoy the advantages of being easy to prepare, with tunable plasmonic absorption, and are generally smaller in size than gold–silica nanoshells. Gold nanorods have been used to ablate tumors in mouse models of colon cancer and squamous cell carcinoma.[119,367–369] El-Sayed and coworkers first demonstrated the use of gold nanorods for *in vivo* photothermal cancer therapy in 2008, showing that the method was capable of inhibiting tumor growth and in many cases inducing complete tumor resorption following a single, 10 min laser exposure (Fig. 18).[6,119] More recently, Bhatia and coworkers further demonstrated the therapeutic efficiency of gold nanorods *in vivo*, where they found that a single intravenous dose of PEG-coated gold nanorods was capable of accumulating at tumor sites in mouse models and that X-ray computed tomography of these tissues could be used to guide subsequent photothermal therapy with high efficacy.[123]

Another class of NIR-absorbing gold nanoparticles is gold nanocages, which was developed by the Xia group.[60,348,350] Gold nanocages are cubic-shape hollow structures with tunable plasmonic optical properties that absorb light in the range of 400–1200 nm, depending on their wall thickness and edge length.[60] Success in using gold nanocages as photothermal therapeutic agents was demonstrated both *in vitro* and *in vivo*.[348,370,371] The advantage of nanocages over nanoshells is that they are smaller in size, generally less than 100 nm, which is important for considering tissue accumulation and elimination. For example, Xia and coworkers used targeted nanocages only 45 nm in edge length and with plasmonic absorption maxima at 810 nm, to ablate SK-BR-3 breast cancer cells in cell culture studies.[348]

There are other gold nanostructures that support LSPR in the NIR region of spectra and are useful for photothermal therapy such as gold–gold sulfide nanoparticles and hollow gold nanoshells. The former nanoparticles absorb in the NIR with a diameter less than 25 nm,

Author Manuscript Author Manuscript Author Manuscript Author Manuscript

which is a great advantage compared to spherical gold nanoparticles at this size (which exhibit one plasmonic peak at 520 nm). At this small diameter, these nanoparticles have high absorption cross-sections and higher absorption efficiencies than other similarly sized gold nanoparticles (98% absorption and 2% scattering of the total optical extinction).[372] Gold–gold sulfide nanoparticles, stabilized with PEG, have been shown to be effective photothermal therapeutics in both *in vitro* and *in vivo* models.[372,373] Similar to gold–gold sulfide nanoparticles, hollow gold nanoshells also absorb light in the NIR and enjoy small sizes compared to gold–silica nanoshells (30 nm in diameter with 8 nm shell thickness).[374] Lu *et al.* used hollow gold nanoshells functionalized with melanocyte-stimulating hormone analog for successful targeting and ablation of melanoma tumors *in vivo*.[375] Table 3 summarizes examples of *in vivo* studies aimed to use gold nanoparticles to treat cancer.

C. Gold nanoparticles as drug delivery vehicles

Nanoparticles have been used in exploratory drug delivery applications due to the following reasons: (i) the high surface area of nanoparticles provides sites for drug loading and enhances solubility and stability of loaded drugs, (ii) the ability to functionalize nanoparticles with targeting ligands to enhance therapeutic potency and decrease side effects, (iii) the advantage of multivalent interactions with cell surface receptors or other biomolecules, (iv) enhanced pharmacokinetics and tumor tissue accumulations compared to free drugs, and (v) biological selectivity which allows nanoscale drugs to preferentially accumulate at tumor sites due to their “leaky” blood vessels—the so-called enhanced permeability and retention (EPR) effect first described by Maeda in 1986.[97,98,100] Classical nanoparticles such as liposomes, polymeric nanoparticles, and protein-based nanoparticles enjoy physical properties such as size and high surface area, but lack the unique optical and photothermal properties of gold nanoparticles. Thus, gold nanoparticles are new agents that are being evaluated for biological sensing, drug delivery, and cancer treatment. In the next sub-sections, we will focus and expound upon the use of gold nanoparticles of different shape/size in drug delivery applications, each categorized by the previously discussed methods in which their active agent is loaded and/or released (Fig. 19).

1. Loading by partitioning (Fig. 19a–b)—As-prepared gold nanoparticles have a monolayer or bilayer of the capping agent, which serves as a stabilizing agent against aggregation or in some cases as a shape-directing agent during the growth of nanoparticles. For any of these reasons, the presence of this mono- or bilayer is advantageous to load drugs and subsequently release it at a diseased site. A mono or bi-layer of capping agents on the surface of gold nanoparticles can be considered as a thin layer of organic solvent, which is able to partition hydrophobic drugs from the surrounding medium.[376] For example, as-prepared gold nanorods have a surfactant (cetyltrimethylammonium bromide, CTAB) bilayer on their surfaces with a thickness of ~3 nm. Alkilany *et al.* showed that hydrophobic molecules such as 1-naphthol can partition efficiently into the CTAB bilayer with a ratio of 1.6 : 1 of naphthol to CTAB on the surface of gold nanorods.[376] Rotello and coworkers prepared spherical gold nanoparticles capped with a monolayer of a polymer that had both a hydrophobic region (interior) and a hydrophilic region (exterior).[132] The hydrophobic region of the nanoparticle polymeric shell was used to load hydrophobic drugs and the hydrophilic region to stabilize the nanoparticles in aqueous media. With this design, they have shown

Author Manuscript Author Manuscript Author Manuscript Author Manuscript

that these nanoparticles are able to partition hydrophobic drugs and release them when nanoparticles interact with cell membrane, without the need for the nanoparticles to enter the cell. The payload was stable in aqueous media and no significant release was observed until the nanoparticles interacted with cells. The authors concluded that the driving force for the observed release is re-partitioning of the drug from the polymer monolayer on the gold nanoparticles to hydrophobic domains in the cellular membrane.[132]

2. Loading by surface complexation (Fig. 19c–e)—The affinity of thiols and amines for gold surfaces is the origin of this loading approach.[142] Drugs with thiols or free amines (as part of their original structure or added without affecting the intrinsic activity of the drug) can anchor themselves to the surface of gold nanoparticles through the formation of Au–S or Au–N bonds.[6,118,119,142] This approach has been used to attach drugs,[115,116,377–379] DNA,[137,239,380,381] and siRNA to the surface of gold nanoparticles. The payload then can be released by various means such as diffusion to cellular membranes (in the case of weaker Au–N), thiol exchange (such as with intracellular glutathione), and external light which triggers release by the photothermal effect (either by breaking the Au–S bond and/or melting the nanoparticle itself).[381]

It is worth noting here that the nature of drug complexation to the gold surface affects its release profile. In the case of thiolated drugs, the Au–S bond can be strong enough to prevent drug release by simple diffusion.[115] Indeed, complexed therapeutics *via* Au–S bonds often need the help of external stimuli to be released such as thiol exchange or external light. In the case of amines, the Au–N bond is much weaker than Au–S and this can provide an advantage for more efficient drug release by diffusion. Burda and coworkers found very different delivery profiles for photodynamic therapy (PDT) cancer drugs when they are attached to the gold surface *via* Au–S or Au–N bonds.[115] In the former case, the attachment of drug molecules to the gold core was strong enough to retard the release where in the latter case, the release profiles were much better in both two-phase system (water : toluene) and inside cells.[115] The authors concluded that weak interactions between gold nanoparticles and drug molecules are favorable to covalent bonding to the gold surface.[115]

A clear advantage of this surface complexation as an approach to attach/release drugs to/from the surface of gold nanoparticle is the fact that loading/release events can be monitored by simple fluorescence microscopy (if the drug fluoresces) or by surface-enhanced Raman spectroscopy (SERS). When a fluorophore is attached to a nanoscale metallic surface, fluorescence quenching is observed due to energy and/or electron transfer from the donor (fluorophore) to the acceptor (gold core).[382,383] This phenomena implies that drug loading and its kinetics can be monitored *via* changes in fluorescence intensity; the reverse scenario can be applied for monitoring drug release *via* increased fluorescence signal into solution/cells.[384] For example, Kim *et al.* employed this technique to monitor the loading of gold nanoparticles with different fluorescent dyes and drugs and monitor their release inside cells.[132] The loading of common polyaromatic drugs (with appreciable UV absorption) are also highly amenable gold nanoparticle-based drug delivery. Dreaden and El-Sayed synthesized a thiol-PEGylated derivative of the breast cancer treatment drug tamoxifen and studied the efficacy of these nanoconjugates in selectively killing breast cancer cells *via* recognition by membrane-estrogen receptor (Fig. 20).[6,118] The authors found that the toxicity of these

Author Manuscript Author Manuscript Author Manuscript Author Manuscript

particles was >10^4 fold greater than free tamoxifen due to accelerated intracellular delivery kinetics (greater than 2.7-fold per ligand molecule). This combined targeting selectivity and enhanced potency provides opportunities for co-targeting/delivery strategies, as well as adjunctive laser photothermal therapy.

3. Loading by attachment to capping agents (Fig. 19f)—Therapeutics can be attached to gold nanoparticles *via* complexation or coupling to terminal functional groups of the capping agents. In these cases, the gold surface is already passivated with various functional groups and the drug attachment proceeds to the outermost layer on top of the particles. For example, Wheate and coworkers employed terminal carboxylic acid moieties from their capping agent (HS–PEG–COOH) on gold nanoparticles to complex platinum anticancer agents and to prepare platinum-tethered gold nanoparticles to kill lung and colon cancer cells.[136] In another example, Mirkin and coworkers used terminal primary amine-functionalized ssDNA on gold nanospheres to couple carboxylic acid-containing prodrugs of platinum through the formation of amide bonds.[167] The Pt prodrug-gold nanoparticles were able to enter cancer cells and their platinum center was reduced from Pt(IV) to Pt(II) to release active cisplatin, a powerful anti-cancer drug. Rothrock and coworkers attached nitric oxide (NO) donor molecules to the terminal amines on gold nanoparticles to produce NO-releasing gold nanospheres for potential applications in vasodilation.[385,386] Rotello and coworkers attached another anticancer drug (5-fluorouracil) to gold nanoparticles with terminal carboxylic acids (from the capping agents) through a photosensitive *o*-nitrobenzyl linkage. Upon irradiation with UV light, drug release was observed due to the cleavage of the photosensitive linker.[139]

Here, we would like to highlight an important note regarding coupling therapeutics to the capping agents on the surface of gold nanoparticles: coupling reactions can often induce nanoparticle aggregation, especially if the coupled drugs are hydrophobic. For example, Zubarev and coworkers prepared gold nanospheres (diameter 2 nm) with a dense shell of paclitaxel (a chemotherapeutic drug) by modifying the paclitaxel with a flexible hexaethylene glycol linker and coupling the linker's carboxylic acid to phenol-terminated gold nanoparticles.[133] The content of the attached organic shells was 67% by weight. However, the presence of the organic shell of paclitaxel around the nanoparticles dramatically decreased the solubility of these nanoparticles in aqueous media.[133]

4. Loading by layer-by-layer assembly (Fig. 19g)—Usually, gold nanoparticles (as synthesized in water) are highly charged due to the presence of charged capping agents on their surfaces. With that in mind, charged drugs can be easily attached to the surfaces of complementary charged gold nanoparticles by electrostatic-conjugation or the related layer-by-layer (LbL) coating.[141,142] The best example for this loading approach is the attachment of nucleic acids (DNA or siRNA) to the surfaces of gold nanoparticles by charge complexation. DNA or siRNA molecules, considered as biological polyelectrolytes with high negative charge, can be assembled on cationic gold nanoparticles for gene delivery and gene silencing.[387–390] It is important to note here that LbL for complementary charged polymers creates a very strong interaction (often irreversible),[391] which may retard the payload release (*e.g.* DNA or siRNA). To overcome this problem, Guo *et al.* used a charge-

Author Manuscript Author Manuscript Author Manuscript Author Manuscript

reversal co-polymer that shifted zeta potential based on pH.[392] At neutral pH, the polymer exhibits net negative charge that enabled it to complex with cationic gold nanoparticles. At acidic pH (inside the endo/lysosomes) the particle exhibited a net positive charge, thus allowing dissociation from the surface of the cationic nanoparticles and releasing the attached DNA or RNA. Guo *et al.* demonstrated that the use of gold nanoparticles with such a charge-reversal polymer is superior to classical polyelectrolytes as gene delivery vehicles and results in higher gene transfection efficiency.[392] Another approach to release complexed DNA or siRNA is to use a biodegradable, charged, complementary polypeptide which interacts with the nucleic acids. For example, Lee *et al.* used the LbL technique to coat gold nanoparticles with multilayers of poly-L-lysine (4 layers) and siRNA (3 layers) without inducing nanoparticle aggregation. Poly-L-lysine has the advantage of being biodegradable (protease-susceptible) and thus allows for sustained release of the complexed siRNA and an extended gene-silencing effect.[393]

5. Loading inside the nanoparticles (into the interior, Fig. 21)—Due to the high total surface area and the presence of internal reservoirs to load therapeutics, hollow gold nanostructures such as gold nanocages and hollow gold nanoshells are excellent candidates for drug delivery applications.[394–396] Gold nanocages, developed by Xia and coworkers, are porous hollow gold nanostructures with internal reservoir and unique optical/photothermal properties which allow them to absorb/scatter light in the NIR region of the electromagnetic spectrum. Gold nanocages were used to develop a ‘smart’ controlled-release drug delivery system in which drug molecules were encapsulated in the hollow interior of the cubes and caged by a dense thermo-sensitive polymer at their exterior surface (the polymer shell preventing release of the drug in the absence of thermal stimuli).[395,397] Since gold nanocubes are excellent light NIR photon absorbers, they were able to release the payload by absorbing NIR light and converting it to heat which melted the thermo-sensitive polymer shell and exposed the pores in the walls of the cube and allowed the entrapped to drug release.[397] The ‘smart’ polymers were attached to the exterior surface by gold–thiol bonds and the interior of the cubes were loaded by simple inward diffusion of the drug from aqueous media (Fig. 21a).[397] The release profile could be controlled by the laser power density and irradiation time without melting the metallic cube or desorbing the polymeric shell. This example highlights the superiority of gold nanoparticles over “classical” nanoparticles such as polymeric nanoparticles when light-triggered release is desired. As previously discussed, the wavelengths at which gold nanoparticles absorb light can be tuned to the NIR, where biological components and tissue absorb/scatter minimal light; however, for non-metallic nanoparticles, UV light is typically used to cleave a photosensitive organic linker.[398] Alvarez-Lorenzo *et al.* recently reported another approach to entrap drugs within the interiors of gold nanocages (Fig. 21b). In a more recent report, Xia and coworkers loaded the interior of these particles with a mixture of a drug and a thermo-sensitive material (the thermo-sensitive-barrier is in the interior and not on the exterior of particles as in the previous case).[394] Upon stimuli (heating by either NIR irradiation or high intensity focused ultrasound), the thermo-sensitive material in the interior was shown to melt, thus allowing the diffusion out of their nanoscale carriers. In this case, the thermo-sensitive material was 1-tetradecanol, which has surfactant-like properties and was thus able to accommodate both hydrophilic and hydrophobic drugs.[394]

Author Manuscript Author Manuscript Author Manuscript Author Manuscript

Hollow gold nanoshells have similar properties to gold nanocages: optical extinction in the NIR, small size, and a hollow interior. However, these particles are not as porous as gold nanocages and thus drug loading steps typically precede the synthesis of the gold shell. For example, Jin and Gao loaded liposomes with fluorescent dyes followed by the formation of a thin shell of gold.[399] The prepared "gold nanocontainer" with encapsulated drug in the interior had tunable optical spectra in the Vis-NIR region.[399] Upon irradiation with light, the generated heat resulted in shell degradation and the payload was released. The advantage of these light-triggered gold nanoparticles over other candidates is that it is "leakage-free" in solution or in blood, minimizing systemic exposure to loaded (and potentially cytotoxic) therapeutics.[399] Rather than continuous and integrated gold nanoshells, Trautman *et al.* used liposomes stabilized by spherical gold nanoparticles.[400] The gold–liposome composite absorbed light in the Vis-NIR and degraded upon irradiation with the proper light (photothermal induced disintegration) and released its payload.[400]

D. Gold nanoparticles as stabilizing agent for other drug delivery vehicles

Besides the great potential for gold nanoparticles as drug delivery carriers, they have also been used to stabilize and enhance the efficiency of other drug delivery carriers such as liposomes and microcapsules. Liposomes are used extensively as drug carriers; however, their poor stability against fusion and non-desired release in blood plasma and/or other organs can limit their use.[401,402] Granick and coworkers studied the effect of nanoparticle adsorption to phospholipid liposomes and they provided solid evidence, using fluorescence and calorimetric tools, that nanoparticles can induce gelation at the site of liposome adsorption (the phase transition temperature is increased by tens of degrees at the site of nanoparticles adsorption).[403] With only 25% of the outer surface area of liposome being occupied with nanoparticles, the nanoparticle-modified liposomes were stable without leaking any of encapsulated payload for 50 days in solution.[402] Rotello and coworkers employed a clever approach to stabilize oil-in-water droplets (smaller than 100 nm) using gold nanoparticles. They prepared oil-in-water droplets with a net negative charge and assembled positively charged gold nanoparticles (2 nm in diameter) at the outer shell of the droplet *via* electrostatic interactions. The strong lateral repulsion forces induced by the nanoparticles at the droplet's surfaces were screened by further addition of a "bridging" protein (namely transferrin). Their strategy resulted in radial particle–lipid and lateral particle–protein interactions which greatly increased stability of the small sized lipid capsule.[395] Zhang and coworkers used gold nanoparticles (with terminal carboxylate functional groups) to stabilize cationic liposomes and to trigger their fusion by pH stimuli.[404] At neutral pH (~7), the carboxylate moieties were deprotonated and their electrostatic interaction with the cationic liposomes was maximal. In mild, acidic conditions (pH ≈ 4.5–5.5) such as that inside cellular endosomes and lysosomes,[405] a significant portion of the carboxylic acids were protonated, inducing dissociation of the particles from the liposome surface and triggering liposomal fusion and subsequent cargo release.[404] In another report, gold nanoparticle-stabilized liposomes were used to selectively release anti-bacterial drugs to sites of infection. Gold nanoparticles functionalized with chitosan were used to stabilize liposomes and prevent fusion events in solution;[406] however, when nanoparticle-stabilized liposomes were in proximity to bacteria, toxins from the bacteria induced pore formation in the liposomal structure, facilitating release of their payload. The authors demonstrated the

Author Manuscript Author Manuscript Author Manuscript Author Manuscript

feasibility of this approach by loading the liposomes with vancomycin, which was released completely in the presence of *Staphylococcus aureus* bacteria, inhibiting the growth of the bacteria.[406]

E. Gold nanoparticles in composite materials to trigger drug release (Fig. 22)

In this section we will discuss the use of gold nanoparticles as a component in composite materials for controlled drug delivery applications (*i.e.* gold nanoparticles are not the drug carrier). Here, gold nanoparticles were incorporated in various types of materials to fabricate gold-containing devices for drug delivery such as thermo-sensitive microcapsules, films, and hydrogels.[407–411] In a recent report, gold nanoparticles were used as local "nanoheaters" which, upon irradiation, absorb light and generate heat sufficient to alter the structure of the matrix and the polymer networking it and increasing its fluidity (when the generated temperature is higher than critical temperature values such as the lowest critical solution temperature (LCST) or the glass transition temperature (T_g) of the matrix). Usually, LCST or T_g for a selected polymer should be slightly higher than the body temperature to maintain matrix integrity until triggered by light irradiation. You *et al.* prepared polymeric microspheres from the biodegradable polymer (poly(lactideco-glycolide), PLGA) and incorporated an anti-cancer drug (paclitaxel) and hollow gold nanospheres (HGN; 35 nm diameter) into the microsphere matrix.[408] HGN particles were introduced to induce drug release from the matrix upon irradiation, owing to the excellent plasmonic light absorption and photothermal effect of HGN in the NIR region. In the absence of irradiation, no significant drug release was observed from the microsphere matrix;[408] however, upon irradiation, efficient cargo release was observed that was dependent on irradiation time/interval, laser power density, and the concentration of HGN present in the matrix.[408]

F. Targeting gold nanoparticles to diseased sites

The idea of targeted drug delivery is attractive since it implies minimal systemic exposure and thus decreased side effects; at the same time it implies high local concentration of therapeutics at the desired target sites for maximum efficacy.[412] There are two general types of targeting approaches for biomedical nanoparticles: (i) passive targeting and (ii) active targeting. Passive targeting takes advantage of the disordered vasculature characteristic of tumors, which allow for selective accumulation for nanoparticles based on the size (which cannot cross normal blood vessels with endothelial tight junctions).[413] This effect is also known as the EPR (enhanced permeability and retention) effect; however, passive targeting, alone, is not very effective due to the following reasons: (i) penetration of molecules into the tumor interstitium, in the case of solid tumors is limited to very short distances (a few cell diameters and can be worse for nanoparticle with low diffusivity),[414,415] (ii) passive targeting is dependent on the size of the nanoparticles and optimal size for EPR can vary from tumor to tumor.[98,416] The active targeting strategies augment passive targeting effects by decorating nanoparticles with recognition moieties which enhance their accumulation at tumor sites. Various recognition moieties have been used with gold nanoparticles including antibodies,[348,358,361,374,375] small peptides,[375,417,418] aptamers,[378,419,420] and small molecules.[6,118,302,421] The high surface area of gold nanoparticles allow for anchoring of a large number of targeting moieties to the surface, which enhances the binding avidity through multivalent epitope binding (similar to that exhibited by bivalent antibodies);[412]

Author Manuscript Author Manuscript Author Manuscript Author Manuscript

however, whether the presence of targeting ligands on the surfaces of gold nanoparticles enhances their tumor-specific accumulation is, to some, debatable. Nie and coworkers compared the tumor uptake of targeted and non-targeted gold nanorods in mice models.[173] The use of gold nanoparticles in such biodistribution studies is ideal since the content of gold can be analyzed with mass spectrometry with an extremely high limit of quantification (there is no endogenous background of gold ions in biological tissues). With this in mind, they found that there is only marginal difference in the total tumor uptake of gold nanorods between targeted and non-targeted particles; however, the investigators also found significant differences in the intra-tumoral cellular distribution of these nanoparticles which varied depending on their targeting ligand.[173] In contrast to these findings, Li and coworkers compared the tumor accumulation of targeted and non-targeted hollow gold nanospheres.[375] Using fluorescence imaging of fluorescein-conjugated nanoparticles, they found three times greater tumor accumulation of the targeted nanoparticles than untargeted (PEGylated) nanoparticles in the tumor sites.[375] Further, they found that intratumoral cellular distribution of the targeted particles is very different from that of the non-targeted nanoparticles; targeted nanoparticles were found throughout the tumor matrix (>200 microns away from blood vessels) while nontargeted particles stayed near the tumor vasculature.[375] Nanoparticle shape/size, targeting ligands, and analytical tools were different in the above two studies, a fact which may preclude direct comparison of their results. One general notion in the literature is that nanoparticle diffusion in solid tumor tissue is the rate-limiting step, and thus, the primary pathway for better intratumoral distribution is that the nanoparticles need to be uptaken by the tumor cells.[412,422]

G. Toxicity of gold nanoparticles

1. *In vitro* models: toxicity and cellular uptake—As with any pharmaceutical drug, therapeutic gold nanoparticles may have undesired side effects upon administration.[423] To understand and evaluate these effects, extensive *in vitro* and *in vivo* toxicological evaluations were performed on various gold nanoparticle types and cell/animal models.[341,424,425] The general conclusion from these studies is that the gold core is benign and biologically inert; however, this is not necessarily true when the gold core size decreases in size below 2 nm, where the surface of the gold nanoparticles shows unusual chemical reactivity.[341] For example, gold nanoparticles with a diameter of 1.4 nm (a 55 gold atom cluster) can act as an efficient chemical catalyst due to their high surface reactivity at this size,[426] which can be also the source of unwanted reactions/side effects in biological systems. For example, it has been shown that gold nanoparticles with a diameter of 1.4 nm exert significant toxicity to culture cells *via* induction of oxidative stress and mitochondrial damage.[23] Generally, gold nanoparticles for drug delivery and photothermal therapy applications have dimensions larger than 10 nm, which is sufficient to decrease its surface reactivity and thus make gold cores benign. This size (>6–8 nm) is also optimal to preclude renal excretion and consequently diminished circulatory half life.[427]

Most studies that have been carried out to evaluate the safety of gold nanoparticle solutions were conducted using *in vitro* models (cultured cells). Despite the importance of starting any toxicological screening using cell models, they do not provide results that can be extrapolated to conclude what the fate of these materials is *in vivo*; however, *in vitro* models

Author Manuscript Author Manuscript Author Manuscript Author Manuscript

are simpler, faster, cheaper, require less regulations, and provide mechanistic and molecular understanding on how nanoparticles enter and interact with cellular components.[428] Various analyses have been employed to assess the toxicological effects of gold nanoparticles on culture cells such as viability assays, reactive oxygen species (ROS) analysis, gene expression analysis, cell–substrate impedance and micromotility analysis (ECIS), and cellular morphology assays.[429–431] Most of these analyses are already applied to evaluate toxicity of small-molecule chemicals and pharmaceutical drugs; however, care should be taken when adapting these assays to evaluate toxicity of gold nanoparticles, which are excellent light absorbers in the visible region and thus can interfere with colorimetric, chemiluminescence-based, and fluorescence assays.[424,429]

For monitoring gold nanoparticle cellular uptake, powerful analytical tools have been used to provide both qualitative and quantitative measurements such as transmission electron microscopy (TEM),[341,429] scanning electron microscopy (SEM),[432] atomic force microscopy (AFM),[433,434] darkfield optical microscopy,[96,269] differential interference contrast (DIC) microscopy,[435,436] and photothermal heterodyne imaging.[437,438] Inductively-coupled plasma mass spectrometry (ICP-MS) has very low detection limits for gold (18 parts per trillion), permitting very rigorous quantification of gold in biological specimens, with the caveat that analyses require digestion and are thus, destructive.[67] TEM for fixed cells is considered the “gold standard” for visualizing nanoparticles in cellular compartments since it provides structural details with nanometre resolution. Moreover, gold nanoparticles are electron dense and can be visualized in TEM images without the need for staining. However, drawbacks of the TEM method includes the long processing time to prepare specimens for imaging, the need to prepare thin specimen samples (50–200 nm in thickness) and therefore many features in the cell can be missed upon sectioning (rods can appear as spheres or shorter rods). Moreover, TEM imaging does not provide *in situ* analysis/information on the uptake process. To this end, Peckys and de Jonge recently reported the use of liquid-SEM to visualize living cells with thickness up to 10 microns without the need to fix or section the cells.[432]

Despite the fact that the gold nanoparticle core is considered inert and non-toxic, gold nanoparticles solutions “as a whole” can induce toxicity. This toxicity could rise from any part rather than the core itself, such as the capping agents used to stabilize gold nanoparticles or its degradation products, leftover chemicals from the synthesis, and remnants from inadequate purification. For example, it has been shown that apparent toxicity of gold nanorod solutions at nanomolar concentrations is not due to the gold nanorod core, but is due to the presence of quaternary ammonium surfactant (CTAB, capping agent) free in the solution.[96,122,439,440] Replacing CTAB by a non-toxic capping agent or preventing CTAB desorption from the surface of gold nanorods to the solution prevented the acute toxicity of gold nanorod in cell culture.[96,341] It is therefore very important to determine the “purity” of gold nanoparticle formulations before conducting toxicological studies (*i.e.* one should determine the level of free surfactant or any other “toxic” species such as metal ions in the solution and try to minimize these levels by adequate purification). As a control experiment, the toxicity of the gold nanoparticle solution “as a whole” should also be compared with the same solution after removing the gold nanoparticles “supernatant” (Fig. 23a).[341] Comparing an original nanoparticle solution with its supernatant has led to the

Author Manuscript Author Manuscript Author Manuscript Author Manuscript

identification of molecular mechanisms for nanoparticle-associated cytotoxicity, resulting from the presence of free small molecules or metal ions in the solution.[96,341,441] This strategy is not confined to gold nanorods or nanoparticles; indeed it should be a general approach for any nanoparticle solution of different shape, size, core composition, and capping agents.[281]

Gold nanoparticle uptake by cultured cells is widely studied and quantified. It is generally agreed that cellular uptake of gold nanoparticles occurs as a function of size, shape, surface functionality/charge, aggregation state of nanoparticles, concentration of nanoparticles, the type of cell, incubation conditions, and type of culture media. In other words: there is no standard dose that is known to be safe, or known to be toxic. Chan and coworkers studied the cellular uptake of antibody-functionalized spherical gold nanoparticles with different sizes (2–100 nm).[442,443] They found that nanoparticles with diameter of 40–50 enter cells more efficiently than both smaller and larger in size (Fig. 24).[442] The explanation for this size-dependent uptake was that at this “proper” size (40–50 nm), antibody-functionalized nanoparticles have the maximum interaction with the receptors at the surface of the cell and thus enter *via* receptor-mediated endocytosis.[442] Besides its size, the shape of a nanoparticle also appears to affect its cellular interactions and uptake. Chan and coworkers compared the cellular uptake of gold nanorods (14×74 nm) with gold nanospheres (either 14 or 74 nm in diameter).[386] They found that cells take 500 and 375% fewer nanorods than 74 and 14 nm spheres, respectively (all particles have citrate as surface capping agent).[443] The surface chemistry and net charge of a gold nanoparticle also has a dramatic effect on its cellular uptake. Many reports claimed that cationic nanoparticles enter cells much more efficiently than anionic nanoparticles with the same size and shape;[390,422,439,441] however, the mechanism for this phenomenon is still debatable. The simple explanation is that the cell membrane is negatively charged and thus cationic nanoparticles interact more efficiently with it. This notion becomes less clear when one considers that nanoparticles in biological media will develop new surfaces and an adsorbed protein corona.[444–447] Moreover, there is experimental evidence that suggests that cationic nanoparticles are not “cationic” in biological medium which also contains negatively charged proteins that can exhibit electrostatic affinity for the gold surface.[96,448,449] For example, cationic gold nanorods (zeta potential +40 mV) become anionic upon mixing with cell growth media containing 10% bovine serum albumin (zeta potential −20 mV).[96] In an interesting recent study by Doorley *et al.*, two-color fluorescence microscopy evidence showed that serum albumin adsorbs to the surfaces of cationic gold nanoparticles in solution and that both bind to the surface of the cell as a single anionic complex;[448] however, the number, orientation, and denaturation state of adsorbed albumin molecules on the surfaces of gold nanoparticles can be very different for gold nanoparticles with different surface charge and thus, different albumin-mediated endocytotic pathways. Albumin has at least four types of surface receptors[450] that can bind and induce endocytosis; therefore albumin can act as an endocytic ligand for non-functionalized nanoparticles.[448] Another point we should mentione here is that even though the cell membrane has a net negative charge, it contains positively charged domains and non-charged domains. Experimentally it has been shown that charge distribution in cell membranes is not homogeneous; indeed, it is largely heterogeneous and contains domains that can bind cationic, anionic, or both macromolecules.[451]

Author Manuscript Author Manuscript Author Manuscript Author Manuscript

2. Remarks on *in vitro* studies to evaluate toxicity and uptake of gold nanoparticles—Before we leave the discussion on the *in vitro* evaluation of gold nanoparticles, we would like to highlight some critical and important recent findings, which should improve the quality of understanding cell–gold nanoparticle interactions and eliminate a large volume of experimental artifacts. For example, how many gold nanoparticles are uptaken by cultured cells? A common tool to answer this question is to expose known number of cells to known number of particles followed by proper and thorough washing. The cells can then be attached and digested using strong acid mixture followed by analysis using ICP-MS. However, the results from ICP-MS may not reflect what entered the cells since ICP-MS is a destructive tool and cannot distinguish between nanoparticles "on" the cell membrane or "in" the cells. Xia and coworkers addressed this point and they provided a simple and effective solution to distinguish both types of nanoparticles (adsorbed *versus* entered, Fig. 23b). They used a mild etching mixture (I_2/KI) to selectively solvate gold nanoparticles on the surface of cells without inducing any observed toxicity to the exposed cells or etching of intracellularly localized nanoparticles.[452]

Another point which should be taken into consideration while carrying out cellular uptake experiments is that nanoparticles could aggregate during the incubation time in the cell media, and thus have intrinsic higher sedimentation rates which can affect the rate and extent of nanoparticle uptake. This is important to consider when comparing cellular uptake of nanoparticles with different physical properties such as size, shape, and surface chemistry. This differential uptake could be due to different aggregation states and thus sedimentation rates and not due to size or charge (Fig. 23c). Xia and coworkers have shown experimentally that the sedimentation rate of nanoparticles in cell culture is a crucial factor that should be taken in consideration when assessing the cellular uptake of gold nanoparticles.[453] Wittmaack studied the sedimentation of nanoparticles and concluded that aggregation of nanoparticles in culture media could enhance nanoparticle–cellular interaction by a factor of 1000, resulting in excessive delivery of nanoparticles to the cells and could result in misinterpreted evaluation of nanoparticle uptake and toxicity.[454]

3. *In vivo* models: toxicity and pharmacokinetics—In order to apply gold nanoparticles as phototherapeutic, drug carrier, and diagnostic imaging platforms, their side effects and pharmacokinetic parameters (absorption, distribution, metabolism, and elimination, ADME) should be evaluated. Compared to *in vitro* toxicological studies, few studies focus on evaluating the toxicity of nanoparticles *in vivo* per se; most data have been collected as part of larger studies with the main focus on demonstrating the medical utility of nanoparticles such as in treating cancers by the photothermal effect.

The main route of administration for gold nanoparticles in research papers is the systemic route, mainly intravenous (Table 3); thus we expect major organs to be exposed to gold nanoparticles, a fact which emphasizes the need for detailed information on the toxicity and partitioning of nanoparticles to different organs. Toxicity of nanoparticles *in vivo* could arise from direct toxicity to cells/tissue (necrotic or apoptotic mechanisms), inducing oxidative stress, or the provocation of local/systematic inflammatory or immunological responses.[455–458] Most studies have suggested that safety in the intravenous administration of gold nanoparticles can be based on general assessments such as animal average weight, loss of

Author Manuscript Author Manuscript Author Manuscript Author Manuscript

appetite, mortality rates, or other gross visual observations;[425] however, other studies show different results and indicate toxicity from intravenous injection of gold nanoparticles. For example, Chen *et al.* studied the toxicity of citrate-capped gold nanoparticles in mouse models as a function of particle size (3–100 nm) and they found that smallest sizes (3, 5 nm) and largest sizes (50 and 100 nm) were not toxic at their doses, while medium sizes (8, 12, 17, 37 nm) induced severe sickness, loss of weight, change in fur color, and most importantly shorter life span.[459] Using pathological examinations, the observed systemic toxicity for these nanoparticles was linked to injury of the liver, spleen, and lungs. The molecular mechanism for the observed toxicity was not elucidated and a clear explanation why only medium sizes are toxic was not provided. In another study, Lasagna-Reeves *et al.* showed that intraperitoneal injections of gold nanoparticles (13 nm, PEG-capped) for 8 days (daily) did not induce any acute side effects. In both studies the surface chemistry and doses of the nanoparticles were different, which makes it difficult to perform a direct comparison of their outcomes. This is the general trend for almost all reported studies, where the doses of gold nanoparticles are widely scattered and varied by a factor of five orders (from 0.01 to 1000 mg gold per kg animal weight).[425] It is very clear that we need to narrow the dosage range and define proven therapeutic-doses to be used for toxicological evaluation.

Typical biodistribution studies start with gold nanoparticles administration, followed by analyzing the content of gold in blood and organs of interest as a function of time (post injection). The content of gold can be analyzed using ICP-MS (as we describe it for quantification of gold in cell culture), with a high limit of quantification (1 ng gold per kg organ).[331] Other analytical methods have also been used to quantify gold content in blood or organs including neutron activation analysis (NAA)[460] and the use of radiolabeled tracers.[374] To visualize/study particles in tissues, TEM, SEM, EDX (energy dispersive X-ray spectroscopy), and XAS (X-ray absorption spectroscopy) are often employed.[425]

Most intravenously injected gold nanoparticles accumulate in the liver and spleen.[425,427] This was explained by the adsorption of blood protein to the nanoparticles followed by opsonization and uptake by the reticuloendothelial system (RES), the part of the immune system that recognizes, captures, filters, and sequesters “foreign” antigens in the spleen and liver. However, the distribution of nanoparticles to different organs occurs as a function of nanoparticle size, shape, and surface chemistry. The presence of anti-fouling molecules such as PEG or antibodies can greatly change the pharmacokinetic parameters of a gold nanoparticle conjugate.[461] For example, Niidome and coworkers showed that displacing CTAB on gold nanorods with PEG molecules increase their circulation half time (5% of CTAB-capped nanorods found in blood after 30 minutes *versus* 54% for PEG-capped gold nanorods).[122] This effect was linked to the ability of PEG to prevent/reduce the non-specific adsorption of plasma proteins onto the surfaces of gold nanorods, thus decreasing the extent of nanoparticle opsonization and uptake by the RES.[122] In a related report, the density of PEG on the surfaces of gold nanorods was shown to also affect their pharmacokinetic profiles in mice, with a higher PEG grafting density resulting in more gold nanoparticles in the tumor and less in the liver.[462] The size effect of gold nanoparticles on their distribution profile is evident by several reports. De Jong *et al.* studied the tissue biodistribution of gold nanoparticles with different sizes (10–250 nm).[463] They found that the smallest size (10 nm) exhibited a wide biodistribution profile and were found in the liver, spleen, testis, lung,

Author Manuscript Author Manuscript Author Manuscript Author Manuscript

blood, and brain after 24 hours post injection. In contrast, larger particles were found only in spleen and kidney (analysis by ICP-MS).[463] In another study by Cho *et al.*, using pegylated nanoparticles with different sizes (4, 13, 100 nm) it has been shown that circulation half lives decreases with increasing the particle size.[449]

The clearance of nanoparticles from tissues after administration is a topic of paramount importance to the evaluation of local inflammation and toxicity (and FDA approval). For small-molecule organic drugs, there are various routes of clearance from the body such as the kidneys (renal/urinary excretion), the hepatobiliary system, the skin and the lungs. However, the case for nanoparticles is not the same since they are larger in size and in many cases cannot cross filtration barriers such as the glomeruli in kidneys (6–8 nm hydrodynamic diameter). For example, biological molecules and proteins with high molecular weight and effective diameter (>70 kDa such as albumin) are excluded from being filtered out of the kidney glomeruli and into the urine.[464] It has been proven experimentally that nanoparticles should have a hydrodynamic diameter less than 5.5 nm to be excreted filtrated and excreted *via* the kidney route.[465] This cutoff value can vary slightly depending on the surface charge with highly cationic nanoparticles less than 8 nm also exhibiting efficient renal excretion.[427] This fact explains why small gold nanoparticles (1.4 nm) were shown to be excreted in the urine (9% of injected dose), while larger nanoparticles (18 nm) accumulated in liver and spleen, and were hardly found in the urine.[466] It is important also to consider the hydrodynamic diameter of gold nanoparticles (measured by light scattering techniques) and not only their core size when predicting clearance properties of nanoparticles. Cho *et al.* noticed that PEG-capped gold nanoparticles with a core diameter of 4 nm and hydrodynamic diameter of 14.8 nm are hardly excreted in the urine and showed similar excretion profile to 13 and 100 nm nanoparticles.[449] Recently, Zing and coworkers found that small core size (2 nm) does not guarantee effective renal clearance due to the ability of these nanoparticles to form larger aggregates in blood.[467] They compared citrate, cystine, and glutathione as capping agents for these small gold nanoparticles and found that the latter is the best for nanoparticle stabilization in blood and thus efficient renal clearance (>50% of injected dose cleared in 24 hours and 65% in 72 hours). The enhanced renal clearance of glutathione-capped gold nanoparticles was linked to its low binding to serum proteins and zwitterionic nature in the blood.[467] Despite the success of using glutathione as a capping agent to enhance renal clearance of small gold nanoparticles, the clearance efficiency was decreased exponentially as a function of hydrodynamic diameter (for 2, 6, and 13 nm nanoparticles; the urine content of gold as the percentage of injected dose was 50, 4, 0.5 after 24 hours).[467] Since most gold nanoparticles that might be used *in vivo* have dimensions larger than 10 nm, more work should be focused in developing new approaches to enhance the total clearance of gold nanoparticles. For example, NIR-absorbing gold nanoparticles can be prepared from assembled small gold nanoparticles on liposomes[400] or within a polymer[468] matrix and upon irradiation the complex can be disintegrated and the small gold nanoparticles cleared (Fig. 21c and 25). However, experimental evaluation for the systemic clearance of these NIR-absorbing plasmonic composites is not yet available in the literature.

4. Environmental and ecological impacts—With the wide production of nanoparticles, potential negative impacts on environment and ecological systems should be

Author Manuscript Author Manuscript Author Manuscript Author Manuscript

carefully evaluated.[469] For gold nanoparticles, little is known about their environmental impact and how they behave in different ecosystems; however, gold nanoparticles are excellent candidates as probes in such studies since they are resistant to dissolution and can be easily detected and quantified. Ferry *et al.* studied the partitioning and distribution of CTAB-capped gold nanorods in model estuarine system containing sediments, microbial biofilms, primary producers (plants), filter feeders (such as clams), grazers (such as snails), and omnivores (fish).[470] Gold nanorods partitioned efficiently into filter feeders (the clam *Mercenaria mercenaria*, which is important shellfish for human consumption), with 5% uptake of total gold nanorods while the filter feeder accounted for less than 0.01% of the model ecosystem total mass. Biofilms, however, (which offer a route into the food-web through being consumed by detritovores) were the main route of entry into the food web.[470] Using another ecosystem model (soil and earthworms), Bertsch and coworkers provided experimental evidences of the ability of citrate-capped gold nanospheres in spiked soil to be uptaken by earthworms, an important ecological receptor species.[471] In a related study, the same group reported the uptake of gold nanoparticles (5, 10, and 15 nm) by plants (primary producers) and their transfer to hornworms (primary consumers) in a size-dependent manner. These studies indicate that gold nanoparticles are bioavailable in different ecosystems and can be transferred from one organism to another in food webs, highlighting a possible mechanism of unintended nanparticles exposure to humans.

VI. Outlook and conclusions

As this review has clearly shown, there is a great deal of current excitement and optimism about the use of gold nanoparticles for a diverse array of biomedical applications. There is an equally clear need to perform careful studies of their longer-term impacts on human and environmental health. We are pleased to note that in the US, the National Cancer Institute has established the Nanotechnology Characterization Laboratory (NCL), which aims to provide an “assay cascade” of nanomaterial characterization, from basic physical properties to *in vivo* animal trials.[472] We might expect that as more and more nanoparticle systems show promise at the research level, more of these materials will be evaluated for clinical impact by the NCL or other groups. One stumbling block already apparent for clinical trials is the issue of scale-up: nanoparticles must be available in multigram quantities, with reproducible batches, for *in vivo* work. A great amount of work is also needed in minimizing the immune system’s response to circulating gold nanoparticles, in order to increase their targeting selectivity; strategies to facilitate the efficient clearance of these particles is also a significant challenge. With the transition of gold nanoparticles from the benchtop to the clinic, we expect that researchers will also learn a great deal about the fundamental interactions between nanoscale materials and biological systems. New insights about fundamental biological functions and properties will also be gleaned from their response to exposure with these exotic nanoscale materials. This, itself, will no doubt result in a significant payoff for the fields of biology *and* nanomedicine. We look forward with great optimism to this new golden age in medicine.

Author Manuscript Author Manuscript Author Manuscript Author Manuscript

Acknowledgments

MAE and ECD acknowledge generous support from the U.S. National Science Foundation Department of Materials Research (Award # 0906822) and the U.S. National Institutes of Health (1U01CA151802-01). X.H. would like to acknowledge support from the University of Memphis Faculty Research Grant, the Spectroscopy Society of Pittsburgh Starter Grant, and the Oak Ridge Associated Universities' Ralph E. Powe Junior Faculty Enhancement Award. CJM acknowledges the support of the U. S. National Science Foundation, the U. S. National Institutes of Health, the Keck Foundation, the USC NanoCenter, and former lab members for all of their hard work.

Biographies

Erik C. Dreaden received his BS in chemistry from the University of Georgia in 2006 working with John L. Stickney. He is currently Center for Drug Design, Development, and Delivery Fellow and a PhD candidate in the School of Chemistry and Biochemistry at Georgia Institute of Technology, studying with Mostafa A. El-Sayed. His research interests include the synthesis, fundamental properties, and oncologic applications of nanoscale materials. In the past, he has conducted research investigating in vivo applications of laser photothermal therapy, surface-enhanced Raman scattering, endocrine-targeted nanoconjugates, experimental and computational plasmonics, plasmon-enhanced photovoltaics, and ultrafast laser spectroscopy.

Alaaldin M. Alkilany received a BSc degree in Pharmacy from Jordan University of Science & Technology, Jordan, in 2000. He worked at Hikma Pharmaceutical-Jordan in the R & D department to develop pharmaceutical formulation and drug delivery systems. In 2010, he was awarded a PhD from the University of Illinois for his work on the synthesis and biomedical applications of gold nanoparticles under the supervision of Professor Catherine Murphy. He is currently a postdoctoral research fellow at Georgia Health Sciences University working in Professor R. William Caldwell's lab to develop engineered gold nanoparticles to target the cardiovascular system.

Author Manuscript Author Manuscript Author Manuscript Author Manuscript

Xiaohua Huang received her BSc from Jilin University in 1996, MSc from Peking University in 2001, and PhD from Georgia Institute of Technology in 2006 with Mostafa A. El-Sayed. After being a postdoctoral fellow at Georgia Institute of Technology in Mostafa A. El-Sayed's lab and Emory University in Shuming Nie's lab, she joined the faculty at the University of Memphis in 2010. Her current research interests are bioconjugated nanoparticles for cancer detection and treatment.

Catherine J. Murphy is the Peter C. and Gretchen Miller Markunas Professor of Chemistry at the University of Illinois at Urbana-Champaign. She received two BS degrees, one in chemistry and one in biochemistry, from UIUC in 1986. She earned her PhD in chemistry (1990) from Wisconsin under the direction of A. B. Ellis. After a postdoctoral stint at Caltech with J. K. Barton, she joined the faculty at the University of South Carolina in 1993. She moved to her present position in 2009. She has been a Senior Editor for the Journal of Physical Chemistry since 2006.

Mostafa A. El-Sayed received his BSc from Ain Shams University in Egypt and his PhD from Florida State with Michael Kasha. After a research fellowship at Harvard and Cal Tech, he joined the faculty at UCLA in 1961 and Georgia Tech in 1994. He is an elected member of the US National Academy of Sciences, an elected fellow of the American Academy of Arts and Sciences, former editor-in-chief of the Journal of Physical Chemistry, and recipient of the US National Medal of Science. His current research includes the optical and electronic properties of nanomaterials and their applications in sensing, nanocatalysis, and nanomedicine.

Author Manuscript Author Manuscript Author Manuscript Author Manuscript

Notes and references

1. Greenwood, NN., Earnshaw, A. Chemistry of the Elements. 2nd. Butterworth-Heinemann; Burlington, MA: 1997.
2. Chen MS, Goodman DW. Science. 2004; 306:252–255. [PubMed: 15331772]
3. Valden M, Lai X, Goodman DW. Science. 1998; 281:1647–1650. [PubMed: 9733505]
4. Green IX, Tang W, Neurock M, Yates JT. Science. 2011; 333:736–739. [PubMed: 21817048]
5. Shaw CF. Chem Rev. 1999; 99:2589–2600. [PubMed: 11749494]
6. Dreaden EC, Mackey MA, Huang X, Kang B, El-Sayed MA. Chem Soc Rev. 2011; 40:3391–3404. [PubMed: 21629885]
7. West JL, Halas NJ. Ann Rev Biomed Eng. 2003; 5:285–292. [PubMed: 14527314]
8. Skrabalak SE, Au L, Li X, Xia Y. Nat Protoc. 2007; 2:2182–2190. [PubMed: 17853874]
9. Faraday M. Philos Trans R Soc London. 1857; 147:145–181.
10. Maxwell JC. Philos Trans R Soc London. 1865; 155:459–512.
11. Data obtained *via* Thompson Reuters-Web of Science topic search for publications in nanomedicine, gold nanomedicine, and gold nanotechnology 11 August, 2011: “ts = (nano*) and ts = (health* or medic* or therap* or diseas* or cancer*)”, “ts = (nano*) and ts = (health* or medic* or therap* or diseas* or cancer*) and “ts = (gold* or Au)”, or “ts = (nano*) and ts = (gold* or Au)”, respectively.
12. Mie G. Ann Phys. 1908; 25:377–445.
13. Knoll M, Ruska E. Z Phys. 1932; 78:318–339.
14. Turkevich J, Stevenson PC, Hillier J. Discuss Faraday Soc. 1951; 11:55–75.
15. Frens G. Nature. 1973; 241:20–22.
16. LaMer VK, Dinegar RH. J Am Chem Soc. 1950; 72:4847–4854.
17. Pong BK, Elim HI, Chong JX, Ji W, Trout BL, Lee JY. J Phys Chem C. 2007; 111:6281–6287.
18. Wang H, Halas NJ. Adv Mater. 2008; 20:820–825.
19. Schmid G, Pfeil R, Boese R, Bandermann F, Meyer S, Calis GHM, van der Velden JWA. Chem Ber. 1981; 114:3634–3642.
20. Weare WW, Reed SM, Warner MG, Hutchison JE. J Am Chem Soc. 2000; 122:12890–12891.
21. Brust M, Walker M, Bethell D, Schiffrin DJ, Whyman R. Chem Commun. 1994:801–802.
22. Shimizu T, Teranishi T, Hasegawa S, Miyake M. J Phys Chem B. 2003; 107:2719–2724.
23. Pan Y, Leifert A, Ruau D, Neuss S, Bornemann J, Schmid G, Brandau W, Simon U, Jahnen-Dechent W. Small. 2009; 5:2067–2076. [PubMed: 19642089]
24. Pan Y, Neuss S, Leifert A, Fischler M, Wen F, Simon U, Schmid G, Brandau W, Jahnen-Dechent W. Small. 2007; 3:1941–1949. [PubMed: 17963284]
25. Faulk WP, Taylor GM. Immunochemistry. 1971; 8:1081–1083. [PubMed: 4110101]
26. Holgate CS, Jackson P, Cowen PN, Bird CC. J Histochem Cytochem. 1983; 31:938–944. [PubMed: 6189883]
27. Hainfeld JF, Slatkin DN, Focella TM, Smilowitz HM. Br J Radiol. 2006; 79:248–253. [PubMed: 16498039]
28. Hainfeld JF, Dilmanian FA, Zhong Z, Slatkin DN, Kalef-Ezra JA, Smilowitz HM. Phys Med Biol. 2010; 55:3045. [PubMed: 20463371]
29. Masuda H, Tanaka H, Baba N. Chem Lett. 1990:621–622.
30. Martin CR. Adv Mater. 1991; 3:457–459.
31. Sau TK, Murphy CJ. Langmuir. 2004; 20:6414–6420. [PubMed: 15248731]
32. Wang ZL, Mohamed MB, Link S, El-Sayed MA. Surf Sci. 1999; 440:L809–L814.
33. Carbó-Argibay E, Rodríguez-González B, Pacifico J, Pastoriza-Santos I, Pérez-Juste J, Liz-Marzán LM. Angew Chem, Int Ed. 2007; 46:8983–8987.
34. Oldenburg SJ, Averitt RD, Westcott SL, Halas NJ. Chem Phys Lett. 1998; 288:243–247.
35. Lu X, Au L, McLellan J, Li ZY, Marquez M, Xia Y. Nano Lett. 2007; 7:1764–1769. [PubMed: 17489641]

Author Manuscript Author Manuscript Author Manuscript Author Manuscript

36. Liang HP, Wan LJ, Bai CL, Jiang L. J Phys Chem B. 2005; 109:7795–7800. [PubMed: 16851906]
37. Kim F, Connor S, Song H, Kuykendall T, Yang P. Angew Chem, Int Ed. 2004; 43:3673–3677.
38. Niu W, Zheng S, Wang D, Liu X, Li H, Han S, Chen J, Tang Z, Xu G. J Am Chem Soc. 2009; 131:697–703. [PubMed: 19102696]
39. Zhang J, Langille MR, Personick ML, Zhang K, Li S, Mirkin CA. J Am Chem Soc. 2010; 132:14012–14014. [PubMed: 20853848]
40. Ming T, Feng W, Tang Q, Wang F, Sun L, Wang J, Yan C. J Am Chem Soc. 2009; 131:16350–16351. [PubMed: 19856912]
41. Personick ML, Langille MR, Zhang J, Harris N, Schatz GC, Mirkin CA. J Am Chem Soc. 2011; 133:6170–6173. [PubMed: 21452816]
42. Ma Y, Kuang Q, Jiang Z, Xie Z, Huang R, Zheng L. Angew Chem, Int Ed. 2008; 47:8901–8904.
43. Millstone JE, Park S, Shuford KL, Qin L, Schatz GC, Mirkin CA. J Am Chem Soc. 2005; 127:5312–5313. [PubMed: 15826156]
44. Hartland GV. Chem Rev. 2011; 111:3858–3887. [PubMed: 21434614]
45. Payne EK, Shuford KL, Park S, Schatz GC, Mirkin CA. J Phys Chem B. 2006; 110:2150–2154. [PubMed: 16471797]
46. Yu YY, Chang SS, Lee CL, Wang CRC. J Phys Chem B. 1997; 101:6661.
47. Gans R. Ann Phys. 1912; 342:881–900.
48. Jana NR, Gearheart L, Murphy CJ. Adv Mater. 2001; 13:1389.
49. Nikoobakht B, El-Sayed MA. Chem Mater. 2003; 15:1957.
50. Grzelczak M, Perez-Juste J, Mulvaney P, Liz-Marzan LM. Chem Soc Rev. 2008; 37:1783–1791. [PubMed: 18762828]
51. Johnson CJ, Dujardin E, Davis SA, Murphy CJ, Mann S. J Mater Chem. 2002; 12:1765–1770.
52. Nikoobakht B, El-Sayed MA. Langmuir. 2001; 17:6368–6374.
53. Murphy CJ, Thompson LB, Chernak DJ, Yang JA, Sivapalan ST, Boulos SP, Huang J, Alkilany AM, Sisco PN. Curr Opin Colloid Interface Sci. 2011; 16:128–134.
54. Khanal BP, Zubarev ER. J Am Chem Soc. 2008; 130:12634–12635. [PubMed: 18754620]
55. Aden AL, Kerker M. J Appl Phys. 1951; 22:1242–1246.
56. Stöber W, Fink A, Bohn E. J Colloid Interface Sci. 1968; 26:62–69.
57. Brinson BE, Lassiter JB, Levin CS, Bardhan R, Mirin N, Halas NJ. Langmuir. 2008; 24:14166–14171. [PubMed: 19360963]
58. Wang H, Brandl DW, Nordlander P, Halas NJ. Acc Chem Res. 2006; 40:53–62.
59. Chen J, McLellan JM, Siekkinen A, Xiong Y, Li ZY, Xia Y. J Am Chem Soc. 2006; 128:14776–14777. [PubMed: 17105266]
60. Skrabalak SE, Chen J, Sun Y, Lu X, Au L, Cobley CM, Xia Y. Acc Chem Res. 2008; 41:1587–1595. [PubMed: 18570442]
61. Liang Z, Susha A, Caruso F. Chem Mater. 2003; 15:3176–3183.
62. Sau TK, Murphy CJ. J Am Chem Soc. 2004; 126:8648–8649. [PubMed: 15250706]
63. Seo D, Park JC, Song H. J Am Chem Soc. 2006; 128:14863–14870. [PubMed: 17105296]
64. Seo D, Yoo CI, Park JC, Park SM, Ryu S, Song H. Angew Chem, Int Ed. 2008; 47:763–767.
65. Shankar SS, Rai A, Ankamwar B, Singh A, Ahmad A, Sastry M. Nat Mater. 2004; 3:482–488. [PubMed: 15208703]
66. Nicewarner-Peña SR, Freeman RG, Reiss BD, He L, Peña DJ, Walton ID, Cromer R, Keating CD, Natan MJ. Science. 2001; 294:137–141. [PubMed: 11588257]
67. Qin L, Park S, Huang L, Mirkin CA. Science. 2005; 309:113–115. [PubMed: 15994551]
68. Hao F, Nehl CL, Hafner JH, Nordlander P. Nano Lett. 2007; 7:729–732. [PubMed: 17279802]
69. Nehl CL, Liao H, Hafner JH. Nano Lett. 2006; 6:683–688. [PubMed: 16608264]
70. Guerrero-Martínez A, Barbosa S, Pastoriza-Santos I, Liz-Marzán LM. Curr Opin Colloid Interface Sci. 2011; 16:118–127.

Author Manuscript Author Manuscript Author Manuscript Author Manuscript

71. Barbosa S, Agrawal A, Rodríguez-Lorenzo L, Pastoriza-Santos I, Alvarez-Puebla R n A, Kornowski A, Weller H, Liz-Marzán LM. Langmuir. 2010; 26:14943–14950. [PubMed: 20804155]
72. Rodriguez-Lorenzo L, Krpetic Z, Barbosa S, Alvarez-Puebla RA, Liz-Marzan LM, Prior IA, Brust M. Integr Biol. 2011; 3:922–926.
73. Khoury CG, Vo-Dinh T. J Phys Chem C. 2008; 112:18849–18859.
74. Rodríguez-Lorenzo L, Álvarez-Puebla RnA, G a de Abajo FJ, Liz-Marzán LM. J Phys Chem C. 2009; 114:7336–7340.
75. Hrelescu C, Sau TK, Rogach AL, Jäckel F, Laurent G, Douillard L, Charra F. Nano Lett. 2011; 11:402–407. [PubMed: 21244014]
76. Kumar, P Senthil, Pastoriza-Santos, I., Rodríguez-González, B., García deAbajo, F Javier, Liz-Marzán, LM. Nanotechnology. 2008; 19:015606. [PubMed: 21730541]
77. Hulteen JC, Van Duyne RP. J Vac Sci Technol, A. 1995; 13:1553–1558.
78. Huang W, Qian W, El-Sayed MA. J Phys Chem B. 2005; 109:18881–18888. [PubMed: 16853430]
79. Fromm DP, Sundaramurthy A, Schuck PJ, Kino G, Moerner WE. Nano Lett. 2004; 4:957–961.
80. Dreaden EC, Near RD, Abdallah T, Talaat MH, El-Sayed MA. Appl Phys Lett. 2011; 98:183115.
81. Xu Q, Rioux RM, Dickey MD, Whitesides GM. Acc Chem Res. 2008; 41:1566–1577. [PubMed: 18646870]
82. Zhang H, Mirkin CA. Chem Mater. 2004; 16:1480–1484.
83. Kim P, Epstein AK, Khan M, Zarzar LD, Lipomi DJ, Whitesides GM, Aizenberg J. Nano Lett. 2011 ASAP.
84. Lu Y, Liu GL, Kim J, Mejia YX, Lee LP. Nano Lett. 2005; 5:119–124. [PubMed: 15792424]
85. Lee J, Hasan W, Stender CL, Odom TW. Acc Chem Res. 2008; 41:1762–1771. [PubMed: 18803410]
86. Hasan W, Lee J, Henzie J, Odom TW. J Phys Chem C. 2007; 111:17176–17179.
87. Zhang H, Li Z, Mirkin CA. Adv Mater. 2002; 14:1472–1474.
88. Liu GL, Lu Y, Kim J, Doll JC, Lee LP. Adv Mater. 2005; 17:2683–2688.
89. Henzie J, Kwak ES, Odom TW. Nano Lett. 2005; 5:1199–1202. [PubMed: 16178210]
90. Shuford KL, Lee J, Odom TW, Schatz GC. J Phys Chem C. 2008; 112:6662–6666.
91. Sweeney CM, Stender CL, Nehl CL, Hasan W, Shuford KL, Odom TW. Small. 2011; 7:2032–2036. [PubMed: 21656907]
92. Luk'yanchuk B, Zheludev NI, Maier SA, Halas NJ, Nordlander P, Giessen H, Chong CT. Nat Mater. 2010; 9:707–715. [PubMed: 20733610]
93. Kroner M, Govorov AO, Remi S, Biedermann B, Seidl S, Badolato A, Petroff PM, Zhang W, Barbour R, Gerardot BD, Warburton RJ, Karrai K. Nature. 2008; 451:311–314. [PubMed: 18202652]
94. Hasan W, Stender CL, Lee MH, Nehl CL, Lee J, Odom TW. Nano Lett. 2009; 9:1555–1558. [PubMed: 19271715]
95. Wust P, Hildebrandt B, Sreenivasa G, Rau B, Gellermann J, Riess H, Felix R, Schlag PM. Lancet Oncol. 2002; 3:487–497. [PubMed: 12147435]
96. Alkilany AM, Nagaria PK, Hexel CR, Shaw TJ, Murphy CJ, Wyatt MD. Small. 2009; 5:701–708. [PubMed: 19226599]
97. Matsumura Y, Maeda H. Cancer Res. 1986; 46:6387–6392. [PubMed: 2946403]
98. Maeda H, Wu J, Sawa T, Matsumura Y, Hori K. J Controlled Release. 2000; 65:271–284.
99. Sato K, Hosokawa K, Maeda M. J Am Chem Soc. 2003; 125:8102–8103. [PubMed: 12837070]
100. Iyer AK, Khaled G, Fang J, Maeda H. Drug Discovery Today. 2006; 11:812–818. [PubMed: 16935749]
101. Bain CD, Troughton EB, Tao YT, Evall J, Whitesides GM, Nuzzo RG. J Am Chem Soc. 1989; 111:321–335.
102. Love JC, Estroff LA, Kriebel JK, Nuzzo RG, Whitesides GM. Chem Rev. 2005; 105:1103–1170. [PubMed: 15826011]

Author Manuscript Author Manuscript Author Manuscript Author Manuscript

103. Bard, AJ., Faulkner, LR. Electrochemical Methods: Fundamentals and Applications. 2. John Wiley & Sons, Inc.; New York: 2001.
104. Hu K, Bard AJ. Langmuir. 1998; 14:4790–4794.
105. Hostetler MJ, Templeton AC, Murray RW. Langmuir. 1999; 15:3782–3789.
106. Sardar R, Funston AM, Mulvaney P, Murray RW. Langmuir. 2009; 25:13840–13851. [PubMed: 19572538]
107. Templeton AC, Wuelfing MP, Murray RW. Acc Chem Res. 2000; 33:27–36. [PubMed: 10639073]
108. Martin BR, Dermody DJ, Reiss BD, Fang M, Lyon LA, Natan MJ, Mallouk TE. Adv Mater. 1999; 11:1021–1025.
109. Walter M, Akola J, Lopez-Acevedo O, Jadzinsky PD, Calero G, Ackerson CJ, Whetten RL, Grönbeck H, Häkkinen H. Proc Natl Acad Sci U S A. 2008; 105:9157–9162. [PubMed: 18599443]
110. Hou W, Dasog M, Scott RWJ. Langmuir. 2009; 25:12954–12961. [PubMed: 19645516]
111. Zhao Y, Perez-Segarra W, Shi QC, Wei A. J Am Chem Soc. 2005; 127:7328–7329. [PubMed: 15898778]
112. Daniel MC, Astruc D. Chem Rev. 2003; 104:293–346.
113. Yee CK, Ulman A, Ruiz JD, Parikh A, White H, Rafailovich M. Langmuir. 2003; 19:9450–9458.
114. Cheng ZL, Skouta R, Vazquez H, Widawsky JR, Schneebeli S, Chen W, Hybertsen MS, Breslow R, Venkataraman L. Nat Nanotechnol. 2011; 6:353–357. [PubMed: 21552252]
115. Cheng Y, Samia AC, Li J, Kenney ME, Resnick A, Burda C. Langmuir. 2010; 26:2248–2255. [PubMed: 19719162]
116. Cheng Y, Meyers JD, Broome AM, Kenney ME, Basilion JP, Burda C. J Am Chem Soc. 2011; 133:2583–2591. [PubMed: 21294543]
117. Flynn NT, Tran TNT, Cima MJ, Langer R. Langmuir. 2003; 19:10909–10915.
118. Dreaden EC, Mwakwari SC, Sodji QH, Oyelere AK, El-Sayed MA. Bioconjugate Chem. 2009; 20:2247–2253.
119. Dickerson EB, Dreaden EC, Huang XH, El-Sayed IH, Chu HH, Pushpanketh S, McDonald JF, El-Sayed MA. Cancer Lett. 2008; 269:57–66. [PubMed: 18541363]
120. Harris JM, Chess RB. Nat Rev Drug Discovery. 2003; 2:214–221. [PubMed: 12612647]
121. Zheng M, Davidson F, Huang X. J Am Chem Soc. 2003; 125:7790–7791. [PubMed: 12822983]
122. Niidome T, Yamagata M, Okamoto Y, Akiyama Y, Takahashi H, Kawano T, Katayama Y, Niidome Y. J Controlled Release. 2006; 114:343–347.
123. von Maltzahn G, Park JH, Agrawal A, Bandaru NK, Das SK, Sailor MJ, Bhatia SN. Cancer Res. 2009; 69:3892–3900. [PubMed: 19366797]
124. Liu Z, Davis C, Cai W, He L, Chen X, Dai H. Proc Natl Acad Sci U S A. 2008; 105:1410–1415. [PubMed: 18230737]
125. Zalipsky S, Hansen CB, Oaks JM, Allen TM. J Pharm Sci. 1996; 85:133–137. [PubMed: 8683436]
126. Gaertner FC, Luxenhofer R, Blechert B, Jordan R, Essler M. J Controlled Release. 2007; 119:291–300.
127. Konradi R, Pidhatika B, Muhlebach A, Textor M. Langmuir. 2008; 24:613–616. [PubMed: 18179272]
128. Niidome Y, Nakamura Y, Honda K, Akiyama Y, Nishioka K, Kawasaki H, Nakashima N. Chem Commun. 2009:1754–1756.
129. Nikoobakht B, Wang J, El-Sayed MA. Chem Phys Lett. 2002; 366:17–23.
130. Nikoobakht B, El-Sayed MA. J Phys Chem A. 2003; 107:3372–3378.
131. Liao H, Hafner JH. Chem Mater. 2005; 17:4636–4641.
132. Kim CK, Ghosh P, Pagliuca C, Zhu ZJ, Menichetti S, Rotello VM. J Am Chem Soc. 2009; 131:1360–1361. [PubMed: 19133720]
133. Gibson JD, Khanal BP, Zubarev ER. J Am Chem Soc. 2007; 129:11653–11661. [PubMed: 17718495]
134. Gole A, Murphy CJ. Langmuir. 2008; 24:266–272. [PubMed: 18052398]

Author Manuscript Author Manuscript Author Manuscript Author Manuscript

135. Oh E, Susumu K, Blanco-Canosa JB, Medintz IL, Dawson PE, Mattoussi H. Small. 2010; 6:1273–1278. [PubMed: 20486227]
136. Brown SD, Nativo P, Smith JA, Stirling D, Edwards PR, Venugopal B, Flint DJ, Plumb JA, Graham D, Wheate NJ. J Am Chem Soc. 2010; 132:4678–4684. [PubMed: 20225865]
137. Rosi NL, Giljohann DA, Thaxton CS, Lytton-Jean AKR, Han MS, Mirkin CA. Science. 2006; 312:1027–1030. [PubMed: 16709779]
138. Seferos DS, Giljohann DA, Hill HD, Prigodich AE, Mirkin CA. J Am Chem Soc. 2007; 129:15477–15479. [PubMed: 18034495]
139. Agasti SS, Chompoosor A, You CC, Ghosh P, Kim CK, Rotello VM. J Am Chem Soc. 2009; 131:5728–5729. [PubMed: 19351115]
140. Gittins DI, Caruso F. J Phys Chem B. 2001; 105:6846–6852.
141. Gole A, Murphy CJ. Chem Mater. 2005; 17:1325–1330.
142. Murphy CJ, Thompson LB, Alkilany AM, Sisco PN, Boulos SP, Sivapalan ST, Yang JA, Chernak DJ, Huang JY. J Phys Chem Lett. 2010; 1:2867–2875.
143. Singh N, Lyon LA. Chem Mater. 2007; 19:719–726.
144. Obare SO, Jana NR, Murphy CJ. Nano Lett. 2001; 1:601–603.
145. Wood KC, Chuang HF, Batten RD, Lynn DM, Hammond PT. Proc Natl Acad Sci U S A. 2006; 103:10207–10212. [PubMed: 16801543]
146. Kim BS, Smith RC, Poon Z, Hammond PT. Langmuir. 2009; 25:14086–14092. [PubMed: 19630389]
147. Smith RC, Riollano M, Leung A, Hammond PT. Angew Chem, Int Ed. 2009; 48:8974–8977.
148. Su XF, Kim BS, Kim SR, Hammond PT, Irvine DJ. ACS Nano. 2009; 3:3719–3729. [PubMed: 19824655]
149. Poon Z, Lee JB, Morton SW, Hammond PT. Nano Lett. 2011; 11:2096–2103. [PubMed: 21524115]
150. Liz-Marzán LM, Giersig M, Mulvaney P. Langmuir. 1996; 12:4329–4335.
151. Banholzer MJ, Harris N, Millstone JE, Schatz GC, Mirkin CA. J Phys Chem C. 2010; 114:7521–7526.
152. Jana NR, Earhart C, Ying JY. Chem Mater. 2007; 19:5074–5082.
153. Mulvaney SP, Musick MD, Keating CD, Natan MJ. Langmuir. 2003; 19:4784–4790.
154. Doering WE, Nie S. Anal Chem. 2003; 75:6171–6176. [PubMed: 14615997]
155. Zavaleta CL, Smith BR, Walton I, Doering W, Davis G, Shojaei B, Natan MJ, Gambhir SS. Proc Natl Acad Sci U S A. 2009; 106:13511–13516. [PubMed: 19666578]
156. Demers LM, Mirkin CA, Mucic RC, Reynolds RA, Letsinger RL, Elghanian R, Viswanadham G. Anal Chem. 2000; 72:5535–5541. [PubMed: 11101228]
157. Link S, El-Sayed MA. J Chem Phys. 2001; 114:2362–2368.
158. Orendorff CJ, Murphy CJ. J Phys Chem B. 2006; 110:3990–3994. [PubMed: 16509687]
159. Dass A, Stevenson A, Dubay GR, Tracy JB, Murray RW. J Am Chem Soc. 2008; 130:5940–5946. [PubMed: 18393500]
160. Weisbecker CS, Merritt MV, Whitesides GM. Langmuir. 1996; 12:3763–3772.
161. Bourg MC, Badia A, Lennox RB. J Phys Chem B. 2000; 104:6562–6567.
162. Rosi NL, Mirkin CA. Chem Rev. 2005; 105:1547–1562. [PubMed: 15826019]
163. Fleischmann M, Hendra PJ, McQuillan AJ. Chem Phys Lett. 1974; 26:163–166.
164. Kneipp, K., Moskovits, M., Kneipp, H. Surface-Enhanced Raman Scattering: Physics and Applications. Springer-Verlang Berlin Heidelberg; New York: 2006.
165. Jeanmaire DL, Van Duyne RP. J Electroanal Chem. 1977; 84:1–20.
166. Albrecht MG, Creighton JA. J Am Chem Soc. 1977; 99:5215–5217.
167. Dhar S, Daniel WL, Giljohann DA, Mirkin CA, Lippard SJ. J Am Chem Soc. 2009; 131:14652–14653. [PubMed: 19778015]
168. Smith WE. Chem Soc Rev. 2008; 37:955–964. [PubMed: 18443681]
169. Doering WE, Piotti ME, Natan MJ, Freeman RG. Adv Mater. 2007; 19:3100–3108.

Author Manuscript Author Manuscript Author Manuscript Author Manuscript

170. Sha MY, Xu H, Penn SG, Cromer R. Nanomedicine (London, U K). 2007; 2:725.
171. Imura K, Okamoto H, Hossain MK, Kitajima M. Nano Lett. 2006; 6:2173–2176. [PubMed: 17034078]
172. Huang X, El-Sayed IH, Qian W, El-Sayed MA. Nano Lett. 2007; 7:1591–1597. [PubMed: 17474783]
173. Huang X, Peng X, Wang Y, Shin DM, El-Sayed MA, Nie S. ACS Nano. 2010; 4:5887–5896. [PubMed: 20863096]
174. Wustholz KL, Henry AI, McMahon JM, Freeman RG, Valley N, Piotti ME, Natan MJ, Schatz GC, Van Duyne RP. J Am Chem Soc. 2010; 132:10903–10910. [PubMed: 20681724]
175. An JH, El-Said WA, Yea CH, Kim TH, Choi JW. J Nanosci Nanotechnol. 2011; 11:4424–4429. [PubMed: 21780469]
176. Tyler TP, Henry AI, Van Duyne RP, Hersam MC. J Phys Chem Lett. 2011; 2:218–222.
177. Rodríguez-Lorenzo L, Álvarez-Puebla R n A, Pastoriza-Santos I, Mazzucco S, Stéphan O, Kociak M, Liz-Marzán LM, García de Abajo FJ. J Am Chem Soc. 2009; 131:4616–4618. [PubMed: 19292448]
178. Nie S, Emory SR. Science. 1997; 275:1102–1106. [PubMed: 9027306]
179. Kneipp K, Kneipp H, Deinum G, Itzkan I, Dasari RR, Feld MS. Appl Spectrosc. 1998; 52:175.
180. Qian X, Peng XH, Ansari DO, Goen QY, Chen GZ, Shin DM, Yang L, Young AN, Wang MD, Nie S. Nat Biotechnol. 2008; 26:83–90. [PubMed: 18157119]
181. Qian XM, Zhou X, Nie SM. J Am Chem Soc. 2008; 130:14934–14938. [PubMed: 18937463]
182. Chon H, Lee S, Son SW, Oh CH, Choo J. Anal Chem. 2009; 81:3029–3034. [PubMed: 19301845]
183. Yoon KJ, Seo HK, Hwang H, Pyo D, Eom IY, Hahn JH, Jung YM. Bull Korean Chem Soc. 2010; 31:1215–1218.
184. Chon H, Lim C, Ha SM, Ahn Y, Lee EK, Chang SI, Seong GH, Choo J. Anal Chem. 2010; 82:5290–5295. [PubMed: 20503972]
185. Wang GF, Lipert RJ, Jain M, Kaur S, Chakraboty S, Torres MP, Batra SK, Brand RE, Porter MD. Anal Chem. 2011; 83:2554–2561. [PubMed: 21391573]
186. El-Said WA, Kim TH, Yea CH, Kim H, Choi JW. J Nanosci Nanotechnol. 2011; 11:768–772. [PubMed: 21446542]
187. Dufek EJ, Ehlert B, Granger MC, Sandrock TM, Legge SL, Herrmann MG, Meikle AW, Porter MD. Analyst. 2010; 135:2811–2817. [PubMed: 20830325]
188. Ryu K, Haes AJ, Park HY, Nah S, Kim J, Chung H, Yoon MY, Han SH. J Raman Spectrosc. 2010; 41:121–124.
189. Grubisha DS, Lipert RJ, Park HY, Driskell J, Porter MD. Anal Chem. 2003; 75:5936–5943. [PubMed: 14588035]
190. Driskell JD, Kwarta KM, Lipert RJ, Porter MD, Neill JD, Ridpath JF. Anal Chem. 2005; 77:6147–6154. [PubMed: 16194072]
191. Neng J, Harpster MH, Zhang H, Mecham JO, Wilson WC, Johnson PA. Biosens Bioelectron. 2010; 26:1009–1015. [PubMed: 20864330]
192. Zhang H, Harpster MH, Park HJ, Johnson PA. Anal Chem. 2011; 83:254–260. [PubMed: 21121693]
193. Porter MD, Lipert RJ, Siperko LM, Wang G, Narayanana R. Chem Soc Rev. 2008; 37:1001–1011. [PubMed: 18443685]
194. Rule KL, Vikesland PJ. Environ Sci Technol. 2009; 43:1147–1152. [PubMed: 19320172]
195. Guven B, Basaran-Akgul N, Temur E, Tamer U, Boyaci IH. Analyst. 2011; 136:740–748. [PubMed: 21125089]
196. Wang YL, Ravindranath S, Irudayaraj J. Anal Bioanal Chem. 2011; 399:1271–1278. [PubMed: 21136046]
197. Sha MY, Xu HX, Natan MJ, Cromer R. J Am Chem Soc. 2008; 130:17214–17215. [PubMed: 19053187]
198. Wang X, Qian XM, Beitler JJ, Chen ZG, Khuri FR, Lewis MM, Shin HJC, Nie SM, Shin DM. Cancer Res. 2011; 71:1526–1532. [PubMed: 21212408]

Author Manuscript Author Manuscript Author Manuscript Author Manuscript

199. Ni J, Lipert RJ, Dawson GB, Porter MD. Anal Chem. 1999; 71:4903–4908. [PubMed: 10565281]
200. Wilson R, Cossins AR, Spiller DG. Angew Chem, Int Ed. 2006; 45:6104–6117.
201. Lutz BR, Dentinger CE, Nguyen LN, Sun L, Zhang JW, Allen AN, Chan S, Knudsen BS. ACS Nano. 2008; 2:2306–2314. [PubMed: 19206397]
202. von Maltzahn G, Centrone A, Park JH, Ramanathan R, Sailor MJ, Hatton TA, Bhatia SN. Adv Mater. 2009; 21:1–6.
203. Ge M, Bao F, Yao JL, Sun R, Gu RA. Acta Chim Sin. 2009; 67:2285–2289.
204. Link S, El-Sayed MA. Annu Rev Phys Chem. 2003; 54:331–366. [PubMed: 12626731]
205. Anker JN, Hall WP, Lyandres O, Shah NC, Zhao J, Van Duyne RP. Nat Mater. 2008; 7:442–453. [PubMed: 18497851]
206. Ringe E, McMahon JM, Sohn K, Cobley C, Xia YN, Huang JX, Schatz GC, Marks LD, Van Duyne RP. J Phys Chem C. 2010; 114:12511–12516.
207. Kreibig, U., Vollmer, M. Optical Properties of Metal Clusters. Springer; Berlin: 1995.
208. Johnson PB, Christy RW. Phys Rev B: Solid State. 1972; 6:4370–4379.
209. Lee SK, El-Sayed MA. J Phys Chem B. 2006; 110:19220–19225. [PubMed: 17004772]
210. Mahmoud MA, El-Sayed MA. J Am Chem Soc. 2010; 132:12704–12710. [PubMed: 20722373]
211. Willets KA, Van Duyne RP. Ann Rev Phys Chem. 2007; 58:267–297. [PubMed: 17067281]
212. Jain PK, El-Sayed MA. J Phys Chem C. 2007; 111:17451.
213. Englebienne P. Analyst. 1998; 123:1599–1603. [PubMed: 9830172]
214. Nath N, Chilkoti A. Anal Chem. 2002; 74:504–509. [PubMed: 11838667]
215. Okamoto Y, Yamaguchi I, Kobayashi T. Opt Lett. 2000; 25:372–374. [PubMed: 18059883]
216. Mayer KM, Lee S, Liao H, Rostro BC, Fuentes A, Scully PT, Nehl CL, Hafner JH. ACS Nano. 2008; 2:687–692. [PubMed: 19206599]
217. Raschke G, Kowarik S, Franzl T, Sonnichsen C, Klar TA, Feldmann J. Nano Lett. 2003; 3:935–938.
218. Baciu CL, Becker J, Janshoff A, Sönnichsen C. Nano Lett. 2008; 8:1724–1728. [PubMed: 18459744]
219. Nusz GJ, Marinakos SM, Curry AC, Dahlin A, Höök F, Wax A, Chilkoti A. Anal Chem. 2008; 80:984–989. [PubMed: 18197636]
220. Dondapati SK, Sau TK, Hrelescu C, Klar TA, Stefani FD, Feldmann J. ACS Nano. 2010; 4:6318–6322. [PubMed: 20942444]
221. Marinakos SM, Chen S, Chilkoti A. Anal Chem. 2007; 79:5278–5283. [PubMed: 17567106]
222. Mayer KM, Hafner JH. Chem Rev. 2011; 111:3828–3857. [PubMed: 21648956]
223. Sonnichsen C, Reinhard BM, Liphardt J, Alivisatos AP. Nat Biotechnol. 2005; 23:741–745. [PubMed: 15908940]
224. Jain PK, Eustis S, El-Sayed MA. J Phys Chem B. 2006; 110:18243. [PubMed: 16970442]
225. Jain PK, Huang W, El-Sayed MA. Nano Lett. 2007; 7:2080.
226. Su KH, Wei QH, Zhang X. Nano Lett. 2003; 3:1087–1090.
227. Elghanian R, Storhoff JJ, Mucic RC, Letsinger RL, Mirkin CA. Science. 1997; 277:1078–1081. [PubMed: 9262471]
228. Storhoff JJ, Elghanian R, Mucic RC, Mirkin CA, Letsinger RL. J Am Chem Soc. 1998; 120:1959–1964.
229. Lazarides AA, Schatz GC. J Phys Chem B. 2000; 104:460–467.
230. Storhoff JJ, Lazarides AA, Mucic RC, Mirkin CA, Letsinger RL, Schatz GC. J Am Chem Soc. 2000; 122:4640–4650.
231. Reinhard BM, Siu M, Agarwal H, Alivisatos AP, Liphardt J. Nano Lett. 2005; 5:2246–2252. [PubMed: 16277462]
232. Reinhard B, Sheikholeslami S, Mastroianni A, Alivisatos AP, Liphardt J. Proc Natl Acad Sci U S A. 2007; 104:2667–2672. [PubMed: 17307879]
233. Rechberger W, Hohenau A, Leitner A, Krenn JR, Lamprecht B, Aussenegg FR. Opt Commun. 2003; 220:137–141.

Author Manuscript Author Manuscript Author Manuscript Author Manuscript

234. Huang W, Qian W, Jain PK, El-Sayed MA. Nano Lett. 2007; 7:3227–3234. [PubMed: 17760479]
235. Jain PK, Huang W, El-Sayed MA. Nano Lett. 2007; 7:2080–2088.
236. Mucic RC, Storhoff JJ, Mirkin CA, Letsinger RL. J Am Chem Soc. 1998; 120:12674–12675.
237. Taton TA, Lu G, Mirkin CA. J Am Chem Soc. 2001; 123:5164–5165. [PubMed: 11457374]
238. Jin R, Wu G, Li Z, Mirkin CA, Schatz GC. J Am Chem Soc. 2003; 125:1643–1654. [PubMed: 12568626]
239. Giljohann DA, Seferos DS, Prigodich AE, Patel PC, Mirkin CA. J Am Chem Soc. 2009; 131:2072–2073. [PubMed: 19170493]
240. Mirkin CA, Letsinger RL, Mucic RC, Storhoff JJ. Science. 1996; 382:607–609.
241. Nam JM, Park SJ, Mirkin CA. J Am Chem Soc. 2002; 124:3820–3821. [PubMed: 11942805]
242. Park SJ, Lazarides AA, Mirkin CA, Brazis PW, Kannewurf CR, Letsinger RL. Angew Chem, Int Ed. 2000; 39:3845–3848.
243. Taton TA, Mucic RC, Mirkin CA, Letsinger RL. J Am Chem Soc. 2000; 122:6305–6306.
244. Dujardin E, Hsin LB, Wang CRC, Mann S. Chem Commun. 2001:1264.
245. Paraba HJ, Junga C, Leeb JH, Park HG. Biosens Bioelectron. 2010; 26:667–673. [PubMed: 20675117]
246. Xin A, Dong Q, Xiong C, Ling L. Chem Commun. 2009:1658–1660.
247. US Pat. 5989921. 1999.
248. The Economist. 2011
249. Bae WK, Lee YK, Cho MS, Ma SK, Kim SW, Kim NH, Choi KC. Yonsei Med J. 2006; 47:437–439. [PubMed: 16807997]
250. Diaz-Vazquez C, Torregrosa-Bertet MJ, Carvajal-Urueña I, Cano-Garcinuño A, Fos-Escrivà E, García-Gallego A, López-Cacho F, Monzón-Fueyo MC, Pérez-Porcuna XM, Ridao-Redondo ML. Pediatr Allergy Immunol. 2009; 20:601–609. [PubMed: 19220775]
251. Mao X, Ma YQ, Zhang AG, Zhang LR, Zeng LW, Liu GD. Anal Chem. 2009; 81:1660–1668. [PubMed: 19159221]
252. Biagini RE, Sammons DL, Smith JP, MacKenzie BA, Striley CAF, Snawder JE, Robertson SA, Quinn CP. Clin Vaccine Immunol. 2006; 13:541–546. [PubMed: 16682473]
253. Laderman EI, Whitworth E, Dumaual E, Jones M, Hudak A, Hogrefe W, Carney J, Groen J. Clin Vaccine Immunol. 2008; 15:159–163. [PubMed: 18003814]
254. Tippkotter N, Stuckmann H, Kroll S, Winkelmann G, Noack U, Scheper T, Ulber R. Anal Bioanal Chem. 2009; 394:863–869. [PubMed: 19306114]
255. Li Q, Liu L, Chen W, Peng C, Wang L, Xu C. Int J Environ Anal Chem. 2009; 89:261–268.
256. Rong-Hwa S, Shiao-Shek T, Der-Jiang C, Yao-Wen H. Food Chem. 2010; 118:462–466.
257. Lindhardt C, Schönenbrücher H, Slaghuis J, Bubert A, Ossmer R. J AOAC Int. 2009; 92:1885–1889. [PubMed: 20166612]
258. Xu H, Mao X, Zeng QX, Wang SF, Kawde AN, Liu GD. Anal Chem. 2009; 81:669–675. [PubMed: 19072289]
259. Yguerabide J, Yguerabide EE. Anal Biochem. 1998; 262:137–156. [PubMed: 9750128]
260. Yguerabide J, Yguerabide EE. Anal Biochem. 1998; 262:157–186. [PubMed: 9750129]
261. Jain PK, Lee KS, El-Sayed IH, El-Sayed MA. J Phys Chem B. 2006; 110:7238–7248. [PubMed: 16599493]
262. Orendorff CJ, Sau TK, Murphy CJ. Small. 2006; 2:636–639. [PubMed: 17193100]
263. Orendorff CJ, Baxter SC, Goldsmith EC, Murphy CJ. Nanotechnology. 2005; 16:2601–2605.
264. Zhu J, Huang L, Zhao J, Wang Y, Zhao Y, Hao L, Lu Y. Mater Sci Eng, B. 2005; 121:199–203.
265. Lee KS, El-Sayed MA. J Phys Chem B. 2005; 109:20331–20338. [PubMed: 16853630]
266. Zsigmondy, RA. Colloids and the ultramicroscope-A manual of colloid chemistry and ultramicroscopy. John Wiley and Sons, Inc.; NY: 1914.
267. Mock J, Barbic M, Smith D, Schultz D, Schultz S. J Chem Phys. 2002; 116:6755–6759.
268. Sokolov K, Follen M, Aaron J, Pavlova I, Malpica A, Lotan R, Richartz-Kortum R. Cancer Res. 2003; 63:1999–2004. [PubMed: 12727808]

Author Manuscript Author Manuscript Author Manuscript Author Manuscript

269. El-Sayed IH, Huang X, El-Sayed MA. Nano Lett. 2005; 5:829–834. [PubMed: 15884879]
270. Huang XH, El-Sayed IH, Qian W, El-Sayed MA. J Am Chem Soc. 2006; 128:2115–2120. [PubMed: 16464114]
271. Loo C, Lowery A, Halas NJ, West JL, Drezek R. Nano Lett. 2005; 5:709–711. [PubMed: 15826113]
272. Loo C, Hirsch L, Lee MH, Chang E, West J, Halas N, Drezek R. Opt Lett. 2005; 30:1012–1014. [PubMed: 15906987]
273. Ding H, Yong KT, Roy I, Pudavar HE, Law WC, Bergey EJ, Prasad PN. J Phys Chem C. 2007; 111:12552–12557.
274. Chanda N, Shukla R, Katti KV, Kannan R. Nano Lett. 2009; 9:1798–1805. [PubMed: 19351145]
275. Kumar S, Harrison N, Richards-Kortum R, Sokolov K. Nano Lett. 2007; 7:1338–1343. [PubMed: 17439187]
276. Oyelere AK, Chen B, Huang X, El-Sayed IH, El-Sayed MA. Bioconjugate Chem. 2007; 18:1490–1497.
277. Qian W, Huang X, Kang B, El-Sayed MA. J Biomed Opt. 2010; 15:046025. [PubMed: 20799827]
278. Stone JW, Sisco PN, Goldsmith EC, Baxter SC, Murphy CJ. Nano Lett. 2007; 7:116–119. [PubMed: 17212449]
279. Saxton MJ, Jacobson K. Annu Rev Biophys Biomol Struct. 1997; 26:373–399. [PubMed: 9241424]
280. Tomishige M, Sako Y, Kusumi A. J Cell Biol. 1998; 142:989–1000. [PubMed: 9722611]
281. Dietrich C, Yang B, Fujiwara T, Kusumi A, Jacobson K. Biophys J. 2002; 82:274–284. [PubMed: 11751315]
282. Rong G, Wang H, Skewis LR, Reinhard BM. Nano Lett. 2008; 8:3386–3393. [PubMed: 18788826]
283. Yang YH, Nam JM. Anal Chem. 2009; 81:2564–2568. [PubMed: 19228043]
284. Fujimoto JG, Brezinsky ME, Tearney GJ, Boppart SA, Bouma B, Hee MR, Southern JF, Swanson EA. Nat Med. 1995; 1:970–972. [PubMed: 7585229]
285. Huang D, Swanson EA, Lin CP, Schuman JS, Stinson WG, Chang W, Hee MR, Flotte T, Gregory K, Puliafito CA. Science. 1991; 254:1178–1181. [PubMed: 1957169]
286. Gobin AM, Lee MH, Halas NJ, James WD, Drezek RA, West JL. Nano Lett. 2007; 7:1929–1934. [PubMed: 17550297]
287. Chen J, Saeki F, Wiley BJ, Cang H, Cobb MJ, Li ZY, Au L, Zhang H, Kimmey MB, Li X, Xia Y. Nano Lett. 2005; 5:473–477. [PubMed: 15755097]
288. Oldenburg AL, Hansen MN, Zweifel DA, Wei A, Boppart SA. Opt Express. 2006; 14:6724–6738. [PubMed: 19516854]
289. Oldenburg AL, Hansen MN, Ralston TS, Wei A, Boppart SA. J Mater Chem. 2009; 19:6407–6411. [PubMed: 20107616]
290. Kin CS, Willder-Smith P, Ahn YC, Liaw LH, Che Z, Kkwon YJ. J Biomed Opt. 2009; 14:034008. [PubMed: 19566301]
291. Mooradian A. Phys Rev Lett. 1969; 22:185–187.
292. Boyd GT, Yu ZH, Shen YR. Phys Rev B: Condens Matter Mater Phys. 1986; 33:7923–7936.
293. Mohamed MB, Volkov V, Link S, El-Sayed MA. Chem Phys Lett. 2000; 317:517–523.
294. Eustis S, El-Sayed MA. J Phys Chem B. 2005; 109:16350–16356. [PubMed: 16853078]
295. Li CZ, Male KB, Hrapovic S, Luong JHT. Chem Commun. 2005:3924–3926.
296. Bouheller A, Beversluis MR, Novootny L. Appl Phys Lett. 2003; 83:5041–5043.
297. Imura K, Nagahara T, Okamoto H. J Am Chem Soc. 2004; 126:12730–12731. [PubMed: 15469240]
298. Wang H, Huff TB, Zweifel DA, He W, Low PS, Wei A, Cheng JX. Proc Natl Acad Sci U S A. 2005; 102:15752–15756. [PubMed: 16239346]
299. Loumaigne M, Richard A, Laverdant J, Nutarelli D, Debarre A. Nano Lett. 2010; 10:2817–2824. [PubMed: 20593772]

Author Manuscript Author Manuscript Author Manuscript Author Manuscript

300. Zhou Y, Wu X, Wang T, Ming T, Wang PN, Zhou LW, Chen JY. J Microsc. 2010; 237:200–207. [PubMed: 20096050]
301. Durr NJ, Larson T, Smith DK, Korgel BA, Sokolov K, Ben-Yakar A. Nano Lett. 2007; 7:941–945. [PubMed: 17335272]
302. Tong L, Zhao Y, Huff TB, Hansen MN, Wei A, Cheng JX. Adv Mater. 2007; 19:3136–3141. [PubMed: 19020672]
303. Huff TB, Hansen MN, Zhao Y, Cheng JX, Wei A. Langmuir. 2007; 23:1596–1599. [PubMed: 17279633]
304. Li JL, Gu M. Biomaterials. 2010; 31:9492–9498. [PubMed: 20932571]
305. He W, Wang H, Hartmann LC, Cheng JX, Low PS. Proc Natl Acad Sci U S A. 2007; 104:11760–11765. [PubMed: 17601776]
306. Park J, Estrada A, Sharp K, Sang K, Schwartz JA, Smith DK, Coleman C, Payne JD, Korgel BA, Dunn AK, Tunnell JW. Opt Express. 2008; 16:1590–1599. [PubMed: 18542237]
307. Park, J., Estrada, A., Schwartz, JA., Diagaradjane, P., Krishnan, S., Coleman, C., Payne, JD., Dunn, AK., Tunnell, JW. Plasmonics in Biology and Medicine VI. Editon. VoDinh, T., Lakowicz, JR., editors. Vol. 7192. Spie-Int Soc Optical Engineering; Bellingham: 2009.
308. Park J, Estrada A, Schwartz JA, Diagaradjane P, Krishnan S, Dunn AK, Tunnell JW. Lasers Surg Med. 2010; 42:630–639. [PubMed: 21399728]
309. Tong L, He W, Zhang YS, Zheng W, Cheng JX. Langmuir. 2009; 25:12454–12459. [PubMed: 19856987]
310. Boyer D, Tamarat P, Maali A, Lounis B, Orrit M. Science. 2002; 297:1160–1163. [PubMed: 12183624]
311. Zharov VP, Lapotko DO. IEEE J Sel Top Quantum Electron. 2005; 11:733–751.
312. Brusnichkin AV, Nedosekin DA, Proskurnin MA, Zharov VP. Appl Spectrosc. 2007; 61:1191–1201. [PubMed: 18028698]
313. Zharov VP, Galanzha EI, Tuchin VV. Cytometry, Part A. 2007; 71A:191–206.
314. Zharov VP, Galanzha EI, Tuchin VV. Opt Lett. 2005; 30:628–630. [PubMed: 15791998]
315. Galanzha EI, Kim JW, Zharov VP. J Biophtonics. 2009; 2:725–735.
316. Kim JW, Galanzha EI, Shashkov EV, Moon HM, Zharov VP. Nat Nanotechnol. 2009; 4:688–694. [PubMed: 19809462]
317. Zharov VP, Galitovsky V, Viegas M. Appl Phys Lett. 2003; 83:4897–4899.
318. Zharov VP, Galitovskaya E, Viegas M. Proc SPIE Int Soc Opt Eng. 2004; 5319:291–300.
319. Xu M, Wang LV. Rev Sci Instrum. 2006; 77:041101.
320. Agarwal A, Huang SW, O'Donnell M, Day KC, Day M, Kotov N, Ashkenazi S. J Appl Phys. 2007; 102:064701.
321. Li PC, Wang CRC, Shieh DB, Wei CW, Liao CK, Poe C, Jhan S, Ding AA, Wu YN. Opt Express. 2008; 16:18605–18615. [PubMed: 19581946]
322. Galanzha EI, Shashkov EV, Kelly T, Kim JW, Yang L, Zharov VP. Nat Nanotechnol. 2009; 4:855–860. [PubMed: 19915570]
323. Galanzha EI, Shashkov EV, Spring PM, Suen JY, Zharov VP. Cancer Res. 2009; 69:7926–7934. [PubMed: 19826056]
324. Nedosekin DA, Sarimollaoglu M, Shashkov EV, Galanzha EI, Zharov VP. Opt Express. 2010; 18:8605–8620. [PubMed: 20588705]
325. Lu W, Huang Q, Geng KB, Wen XX, Zhou M, Guzatov D, Brecht P, Su R, Oraevsky A, Wang LV, Li C. Biomaterials. 2010; 31:2617–2626. [PubMed: 20036000]
326. Kim C, Song HM, Cai X, Yao J, We A, Wang LX. J Mater Chem. 2011; 11:2841–2844.
327. Wang B, Yantsen E, Larson T, Karpiouk AB, Sethuraman S, Su JL, Sokolov K, Emelianov SY. Nano Lett. 2009; 9:2212–2217. [PubMed: 18844426]
328. Kim K, Huang SW, Ashkenazi S, O'Donnell M, Agarwal A, Kotov NA, Denny MF, Kaplan MJ. Appl Phys Lett. 2007; 90:223901.
329. Chamberland DL, Agarwal A, Kotov N, Fowlkes JB, Carson PL, Wang X. Nanotechnology. 2008; 19:095101. [PubMed: 21817663]

Author Manuscript Author Manuscript Author Manuscript Author Manuscript

330. Wang GF, Sun W, Luo Y, Fang N. J Am Chem Soc. 2010; 132:16417–16422. [PubMed: 21043495]
331. Wang L, Li YF, Zhou L, Liu Y, Meng L, Zhang K, Wu X, Zhang L, Li B, Chen C. Anal Bioanal Chem. 2010; 396:1105–1114. [PubMed: 20016883]
332. Wang GF, Stender AS, Sun W, Fang N. Analyst. 2010; 135:215–221. [PubMed: 20098755]
333. Sun W, Wang GF, Fang N, Yeung ES. Anal Chem. 2009; 81:9203–9208. [PubMed: 19788254]
334. Luo Y, Sun W, Gu Y, Wang GF, Fang N. Anal Chem. 2010; 82:6675–6679. [PubMed: 20614872]
335. Popovtzer R, Agrawal A, Kotov NA, Popovtzer A, Balter J, Carey TE, Kopelman R. Nano Lett. 2008; 8:4593–4596. [PubMed: 19367807]
336. Cai QY, Kim SH, Choi KS, Kim SY, Byun SJ, Kim KW, Park SH, Juhng SK, Yoon KH. Invest Radiol. 2007; 42:797–806. [PubMed: 18007151]
337. Higby GJ. Gold Bull. 1982; 15:130–140. [PubMed: 11614517]
338. Borg G, Allander E, Lund B, Berg E, Brodin U, Pettersson H, Trang L. J Rheumatol. 1988; 15:1747–1754. [PubMed: 14552308]
339. Lewis MG, Dafonseca S, Chomont N, Palamara AT, Tardugno M, Mai A, Collins M, Wagner WL, Yalley-Ogunro J, Greenhouse J, Chirullo B, Norelli S, Garaci E, Savarino A. AIDS. 2011; 25:1347–1356. [PubMed: 21505294]
340. Butler EB, Scardino PT, Teh BS, Uhl BM, Guerriero WG, Carlton CE, Berner BM, Dennis WS, Carpenter LS, Lu HH, Chiu JK, Kent TS, Woo SY. Semin Surg Oncol. 1997; 13:406–418. [PubMed: 9358587]
341. Alkilany AM, Murphy CJ. J Nanopart Res. 2010; 12:2313–2333. [PubMed: 21170131]
342. Jia HY, Liu Y, Zhang XJ, Han L, Du LB, Tian Q, Xut YC. J Am Chem Soc. 2009; 131:40–41. [PubMed: 19072650]
343. Mukherjee P, Bhattacharya R, Wang P, Wang L, Basu S, Nagy JA, Atala A, Mukhopadhyay D, Soker S. Clin Cancer Res. 2005; 11:3530–3534. [PubMed: 15867256]
344. Kang B, Mackey MA, El-Sayed MA. J Am Chem Soc. 2010; 132:1517–1519. [PubMed: 20085324]
345. Huang X, Jain PK, El-Sayed IH, El-Sayed MA. Lasers Med Sci. 2008; 23:217–228. [PubMed: 17674122]
346. Murphy CJ, Gole AM, Stone JW, Sisco PN, Alkilany AM, Goldsmith EC, Baxter SC. Acc Chem Res. 2008; 41:1721–1730. [PubMed: 18712884]
347. Norman RS, Stone JW, Gole A, Murphy CJ, Sabo-Attwood TL. Nano Lett. 2008; 8:302–306. [PubMed: 18062714]
348. Chen J, Wang D, Xi J, Au L, Siekkinen A, Warsen A, Li ZY, Zhang H, Xia Y, Li X. Nano Lett. 2007; 7:1318–1322. [PubMed: 17430005]
349. Lal S, Clare SE, Halas NJ. Acc Chem Res. 2008; 41:1842–1851. [PubMed: 19053240]
350. Cobley CM, Au L, Chen J, Xia Y. Expert Opin Drug Delivery. 2010; 7:577–587.
351. Kennedy LC, Bickford LR, Lewinski NA, Coughlin AJ, Hu Y, Day ES, West JL, Drezek RA. Small. 2011; 7:169–183. [PubMed: 21213377]
352. O'Neal DP, Hirsch LR, Halas NJ, Payne JD, West JL. Cancer Lett. 2004; 209:171–176. [PubMed: 15159019]
353. El-Sayed MA. Acc Chem Res. 2001; 34:257–264. [PubMed: 11308299]
354. Alkilany AM, Thompson LB, Boulos SP, Sisco PN, Murphy CJ. Adv Drug Delivery Rev. 2011 in press.
355. Weissleder R. Nat Biotechnol. 2001; 19:316–317. [PubMed: 11283581]
356. Hirsch LR, Stafford RJ, Bankson JA, Sershen SR, Rivera B, Price RE, Hazle JD, Halas NJ, West JL. Proc Natl Acad Sci U S A. 2003; 100:13549–13554. [PubMed: 14597719]
357. Loo C, Lin A, Hirsch L, Lee MH, Barton J, Halas N, West J, Drezek R. Technol Cancer Res Treat. 2004; 3:33–40. [PubMed: 14750891]
358. Lowery AR, Gobin AM, Day ES, Halas NJ, West JL. Int J Nanomed. 2006; 1:149–154.
359. Gobin AM, Moon JJ, West JL. Int J Nanomed. 2008; 3:351–358.

Author Manuscript Author Manuscript Author Manuscript Author Manuscript

360. Stern JM, Stanfield J, Lotan Y, Park S, Hsieh JT, Cadeddu JA. J Endourol. 2007; 21:939–943. [PubMed: 17867958]
361. Bernardi RJ, Lowery AR, Thompson PA, Blaney SM, West JL. J Neurooncol. 2008; 86:165–172. [PubMed: 17805488]
362. Liu SY, Liang ZS, Gao F, Luo SF, Lu GQ. J Mater Sci: Mater Med. 2010; 21:665–674. [PubMed: 19834788]
363. Puvanakrishnan P, Park J, Diagaradjane P, Schwartz JA, Coleman CL, Gill-Sharp KL, Sang KL, Payne JD, Krishnan S, Tunnell JW. J Biomed Opt. 2009; 14:024044. [PubMed: 19405772]
364. Schwartz JA, Shetty AM, Price RE, Stafford RJ, Wang JC, Uthamanthil RK, Pham K, McNichols RJ, Coleman CL, Payne JD. Cancer Res. 2009; 69:1659–1667. [PubMed: 19208847]
365. Huang X, Neretina S, El-Sayed MA. Adv Mater. 2009; 21:4880–4910. [PubMed: 25378252]
366. Jain PK, Huang XH, El-Sayed IH, El-Sayed MA. Acc Chem Res. 2008; 41:1578–1586. [PubMed: 18447366]
367. Goodrich GP, Bao L, Gill-Sharp K, Sang KL, Wang J, Payne JD. J Biomed Opt. 2010; 15:018001. [PubMed: 20210487]
368. Choi WI, Kim JY, Kang C, Byeon CC, Kim YH, Tae G. ACS Nano. 2011; 5:1995–2003. [PubMed: 21344891]
369. Jang B, Park JY, Tung CH, Kim IH, Choi Y. ACS Nano. 2011; 5:1086–1094. [PubMed: 21244012]
370. Au L, Zheng D, Zhou F, Li ZY, Li X, Xia Y. ACS Nano. 2008; 2:1645–1652. [PubMed: 19206368]
371. Chen J, Glaus C, Laforest R, Zhang Q, Yang M, Gidding M, Welch MJ, Xia Y. Small. 2010; 6:811–817. [PubMed: 20225187]
372. Gobin AM, Watkins EM, Quevedo E, Colvin VL, West JL. Small. 2010; 6:745–752. [PubMed: 20183810]
373. Day ES, Bickford LR, Slater JH, Riggall NS, Drezek RA, West JL. Int J Nanomed. 2010; 5:445–454.
374. Melancon MP, Lu W, Yang Z, Zhang R, Cheng Z, Elliot AM, Stafford J, Olson T, Zhang JZ, Li C. Mol Cancer Ther. 2008; 7:1730–1739. [PubMed: 18566244]
375. Lu W, Xiong C, Zhang G, Huang Q, Zhang R, Zhang JZ, Li C. Clin Cancer Res. 2009; 15:876–886. [PubMed: 19188158]
376. Alkilany AM, Frey RL, Ferry JL, Murphy CJ. Langmuir. 2008; 24:10235–10239. [PubMed: 18700748]
377. Cheng Y, Samia AC, Meyers JD, Panagopoulos I, Fei B, Burda C. J Am Chem Soc. 2008; 130:10643–10647. [PubMed: 18642918]
378. Kim D, Jeong YY, Jon S. ACS Nano. 2010; 4:3689–3696. [PubMed: 20550178]
379. Papp I, Sieben C, Ludwig K, Roskamp M, Bottcher C, Schlecht S, Herrmann A, Haag R. Small. 2010; 6:2900–2906. [PubMed: 21104827]
380. Poon L, Zandberg W, Hsiao D, Erno Z, Sen D, Gates BD, Branda NR. ACS Nano. 2010; 4:6395–6403. [PubMed: 20958080]
381. Jain PK, Qian W, El-Sayed MA. J Am Chem Soc. 2006; 128:2426–2433. [PubMed: 16478198]
382. Dulkeith E, Morteani AC, Niedereichholz T, Klar TA, Feldmann J, Levi SA, van Veggel FC, Reinhoudt DN, Moller M, Gittins DI. Phys Rev Lett. 2002; 89:203002. [PubMed: 12443474]
383. Sapsford KE, Berti L, Medintz IL. Angew Chem, Int Ed. 2006; 45:4562–4589.
384. Hong R, Han G, Fernandez JM, Kim BJ, Forbes NS, Rotello VM. J Am Chem Soc. 2006; 128:1078–1079. [PubMed: 16433515]
385. Rothrock AR, Donkers RL, Schoenfisch MH. J Am Chem Soc. 2005; 127:9362–9363. [PubMed: 15984851]
386. Polizzi MA, Stasko NA, Schoenfisch MH. Langmuir. 2007; 23:4938–4943. [PubMed: 17375944]
387. Huang HC, Barua S, Kay DB, Rege K. ACS Nano. 2009; 3:2941–2952. [PubMed: 19856978]
388. Bonoiu AC, Mahajan SD, Ding H, Roy I, Yong KT, Kumar R, Hu R, Bergey EJ, Schwartz SA, Prasad PN. Proc Natl Acad Sci U S A. 2009; 106:5546–5550. [PubMed: 19307583]

Author Manuscript Author Manuscript Author Manuscript Author Manuscript

389. Chakravarthy KV, Bonoiu AC, Davis WG, Ranjan P, Ding H, Hu R, Bowzard JB, Bergey EJ, Katz JM, Knight PR, Sambhara S, Prasad PN. Proc Natl Acad Sci U S A. 2010; 107:10172–10177. [PubMed: 20498074]
390. Ghosh PS, Kim CK, Han G, Forbes NS, Rotello VM. ACS Nano. 2008; 2:2213–2218. [PubMed: 19206385]
391. Caruso F, Caruso RA, Mohwald H. Science. 1998; 282:1111–1114. [PubMed: 9804547]
392. Guo S, Huang Y, Jiang Q, Sun Y, Deng L, Liang Z, Du Q, Xing J, Zhao Y, Wang PC, Dong A, Liang XJ. ACS Nano. 2010; 4:5505–5511. [PubMed: 20707386]
393. Lee SK, Han MS, Asokan S, Tung CH. Small. 2011; 7:364–370. [PubMed: 21294265]
394. Moon GD, Choi SW, Cai X, Li WY, Cho EC, Jeong U, Wang LV, Xia YA. J Am Chem Soc. 2011; 133:4762–4765. [PubMed: 21401092]
395. Yang XC, Samanta B, Agasti SS, Jeong Y, Zhu ZJ, Rana S, Miranda OR, Rotello VM. Angew Chem, Int Ed. 2011; 50:477–481.
396. You J, Zhang G, Li C. ACS Nano. 2010; 4:1033–1041. [PubMed: 20121065]
397. Yavuz MS, Cheng YY, Chen JY, Cobley CM, Zhang Q, Rycenga M, Xie JW, Kim C, Song KH, Schwartz AG, Wang LHV, Xia YN. Nat Mater. 2009; 8:935–939. [PubMed: 19881498]
398. Alvarez-Lorenzo C, Bromberg L, Concheiro A. Photochem Photobiol. 2009; 85:848–860. [PubMed: 19222790]
399. Jin Y, Gao X. J Am Chem Soc. 2009; 131:17774–17776. [PubMed: 19928855]
400. Troutman TS, Barton JK, Romanowski M. Adv Mater. 2008; 20:2604–2608. [PubMed: 21494416]
401. Torchilin VP. Nat Rev Drug Discovery. 2005; 4:145–160. [PubMed: 15688077]
402. Zhang L, Granick S. Nano Lett. 2006; 6:694–698. [PubMed: 16608266]
403. Wang B, Zhang L, Bae SC, Granick S. Proc Natl Acad Sci U S A. 2008; 105:18171–18175. [PubMed: 19011086]
404. Pornpattananangkul D, Olson S, Aryal S, Sartor M, Huang CM, Vecchio K, Zhang L. ACS Nano. 2010; 4:1935–1942. [PubMed: 20235571]
405. Mellman I, Fuchs R, Helenius A. Annu Rev Biochem. 1986; 55:663–700. [PubMed: 2874766]
406. Pornpattananangkul D, Zhang L, Olson S, Aryal S, Obonyo M, Vecchio K, Huang CM. J Am Chem Soc. 2011; 133:4132–4139. [PubMed: 21344925]
407. Hribar KC, Lee MH, Lee D, Burdick JA. ACS Nano. 2011; 5:2948–2956. [PubMed: 21384864]
408. You J, Shao R, Wei X, Gupta S, Li C. Small. 2010; 6:1022–1031. [PubMed: 20394071]
409. Sershen SR, Westcott SL, Halas NJ, West JL. J Biomed Mater Res. 2000; 51:293–298. [PubMed: 10880069]
410. Bikram M, Gobin AM, Whitmire RE, West JL. J Controlled Release. 2007; 123:219–227.
411. Charati MB, Lee I, Hribar KC, Burdick JA. Small. 2010; 6:1608–1611. [PubMed: 20603882]
412. Ruoslahti E, Bhatia SN, Sailor MJ. J Cell Biol. 2010; 188:759–768. [PubMed: 20231381]
413. Ferrari M. Nat Rev Cancer. 2005; 5:161–171. [PubMed: 15738981]
414. Hambley TW, Hait WN. Cancer Res. 2009; 69:1259–1262. [PubMed: 19208831]
415. Hait WN, Hambley TW. Cancer Res. 2009; 69:1263–1267. discussion 1267. [PubMed: 19208830]
416. Sugahara KN, Teesalu T, Karmali PP, Kotamraju VR, Agemy L, Girard OM, Hanahan D, Mattrey RF, Ruoslahti E. Cancer Cell. 2009; 16:510–520. [PubMed: 19962669]
417. Tkachenko AG, Xie H, Coleman D, Glomm W, Ryan J, Anderson MF, Franzen S, Feldheim DL. J Am Chem Soc. 2003; 125:4700–4701. [PubMed: 12696875]
418. de la Fuente JM, Berry CC. Bioconjugate Chem. 2005; 16:1176–1180.
419. Liu J, Lu Y. Nat Protoc. 2006; 1:246–252. [PubMed: 17406240]
420. Pavlov V, Xiao Y, Shlyahovsky B, Willner I. J Am Chem Soc. 2004; 126:11768–11769. [PubMed: 15382892]
421. Dixit V, Van den Bossche J, Sherman DM, Thompson DH, Andres RP. Bioconjugate Chem. 2006; 17:603–609.

Author Manuscript Author Manuscript Author Manuscript Author Manuscript

422. Kim B, Han G, Toley BJ, Kim CK, Rotello VM, Forbes NS. Nat Nanotechnol. 2010; 5:465–472. [PubMed: 20383126]
423. Nel A, Xia T, Madler L, Li N. Science. 2006; 311:622–627. [PubMed: 16456071]
424. Lewinski N, Colvin V, Drezek R. Small. 2008; 4:26–49. [PubMed: 18165959]
425. Khlebtsov N, Dykman L. Chem Soc Rev. 2011; 40:1647–1671. [PubMed: 21082078]
426. Turner M, Golovko VB, Vaughan OPH, Abdulkin P, Berenguer-Murcia A, Tikhov MS, Johnson BFG, Lambert RM. Nature. 2008; 454:U981–U931.
427. Longmire M, Choyke PL, Kobayashi H. Nanomedicine. 2008; 3:703–717. [PubMed: 18817471]
428. Nel AE, Maedler L, Velegol D, Xia T, Hoek EMV, Somasundaran P, Klaessig F, Castranova V, Thompson M. Nat Mater. 2009; 8:543–557. [PubMed: 19525947]
429. Marquis BJ, Love SA, Braun KL, Haynes CL. Analyst. 2009; 134:425–439. [PubMed: 19238274]
430. Kandasamy K, Choi CS, Kim S. Nanotechnology. 2010; 21:375501. [PubMed: 20714049]
431. Male KB, Lachance B, Hrapovic S, Sunahara G, Luong JH. Anal Chem. 2008; 80:5487–5493. [PubMed: 18553941]
432. Peckys DB, de Jonge N. Nano Lett. 2011; 11:1733–1738. [PubMed: 21410218]
433. Muñoz Javier A, Kreft O, Alberola A Piera, Kirchner C, Zebli B, Susha AS, Horn E, Kempter S, Skirtach AG, Rogach AL, Rädler J, Sukhorukov GB, Benoit M, Parak WJ. Small. 2006; 2:394–400. [PubMed: 17193058]
434. Shukla R, Bansal V, Chaudhary M, Basu A, Bhonde RR, Sastry M. Langmuir. 2005; 21:10644–10654. [PubMed: 16262332]
435. Ryan JA, Overton KW, Speight ME, Oldenburg CM, Loo L, Robarge W, Franzen S, Feldheim DL. Anal Chem. 2007; 79:9150–9159. [PubMed: 17973401]
436. Gu Y, Sun W, Wang G, Fang N. J Am Chem Soc. 2011; 133:5720–5723. [PubMed: 21438558]
437. Berciaud S, Cognet L, Blab GA, Lounis B. Phys Rev Lett. 2004; 93:257402. [PubMed: 15697940]
438. Leduc C, Jung JM, Carney RR, Stellacci F, Lounis B. ACS Nano. 2011; 5:2587–2592. [PubMed: 21388224]
439. Hauck TS, Ghazani AA, Chan WCW. Small. 2008; 4:153–159. [PubMed: 18081130]
440. Takahashi H, Niidome Y, Niidome T, Kaneko K, Kawasaki H, Yamada S. Langmuir. 2006; 22:2–5. [PubMed: 16378388]
441. Alkilany AM, Nagaria PK, Wyatt MD, Murphy CJ. Langmuir. 2010; 26:9328–9333. [PubMed: 20356032]
442. Jiang W, Kim BYS, Rutka JT, Chan WCW. Nat Nanotechnol. 2008; 3:145–150. [PubMed: 18654486]
443. Chithrani BD, Ghazani AA, Chan WCW. Nano Lett. 2006; 6:662–668. [PubMed: 16608261]
444. Lynch I, Dawson KA. Nano Today. 2008; 3:40–47.
445. Lynch I, Cedervall T, Lundqvist M, Cabaleiro-Lago C, Linse S, Dawson KA. Adv Colloid Interface Sci. 2007; 134–135:167–174.
446. Lundqvist M, Stigler J, Elia G, Lynch I, Cedervall T, Dawson KA. Proc Natl Acad Sci U S A. 2008; 105:14265–14270. [PubMed: 18809927]
447. Cedervall T, Lynch I, Foy M, Berggad T, Donnelly SC, Cagney G, Linse S, Dawson KA. Angew Chem, Int Ed. 2007; 46:5754–5756.
448. Doorley GW, Payne CK. Chem Commun. 2011; 47:466–468.
449. Cho WS, Cho M, Jeong J, Choi M, Han BS, Shin HS, Hong J, Chung BH, Cho MH. Toxicol Appl Pharmacol. 2010; 245:116–123. [PubMed: 20193702]
450. Schnitzer JE, Oh P. J Biol Chem. 1994; 269:6072–6082. [PubMed: 8119952]
451. Ghitescu L, Fixman A. J Cell Biol. 1984; 99:639–647. [PubMed: 6430915]
452. Cho EC, Xie J, Wurm PA, Xia Y. Nano Lett. 2009; 9:1080–1084. [PubMed: 19199477]
453. Cho EC, Zhang Q, Xia Y. Nat Nanotechnol. 2011; 6:385–391. [PubMed: 21516092]
454. Wittmaack K. ACS Nano. 2011; 5:3766–3778. [PubMed: 21446668]
455. Fischer HC, Chan WCW. Curr Opin Biotechnol. 2007; 18:565–571. [PubMed: 18160274]

Author Manuscript Author Manuscript Author Manuscript Author Manuscript

456. Gwinn MR, Vallyathan V. Environ Health Perspect. 2006; 114:1818–1825. [PubMed: 17185269]
457. Kreyling WG, Semmler-Behnke M, Moller W. J Nanopart Res. 2006; 8:543–562.
458. Dobrovolskaia MA, McNeil SE. Nat Nanotechnol. 2007; 2:469–478. [PubMed: 18654343]
459. Chen YS, Hung YC, Liau I, Huang GS. Nanoscale Res Lett. 2009; 4:858–864. [PubMed: 20596373]
460. Hillyer JF, Albrecht RM. Microsc Microanal. 1998; 4:481–490. [PubMed: 9990870]
461. Gref R, Minamitake Y, Peracchia MT, Trubetskoy V, Torchilin V, Langer R. Science. 1994; 263:1600–1603. [PubMed: 8128245]
462. Akiyama Y, Mori T, Katayama Y, Niidome T. J Controlled Release. 2009; 139:81–84.
463. De Jong WH, Hagens WI, Krystek P, Burger MC, Sips AJAM, Geertsma RE. Biomaterials. 2008; 29:1912–1919. [PubMed: 18242692]
464. Caulfield JP, Farquhar MG. J Cell Biol. 1974; 63:883–903. [PubMed: 4612049]
465. Choi HS, Liu W, Misra P, Tanaka E, Zimmer JP, Ipe BI, Bawendi MG, Frangioni JV. Nat Biotechnol. 2007; 25:1165–1170. [PubMed: 17891134]
466. Semmler-Behnke M, Kreyling WG, Lipka J, Fertsch S, Wenk A, Takenaka S, Schmid G, Brandau W. Small. 2008; 4:2108–2111. [PubMed: 19031432]
467. Zhou C, Long M, Qin Y, Sun X, Zheng J. Angew Chem, Int Ed. 2011; 50:3168–3172.
468. Tam JM, Tam JO, Murthy A, Ingram DR, Ma LL, Travis K, Johnston KP, Sokolov KV. ACS Nano. 2010; 4:2178–2184. [PubMed: 20373747]
469. Colvin VL. Nat Biotechnol. 2003; 21:1166–1170. [PubMed: 14520401]
470. Ferry JL, Craig P, Hexel C, Sisco P, Frey R, Pennington PL, Fulton MH, Scott IG, Decho AW, Kashiwada S, Murphy CJ, Shaw TJ. Nat Nanotechnol. 2009; 4:441–444. [PubMed: 19581897]
471. Judy JD, Unrine JM, Bertsch PM. Environ Sci Technol. 2011; 45:776–781. [PubMed: 21128683]
472. McNeil, SE., editor. Characterization of Nanoparticles Intended for Drug Delivery. Humana Press, Springer; New York: 2011.

Author Manuscript Author Manuscript Author Manuscript Author Manuscript

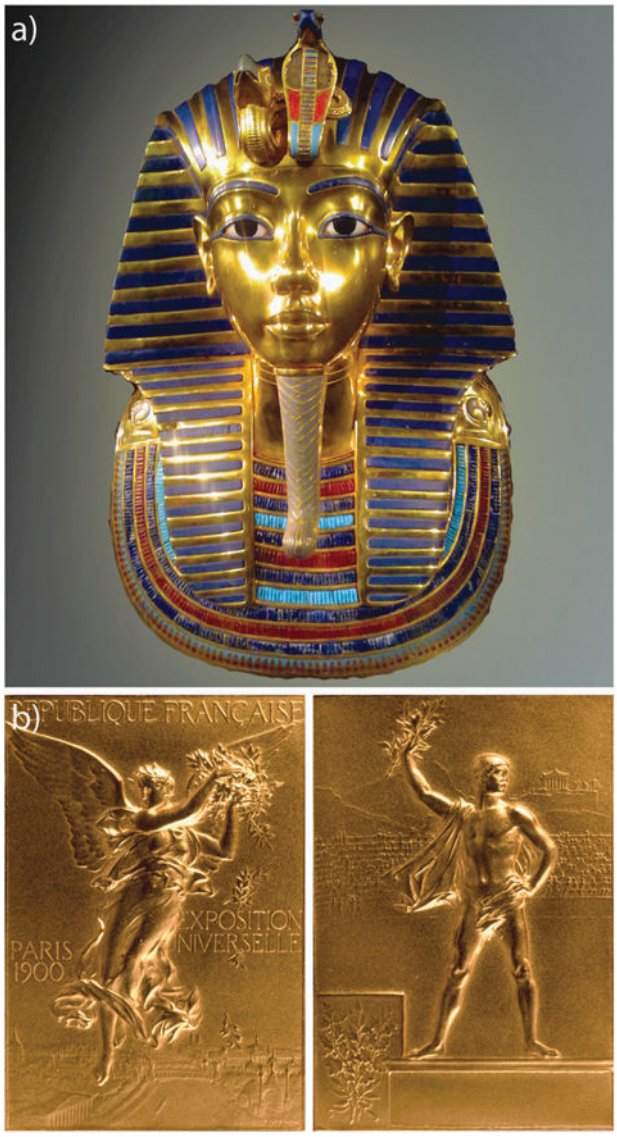

Fig. 1.

(a) Golden burial mask of Egyptian Pharaoh Tutankhamun (King Tut) of the 18th Dynasty (*ca.* 1323 BC). (b) A gold medal presented at the Games of the II Olympiad (Paris, France; 1900). While bulk gold is highly un-reactive and predominantly reflects light, nanoscale gold can be highly reactive, exhibiting pharmacologic properties and the ability to absorb, transfer, and convert light energy into heat. The mask in (a), discovered in 1922 by Howard Cater, consists of solid gold with inlaid glass and stone (21 cm high and *ca.* 11 kg). Prior to the 1900 Olympics in (b), athletes received only silver and copper medals which easily oxidize. The winged goddess Nike is shown on the front in (b); a victorious athlete holding a laurel branch is shown on the back with The Acropolis in the background. Image (a) by James A. Buckley. Image (b) reprinted with permission from the International Olympic Committee. Copyright IOC.

Author Manuscript Author Manuscript Author Manuscript Author Manuscript

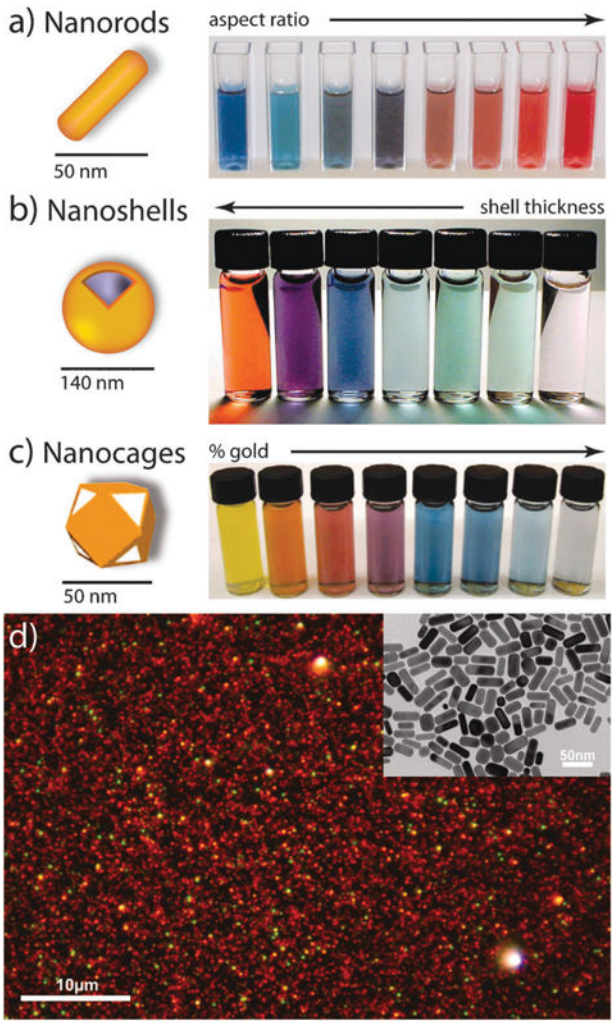

Fig. 2.

Gold nanoparticles commonly applied in biomedical applications. (a) Gold nanorods, (b) silica–gold core–shell nanoparticles, and (c) gold nanocages. The intense color of these nanoparticles arises from the collective excitation of their conduction electrons, or surface plasmon resonance modes, which results in photon absorption at wavelengths which varies with (a) aspect ratio, (b) shell thickness, and/or (c) galvanic displacement by gold. (d) Optical dark-field scattering micrograph of gold nanorods (electron micrograph in the inset) showing resonant scattering from their transverse (short-axis) plasmon mode (green) and their lower energy, longitudinal (long-axis) plasmon mode (red)). Image (a) by X. Huang, (b) by C. Radloff and N.J. Halas, and (d) by C. Rosman and C. Sönnichsen. Figures adapted with permission from (b) ref. 7 and (c) ref. 8. Copyright (a) 2003 Annual Reviews and (b) 2007 Macmillan Publishers Ltd.: Nature Publishing Group.

Author Manuscript Author Manuscript Author Manuscript Author Manuscript

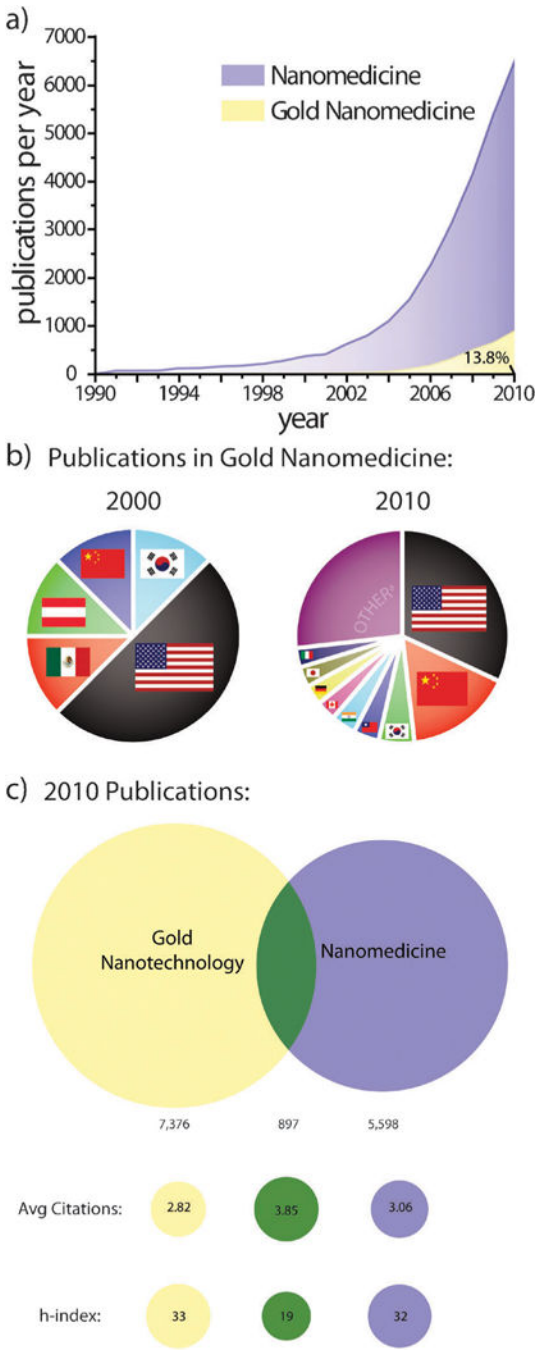

Fig. 3.

Worth more than its weight: exponential growth in the number of publications on gold nanotechnology and nanomedicine over the past two decades.[11] (a) Annual publications in nanomedicine dramatically increased following award of the 1996 Nobel Prize in Chemistry to Kroto, Curl, and Smalley for their discovery of fullerenes. Medicinal applications of gold nanotechnologies further added to this growth following US President Bill Clinton's formation of the National Nanotechnology Infrastructure Network (NNIN) in 2000 and US President George H. W. Bush's expansion of the program in 2003 with the 21st Century

Author Manuscript Author Manuscript Author Manuscript Author Manuscript

Nanotechnology Research and Development Act. (b) Contributions from various countries to publications on gold nanomedicine in 2000 and 2010. Publications in 2000 were limited to just 5 countries while those in 2010 included more than 50. Other countries[a] represent those with <2.9%. (c) Overlap between publications on gold nanotechnology and nanomedicine in 2010 and comparison of their corresponding average number of citations and h-indices. Note that publication data in (a) is not cumulative.

Author Manuscript Author Manuscript Author Manuscript Author Manuscript

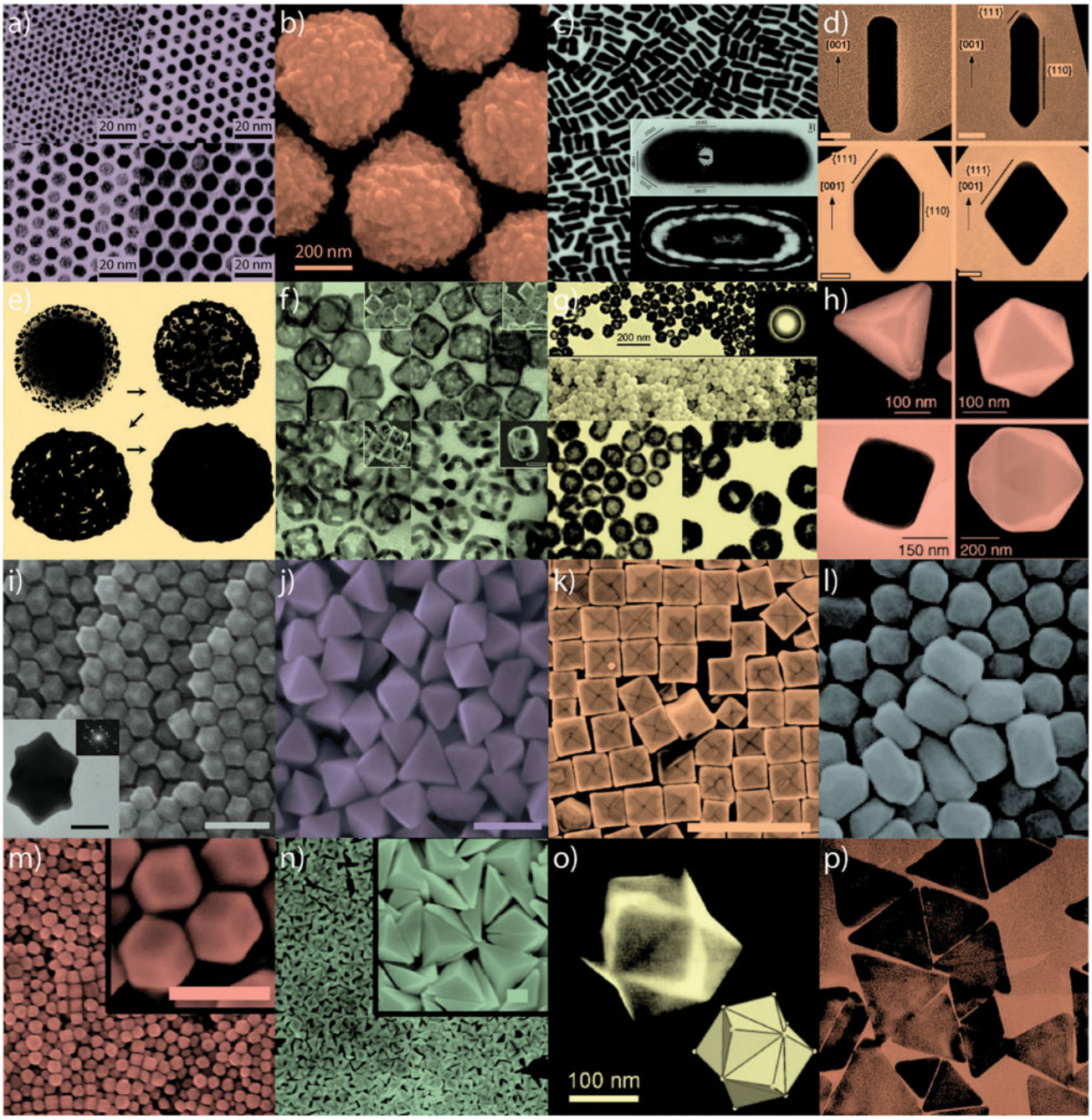

Fig. 4.

Gold nanoparticles of various size and shape with potential applications in biomedicine. Small (a) and large (b) nanospheres, (c) nanorods, (d) sharpened nanorods, (e) nanoshells, (f) nanocages/frames, (g) hollow nanospheres, (h) tetrahedra/octahedra/cubes/icosahedra, (i) rhombic dodecahedra, (j) octahedra, (k) concave nanocubes, (l) tetrahexahedra, (m) rhombic dodecahedra, (n) obtuse triangular bipyramids, (o) trisoctahedra, and (p) nanoprisms. Figures adapted with permission from (a) ref. [22], (b) ref. [17], (c) ref. [31] and [32], (d) ref. [33], (e) ref. [34], (f) ref. [35], (g) ref. [36], (h) ref. [37], (i–j) ref. [38], (k) ref. [39], (l) ref. [40], (m–n) ref. [41], (o) ref. [42], and (p) ref. [43]. Copyright (a) 2003 American Chemical Society, (b) 2008 Wiley-VCH

Author Manuscript Author Manuscript Author Manuscript Author Manuscript

Verlag GmbH & Co., (c) 2004 American Chemical Society and 1999 Elsevier Science B.V., (d) 2007 Wiley-VCH Verlag GmbH & Co., (e) 1998 Elsevier Science B.V., (f) 2007 American Chemical Society, (g) 2005 American Chemical Society, (h) 2004 Wiley-VCH Verlag GmbH & Co., (i–j) 2009 American Chemical Society, (k) 2010 American Chemical Society, (l) 2009 American Chemical Society, (m–n) 2011 American Chemical Society, (o) 2008 VCH Verlag GmbH & Co., and (p) 2005 American Chemical Society.

Author Manuscript Author Manuscript Author Manuscript Author Manuscript

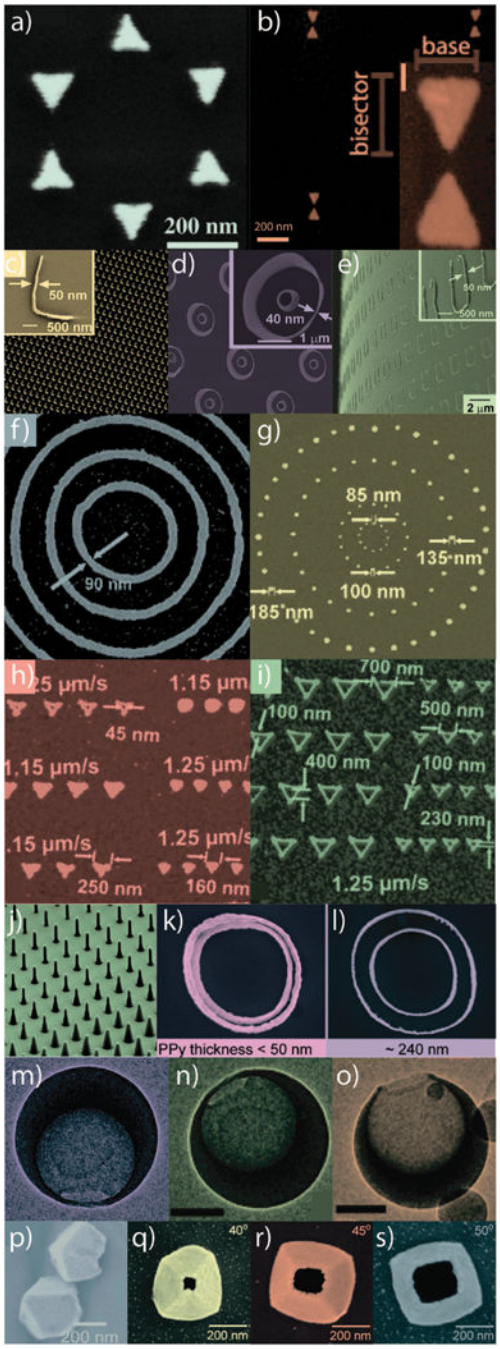

Fig. 5.

Exemplary gold nanostructures obtained by various “top-down” synthetic approaches. (a) Nanosphere lithography (NSL), (b) electron-beam lithography (EBL), (c–e) nanoskiving, (f–i) dip-pen lithography (DPL), (j–l) structural transformation by electro-deposition on patterned substrates (STEPS), (m–o) nanocrescent synthesis, and (p–s) nanopyramid synthesis. Figures adapted with permission from (a) ref. [78], (b) ref. [80], (c–e) ref. [81], (f–i) ref. [82], (j–l) ref. [83], (m–o) ref. [84], and (p–s) ref. [85], [86]. Copyright (a) 2005 American Chemical Society, (b) 2011 American Institute of Physics, (c–e) 2008 American Chemical Society, (f–

Author Manuscript Author Manuscript Author Manuscript Author Manuscript

i) 2004 American Chemical Society, (j–l) 2011 American Chemical Society, (m–o) 2005 American Chemical Society, (p) 2007 American Chemical Society, and (q–s) 2008 American Chemical Society.

Author Manuscript Author Manuscript Author Manuscript Author Manuscript

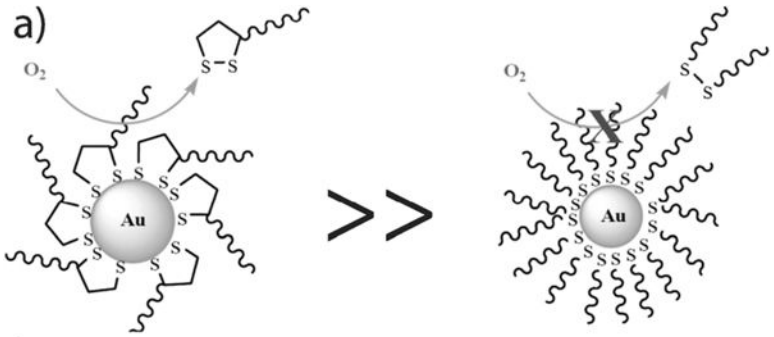

b) percent oxidative desorption of dithiolate and thiolate molecules

time (h)	dithiolate-AuNPs	(mono)thiolate-AuNPs
0	0 %	0 %
2	12.5 %	0 %
24	13.7 %	0 %
48	16.1 %	0 %
72	19.0 %	0 %

Fig. 6.

Comparison of dithiolate and thiolate oxidative desorption from gold nanoparticles (a) over a 73 hour period (b). Figure/data adapted with permission from ref. 110. Copyright 2009 American Chemical Society.

Author Manuscript Author Manuscript Author Manuscript Author Manuscript

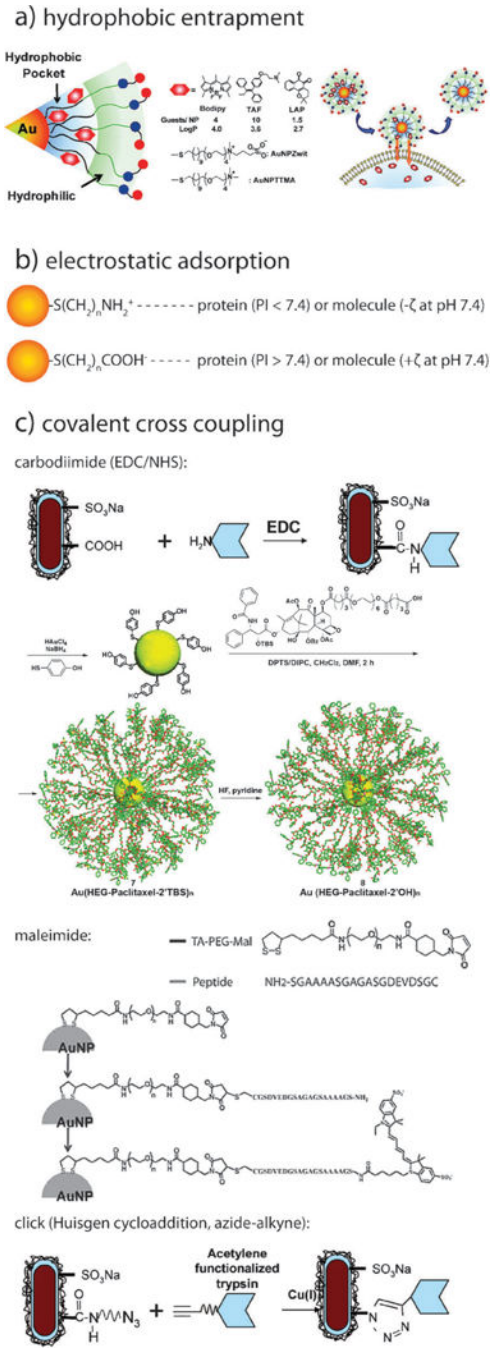

Fig. 7.

Schematics illustrating various methods by which gold nanoparticles can be conjugated with biofunctional molecules. (a) hydrophobic entrapment, (b) electrostatic adsorption, and (c) covalent cross coupling by carbodiimide, maleimide, and click chemistry. Figures adapted with permission from (a) ref. [132] and (c) ref. [134], [133], and [135]. Copyright (a) 2009 American Chemical Society and (c) 2007 American Chemical Society and 2010 Wiley-VCH Verlag GmbH & Co.

Author Manuscript Author Manuscript Author Manuscript Author Manuscript

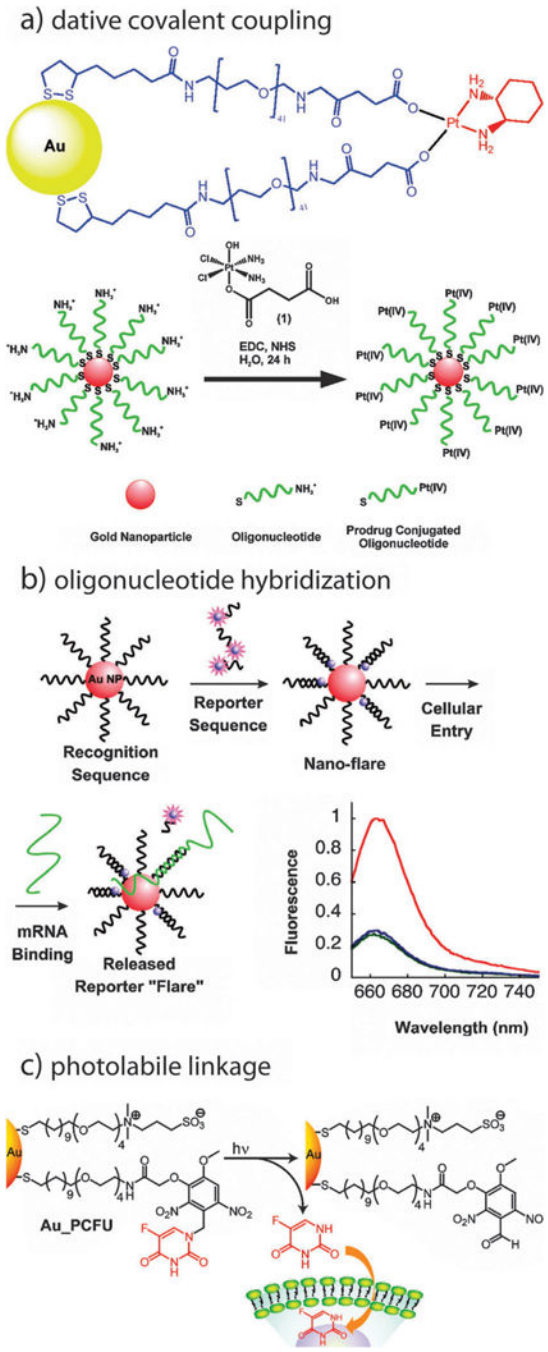

Fig. 8.

Schematics illustrating additional methods by which gold nanoparticles can be conjugated with biofunctional molecules. (a) dative covalent bonding, (b) oligonucleotide hybridization, and (c) and photolabile linkage. Figures adapted with permission from (a) ref. [136], [167], (b) ref. [138], and (c) ref. [139]. Copyright (a) 2010 and 2009, (b) 2007, and (c) 2009 American Chemical Society.

Author Manuscript Author Manuscript Author Manuscript Author Manuscript

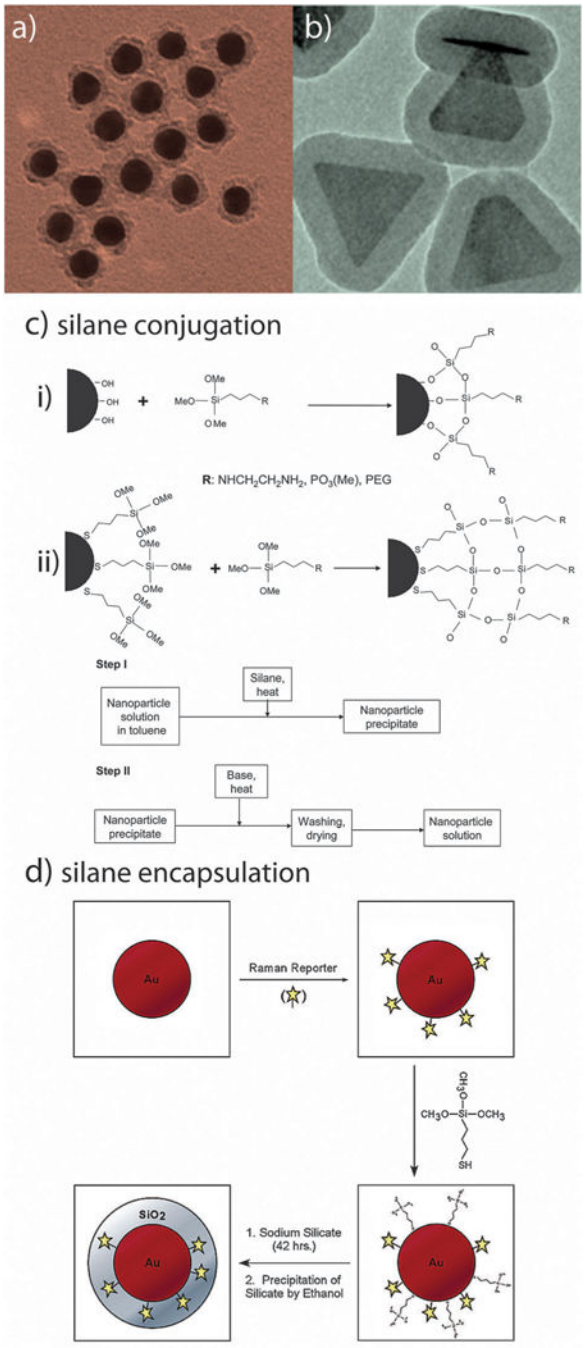

Fig. 9.

Silane conjugation chemistry for biomedical gold nanoparticle conjugates. Silica shell (Stöber) functionalized (a) gold nanospheres and (b) gold nanoprisms. Reaction schemes (c) for conjugation to (i) hydroxyl-and (ii) silane-functionalized gold nanoparticles. Reaction scheme (d) for the encapsulation of bioanalytically- and/or therapeutically-relevant molecules about gold nanoparticles. Figures adapted with permission from (a) ref. [150] (b) ref. [151] (c) ref. [152] and (d) ref. [154]. Copyright (a) 1996, (b) 2010, (c) 2007, and (d) 2003 American Chemical Society.

Author Manuscript Author Manuscript Author Manuscript Author Manuscript

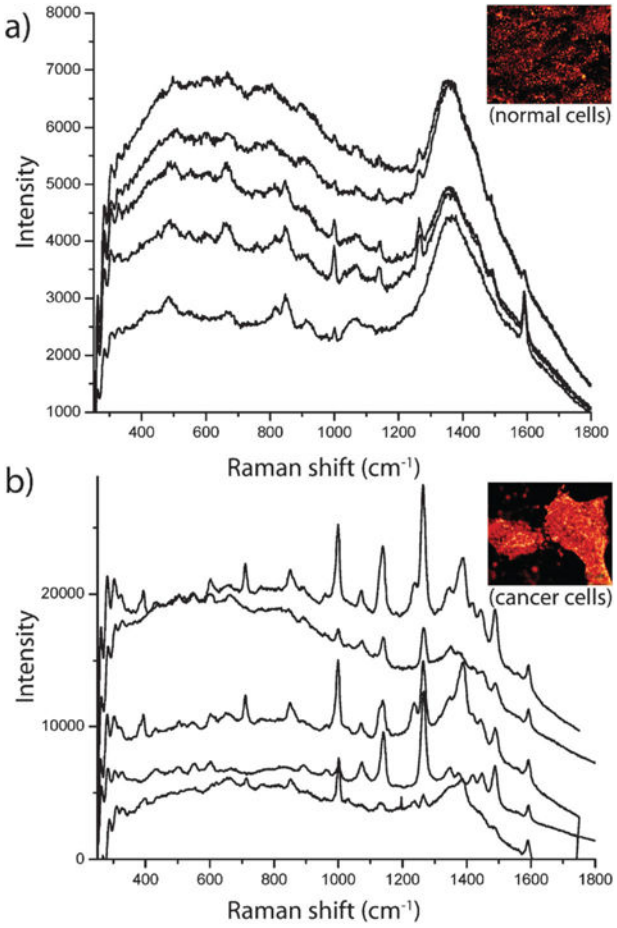

Fig. 10.

SERS detection of cancer cells using immunolabeled gold nanorods. (a) SERS spectra of normal HaCaT cells incubated with anti-EGFR antibody conjugated gold nanorods. (b) SERS spectra of HSC cancer cells incubated with anti-EGFR antibody conjugated gold nanorods. Cancer cells in (b) show stronger, sharper and better resolved SERS signals than normal cells in (a) due to the specific binding of immunolabeled gold nanorods with receptors on the cancer cell surface, suggesting that SERS may serve as a clinical diagnostic tool. The sharper and stronger Raman signals in (b) result from electromagnetic field enhancement due to interparticle coupling between immunolabeled nanorods and their alignment along the cellular membrane surface. Figures adapted with permission from ref. [172]. Copyright 2007 American Chemical Society.

Author Manuscript Author Manuscript Author Manuscript Author Manuscript

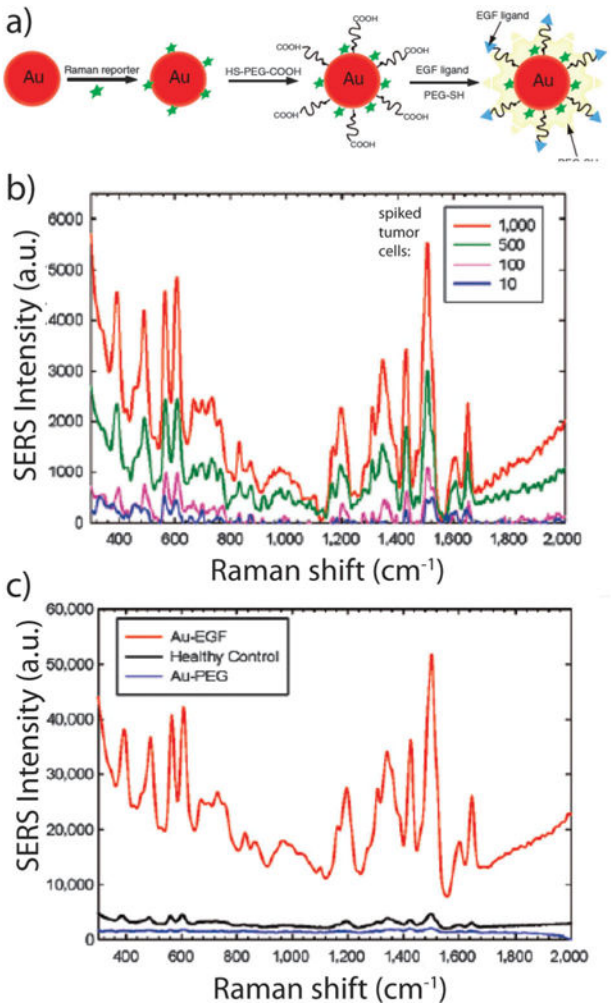

Fig. 11.

SERS detection of circulating tumor cells in patient blood samples. (a) Schematic illustration of SERS nanoparticles and their conjugation with epidermal growth factor peptides. (b) SERS spectra of different numbers of Tu212 cancer cells spiked into mouse white blood cells. (c) SERS spectra of blood sample from a patient incubated with targeted and non-targeted SERS nanoparticles, as well as a blood sample from a healthy donor incubated with targeted SERS nanoparticles. The SERS nanoparticles can detect circulating tumor cells with a sensitivity of 5–50 cells per mL blood. The strong signals from cancer patient indicates highly specific and sensitive detection of circulating tumor cells in blood system. Figures adapted with permission from ref. [198]. Copyright 2011 American Association for Cancer Research.

Author Manuscript Author Manuscript Author Manuscript Author Manuscript

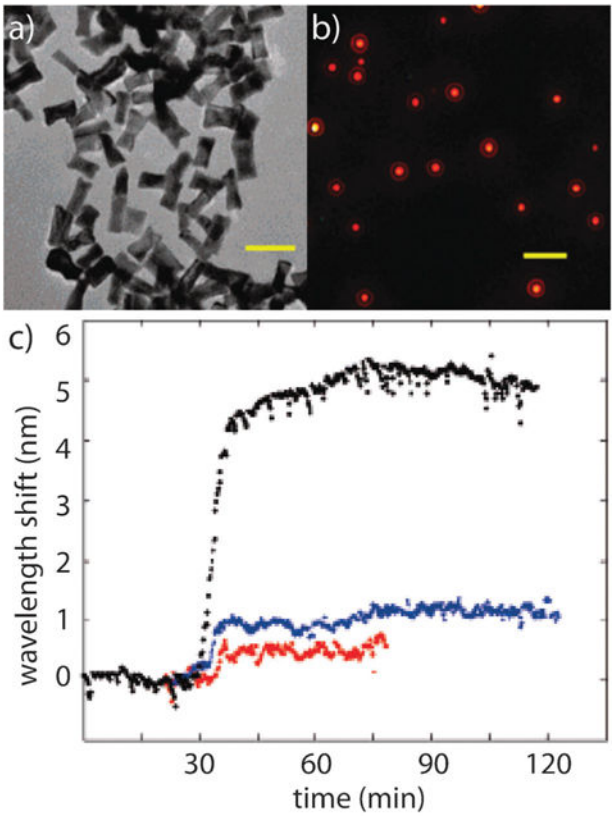

Fig. 12.

A single particle localized surface plasmon resonance (LSPR) assay for biomolecular detection. (a) Electron micrographs of gold nanorods. (b) Optical dark-field scattering microscopy of gold nanorods. (c) Real-time measurement of the binding of streptavidin and biotin by monitoring the light scattering spectra of a single biotin-conjugated gold nanorod. Black, blue, and red curves represent the spectral shift over time when biotin-conjugated gold nanorods were incubated in 130 nM, 10 nM and 1 nM streptavidine in PBS. The gold nanorods showed a sensitivity of streptavidin detection down to 1 nM. Figures adapted with permission from ref. [219]. Copyright 2008 American Chemical Society.

Author Manuscript Author Manuscript Author Manuscript Author Manuscript

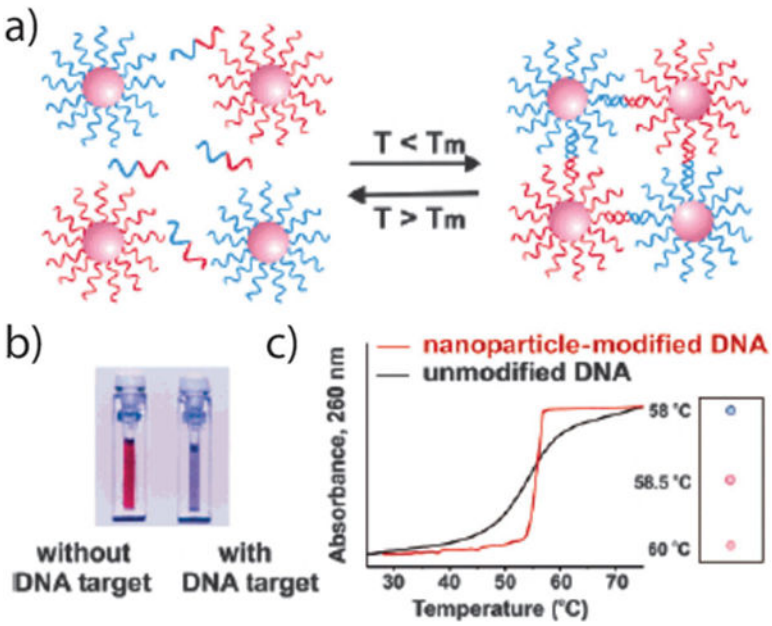

Fig. 13.

DNA detection using gold nanoparticles. (a) Schematic illustration of DNA detection based on hybridization-induced gold nanoparticle aggregation. (b) Visualization of gold nanoprobes with and without the presence of target DNA. (c) Monitoring the aggregation process by spotting the solution on a silica support. Black and red curves: in the presence of complementary DNA target, the oligonucleotides on the surfaces of the gold nanoparticles will bind to the target and induce aggregation of gold nanoparticles and a blue color change. Figures adapted with permission from ref. [227] and [162]. Copyright 1997 American Association for the Advancement of Science and 2005 American Chemical Society.

Author Manuscript Author Manuscript Author Manuscript Author Manuscript

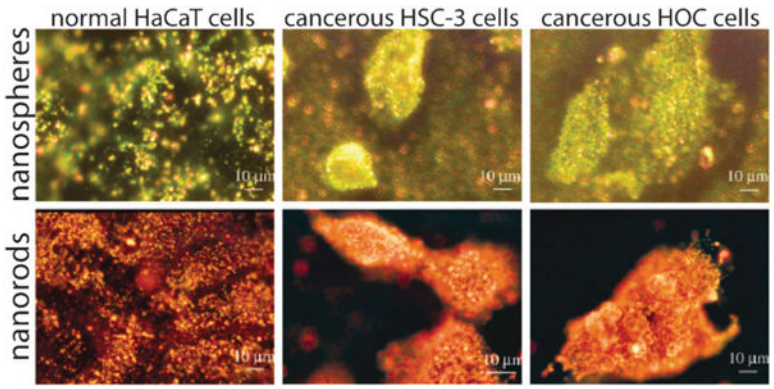

Fig. 14.

Cancer diagnostics using gold nanorod-enhanced light scattering. Optical dark-field microscopy of normal HaCaT cells and cancerous HSC and HOC cells incubated with anti-EGFR antibody-conjugated gold nanospheres (top panels, left to right). Optical dark-field microscopy of normal HaCaT cells and cancerous HSC and HOC cells incubated with anti-EGFR antibody-conjugated gold nanorods (lower panel, left to right). Anti-EGFR conjugated gold nanoparticles specifically bound to cancer cells, scattering strongly under dark-field microscopy and thus enabling detection of malignant cells. Figures adapted with permission from ref. [270]. Copyright 2006 American Chemical Society.

Author Manuscript Author Manuscript Author Manuscript Author Manuscript

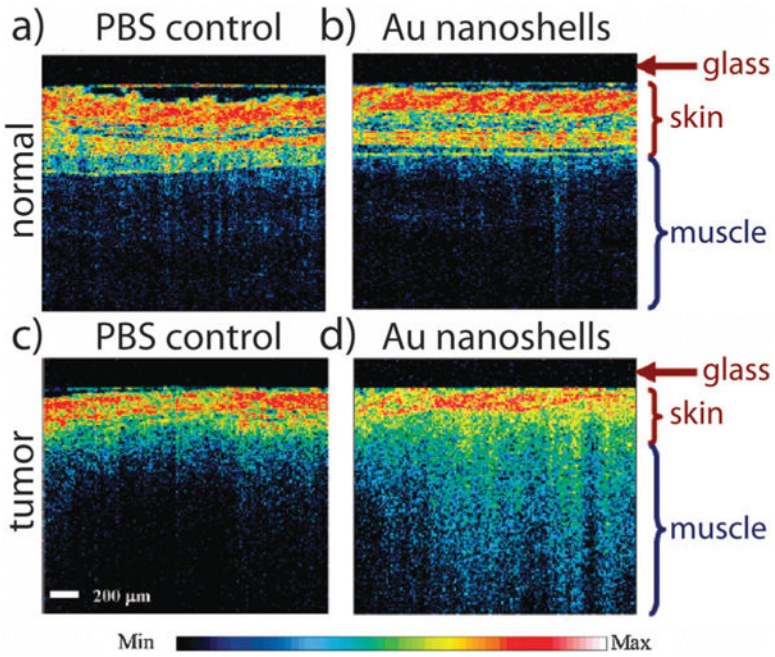

Fig. 15.

Tumor diagnosis by using gold nanoshell-enhanced optical coherence tomography imaging. Optical coherent tomography image of (a) normal tissue injected with saline, (b) normal tissue injected with gold nanoshells, (c) tumor tissue injected with saline, and (d) tumor tissue injected with gold nanoshells. A significant increase in image contrast from tumor tissue is observed compared with normal tissue or tumor tissue injected with PBS solution. Figures adapted with permission from ref. [286]. Copyright 2007 American Chemical Society.

Author Manuscript Author Manuscript Author Manuscript Author Manuscript

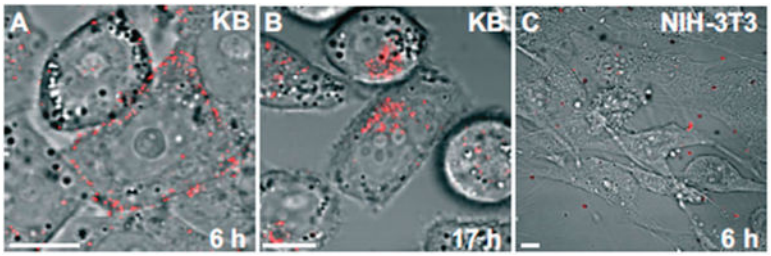

Fig. 16.

Two-photon luminescence (TPL) imaging of the accumulation and uptake of small-molecule targeted gold nanorods. (A) KB cancer cells incubated with folate-conjugated gold nanorods for 6 h. (B) KB cancer cells incubated with folate-conjugated gold nanorods for 17 h. (C) Normal NIH-3T3 cells incubated with folate-conjugated gold nanorods. Due to the strong two photon luminescence signals from gold nanorods, the location of the nanorods could be clearly visualized. At 6 h, the nanorods were accumulated on the cell membrane of cancer cells. At 17 h, the nanorods were internalized into the cancer cells. Functionalized gold nanorods did not show nonspecific binding to normal cells. Figures adapted with permission from ref. [302]. Copyright 2007 Wiley-VCH Verlag GmbH & Co.

Author Manuscript Author Manuscript Author Manuscript Author Manuscript

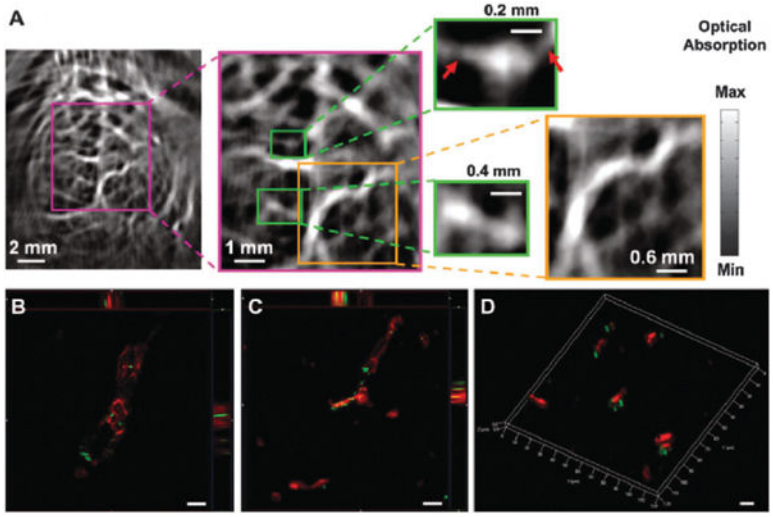

Fig. 17.

Photoacoustic imaging of blood vessels in the mouse brain using gold nanocages. (A) Photoacoustic image of a mouse brain larger (yellow-framed picture) and small (green-framed picture) blood vessels 2 h after intravenous injection of poly(ethylene glycol)-conjugated gold nanocages. (B–D) Optical images of mouse brain vessels 2 h after injecting poly(ethylene glycol)-conjugated gold nanocages. Blood vessels are stained with anti-CD13 antibody (red). Gold nanocages are imaged by dark-field scattering microscopy (pseudogreen). Gold nanocages enhanced the photoacoustic signals of blood vessels in the mouse brain, revealing a clear and detailed structure vasculature as small as 100 μm in diameter. Figures adapted with permission from ref. [325]. Copyright 2010 Elsevier B.V.

Author Manuscript Author Manuscript Author Manuscript Author Manuscript

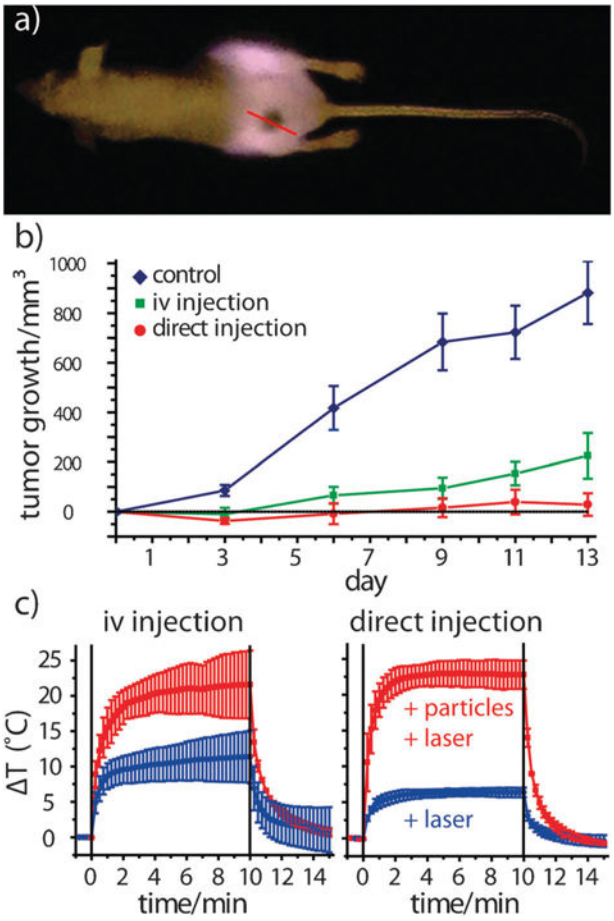

Fig. 18.

Laser photothermal cancer therapy using gold nanorod contrast agents. PEGylated gold nanorods were intravenously and locally injected in carcinoma-bearing mice. (a) NIR transmission images obtained with a simple cell phone camera and an inexpensive NIR-diode laser show substantial laser attenuation due to absorption by nanorods accumulated at the rear flank tumor site. (b) Change in tumor volume over two weeks following a single laser exposure, indicating significant tumor growth remission for both direct and intravenous nanorod administration, as well as resorption of >57% of the directly-injected tumors and 25% of the intravenously-treated tumors. (c) Real-time, intratumoral thermal transient measurements correlating enhanced heating of nanorod-treated tumors with tumor resorption/remission. Reprinted with permission from ref. [119]. Copyright 2008 Elsevier Science B.V.

Author Manuscript Author Manuscript Author Manuscript Author Manuscript

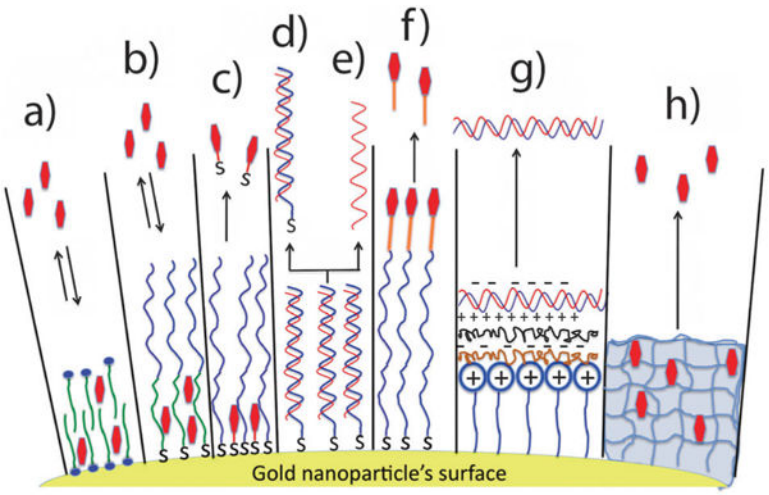

Fig. 19.

Illustration demonstrating various approaches to loading/ unloading therapeutics into/from gold nanoparticles. Partitioning and diffusion-driven release of hydrophobic drug molecules in (a) a surfactant bilayer or (b) an amphiphilic corona layer. (c) Anchoring drugs directly to the surfaces of gold nanoparticles through Au–S or Au–N bonds (capping agent in blue is hydrophilic polymer, *e.g.* PEG, to enhance the overall solubility of the system). Release is triggered by the photothermal effect, thiol exchange (*e.g.* glutathione exchange), or simple diffusion to the cell membranes (in the case of Au–N). (d–e) Double-stranded DNA-loaded gold nanoparticles *via* Au–S bonding. The release of double (d) or single (e) stranded DNA is controlled by an applied laser. (f) Therapeutic agents are coupled/complexed to terminal functional groups of the capping agent *via* a cleavable linker. Release can be triggered by hydrolysis, light, heat, and/or pH changes. (g) Loading charged biomolecules (*e.g.* DNA or siRNA) onto the surfaces of gold nanoparticles by electrostatic assembly (LbL coating, see text for details). Release of payload can be triggered by the use of charge-reversal polyelectrolytes combined with pH change. (h) Drug molecules are incorporated into the matrix of a thermosensitive, crosslinked polymer. Release can be triggered by the photothermal heating by gold nanoparticles also incorporated into the matrix.

Author Manuscript Author Manuscript Author Manuscript Author Manuscript

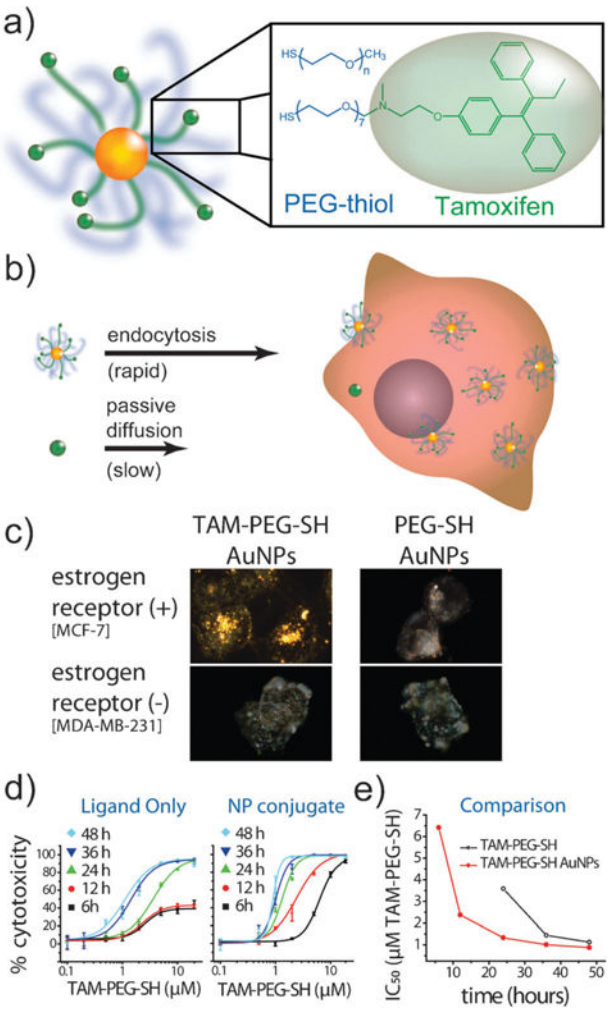

Fig. 20.

Enhanced breast cancer drug delivery using tamoxifen-gold nanoparticle conjugates. (a) A thiol-PEGyalted derivative of the estrogen receptor antagonist, tamoxifen, was conjugated to gold nanoparticles, allowing (b) increasingly rapid and selective drug delivery to breast cancer cells which overexpress the hormone receptor, estrogen receptor. (c) Dark-field scattering microscopy of breast cancer cells showing estrogen receptor-selective intracellular particle delivery. (d–e) Dose–response kinetics indicate accelerated drug transport rates *via* nanoparticle endocytosis *versus* passive diffusion of the free drug, resulting in $>10^4$-fold enhanced potency (2.7-fold per drug molecule). Reprinted with permission from ref. [118] Copyright 2009 American Chemical Society.

Author Manuscript Author Manuscript Author Manuscript Author Manuscript

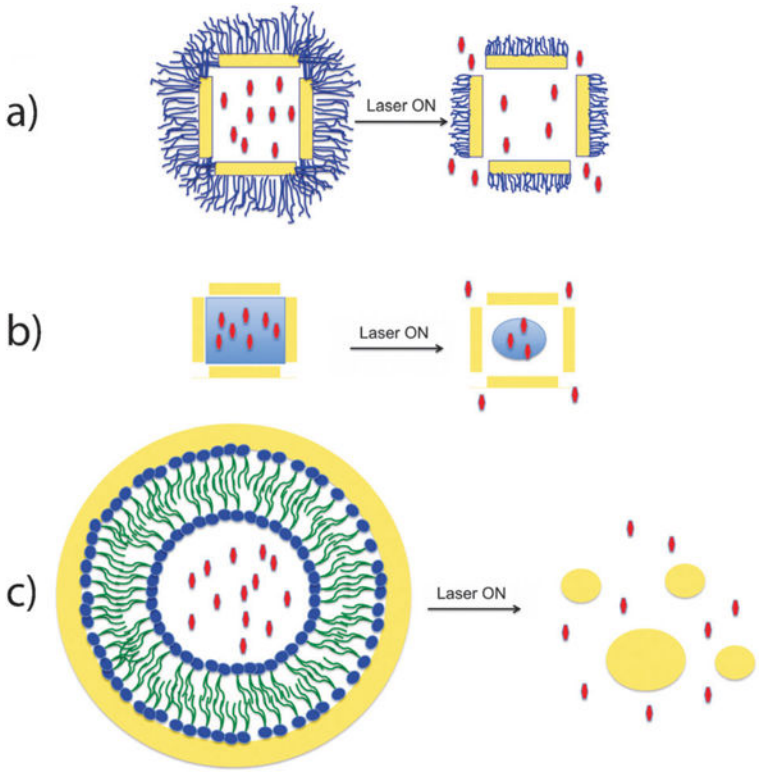

Fig. 21.

Examples of loading drugs into interior reservoirs of gold nanoparticles. (a) Gold nanocages (hollow gold cubes with porous walls) are functionalized with a thermosensitive polymer brush layer at their exterior surface to cage drug molecules in their interior. Laser irradiation induces local heat flux and thus, collapse of the thermo-sensitive polymer to release the caged drug molecules. (b) Gold nanocages with the drugs dispersed into a thermosensitive material in the interior of the nanoparticles. Laser irradiation results in phase-change (melting) of the thermosensitive “filler” and thus enhances drug release. (c) A gold nanoshell covers a liposome carrying drugs in its interior. Gold nanoshells absorb light and convert it to heat and these events result in disintegration and clearance of the carrier, as well as release of its encapsulated drugs.

Author Manuscript Author Manuscript Author Manuscript Author Manuscript

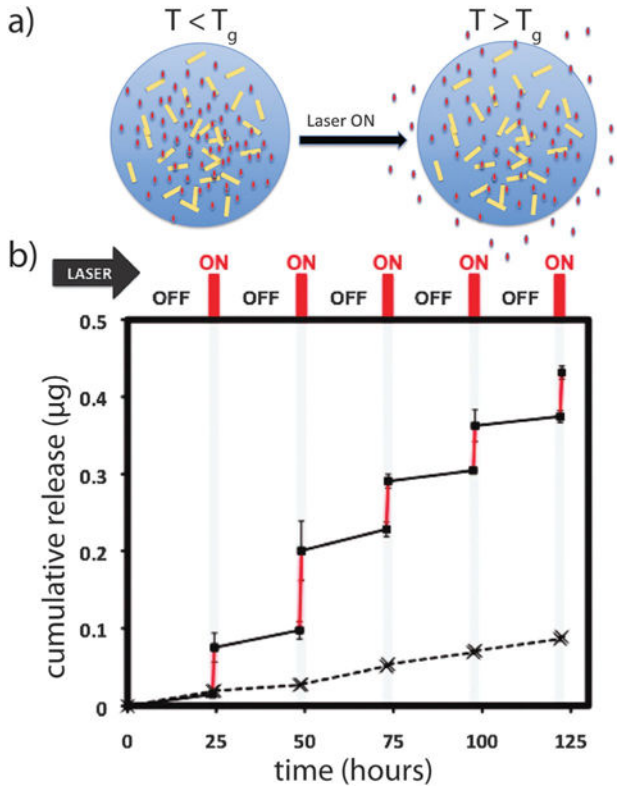

Fig. 22.

(a) Illustration demonstrating the use of gold nanoparticles in a composite material to enable light-triggered drug delivery. Gold nanorods distributed in a polymeric microsphere matrix act as localized nanoheaters upon light irradiation. Gold nanorods absorb light and convert it into heat which changes the polymeric matrix from a glassy state to a rubbery state and allowing enhanced drug diffusion and release. (b) Experiential results showing drug release as a function of laser irradiation cycles/duration for a microsphere matrix containing gold nanorods. Squares: with laser; X: no laser. Laser λ_{max} = 808 nm; T_g = glass transition temperature.[407] Panel (b) is adapted with permission from ref. [407]. Copyright 2011 American Chemical Society.

Author Manuscript Author Manuscript Author Manuscript Author Manuscript

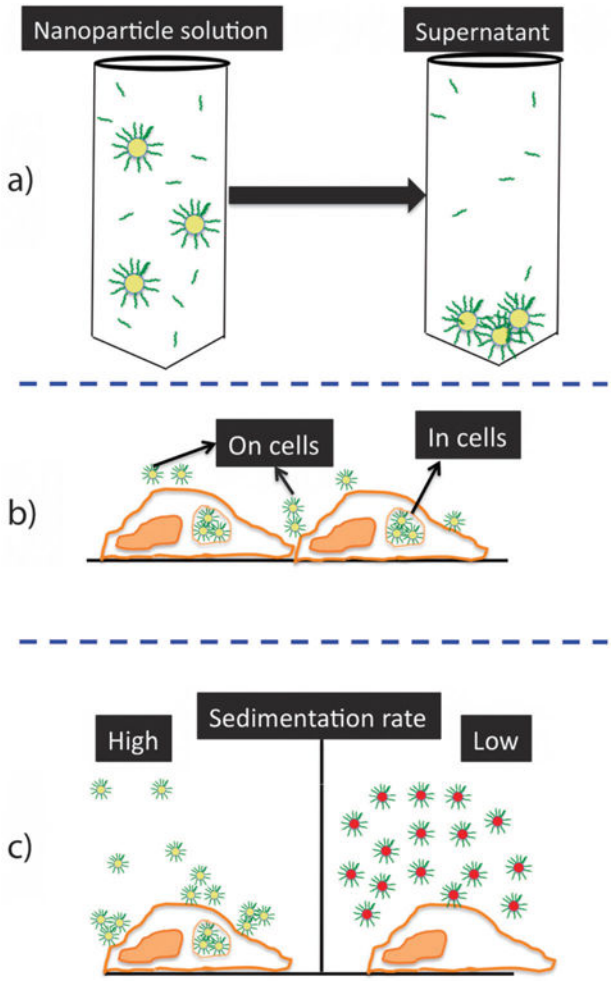

Fig. 23.

Illustration demonstrating potential sources of data artifacts obtained when performing *in vitro* cellular toxicity and uptake studies with nanomaterials. (a) Toxicity could be due to free chemicals in solution and not to the particles themselves; thus, comparing the toxicity of nanoparticle solution with its supernatant is an important control. (b) Nanoparticles could adsorb to the cell surface (on cells) or enter to the inside (in cells). Quantification of gold content in collected cells cannot differentiate between both types of interactions and may result in an overestimated uptake. (c) Differential cellular uptake of nanoparticles could be due to different sedimentation rates. Nanoparticles with a high sedimentation rate (c, left) reach the nanoparticle– cell interaction zone faster than nanoparticles with a low sedimentation rate (c, right) and thus exhibit higher uptake. Ignoring this factor could result in erroneous correlation between uptake and other factors such as size, charge, and surface chemistry.

Author Manuscript Author Manuscript Author Manuscript Author Manuscript

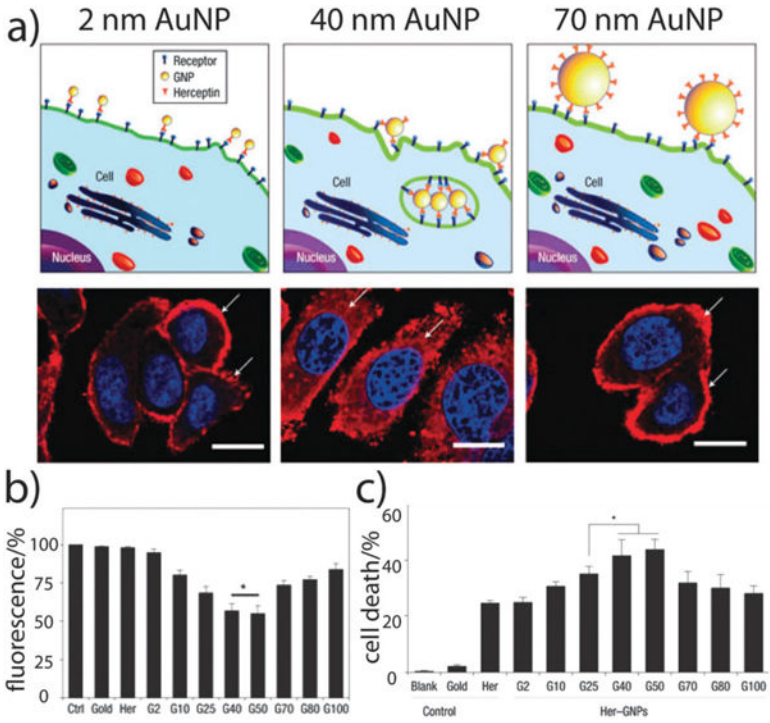

Fig. 24.

(a) Illustration demonstrating binding of gold nanoparticles (G2, G40, G70 for 2, 40, 70 nm diameter) functionalized with Herceptin antibodies, which recognize receptors on the cell surface (HER2/neu, ErbB2). G40 interacts with the receptors more efficiently due to its unique size and propensity for endocytosis. Lower panel: fluorescence images of the cellular distribution of ErbB2 (red) after treatment with fluorescently-labeled G2, G40, and G70. Note that only in the case of G40 treatment, that particles redistributed form the cell surface to the cytoplasm due to efficient endocytosis. (b) Increase in relative fluorescence intensity following nanoparticle uptake was found to correlate with (c) subsequent cell death. Nuclei are stained blue, scale bar = 10 mm, $*p < 0.05$, error bars ±sd, $n = 4$. Adapted with permission from ref. [442]. Copyright 2008 Macmillan Publishers Ltd.: Nature Publishing Group.

Author Manuscript Author Manuscript Author Manuscript Author Manuscript

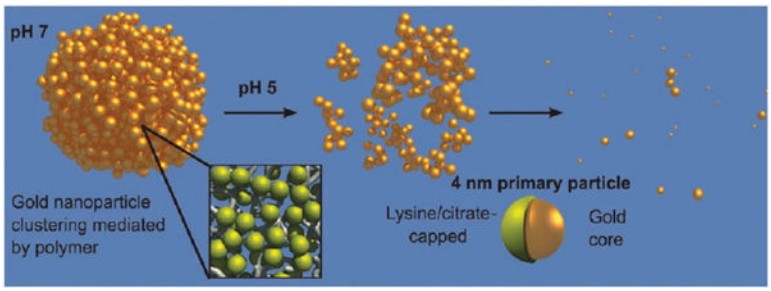

Fig. 25.

Illustration of a biodegradable nanoparticle–polymer composite. Gold nanoparticles (4 nm in diameter) are used as building blocks to form NIR-absorbing plasmonic nanoparticle upon interaction with a biodegradable polymer. The formed nanoclusters can be dissociated to smaller aggregates and ultimately to their initial building blocks by pH drop inside acidic compartments of the cell. Disintegration of nanoparticles to smaller fragments is advantageous to enhance the total urinary clearance of nanoparticles from the body. Adapted with permission from ref. [468]. Copyright 2010 American Chemical Society.

Author Manuscript Author Manuscript Author Manuscript Author Manuscript

Table 1

Various reviews on gold nanotechnology and its use in biomedicine. Please note that this table is by no means comprehensive or indicative of the importance of these works relative to others. We apologize in advance to our friends, colleagues whose publications were unintentionally omitted

Topic	Reference
Anisotropic nanoparticles	C. J. Murphy, T. K. Sau, A. M. Gole, C. J. Orendorff, J. Gao, L. Gou, S. E. Hunyadi and T. Li, Anisotropic metal nanoparticles: synthesis, assembly, and optical applications, *J. Phys. Chem. B*, 2005, **109**, 13857–13870.
Biodiagnostics	N. L. Rosi and C. A. Mirkin, Nanostructures in biodiagnostics, *Chem. Rev.*, 2005, **105**, 1547–1562. J. N. Anker, W. P. Hall, O. Lyandres, N. C. Shah, J. Zhao and R. P. Van Duyne, Biosensing with plasmonic nanosensors, *Nat. Mater.*, 2008, **7**, 442–453. K. M. Mayer and J. H. Hafner, Localized surface plasmon resonance sensors, *Chem. Rev.*, 2011, **111**, 3828–3857.
Biodistribution	N. Khlebtsov and L. Dykman, Biodistribution and toxicity of engineered gold nanoparticles: a review of *in vitro* and *in vivo* studies, *Chem. Soc. Rev.*, 2011, **40**, 1647–1671.
Bio-nanotechnology	E. Katz and I. Willner, Intergrated nanoparticle–biomolecule hybrid system: synthesis, properties, and applications, *Angew. Chem., Int. Ed.*, 2004, **43**, 6042–6108. X. Huang, P. K. Jain, I. H. EI-Sayed and M. A. EI-Sayed, Gold nanoparticles: interesting optical properties and recent applications in cancer diagnostics and therapy, *Nanomedicine*, 2007, **2**, 681–693. C. J. Murphy, A. M. Gole, J. W. Stone, P. N. Sisco, A. M. Alkilany, E.C. Goldsmith and S. C. Baxter, Gold nanoparticles in biology: beyond toxicity to cellular imaging, *Acc. Chem. Res.*, 2008, **48**, 1721–1730. D. F. Moyano and V. M. Rotello, Nano meets biology: structure and function at the nanoparticle interface, *Langmuir*, 2011, **27**(17), 10376–10385.
Bio-nanotechnology and nanomedicine	M. Hu, J. Chen, Z.-Y. Li, L. Au, G. V. Hartland, X. Li, M. Marquez and Y. Xia, Gold nanostructures: engineering their plasmonic properties for biomedical applications, *Chem. Soc. Rev.*, 2006, **35**, 1084–1094. E. Boisselier and D. Astruc, Gold nanoparticles in nanomedicine: preparations, imaging, diagnostics, therapies and toxicity, *Chem. Soc. Rev.*, 2009, **38**, 1759–1782. D. A. Giljohann, D. S. Seferos, W. L. Daniel, M. D. Masssich, P. C. Patel and C. A. Mirkin, Gold nanoparticles for biology and medicine, *Angew. Chem., Int. Ed.*, 2010, **49**, 3280–3294.
Cancer nanotechnology	E. C. Dreaden, M. A. Mackey, X. Huang, B. Kang and M. A. EI-Sayed, Beating cancer in multiple ways using nanogold, *Chem. Soc. Rev.*, 2011, **40**, 3391–3404.
Clusters	A. C. Templeton, M. P. Wuelfing and R. W. Murray, Monolayers protected cluster molecules, *Acc. Chem. Res.*, 2000, **33**, 27–36. R. L. Whetten, M. N. Shafigullin, J. T. Khoury, T. G. Schaaff, I. Vazmar, M. M. Alvarez and A. Wilkinson, Crystal structures of molecular gold nanocrystal arrays, *Acc. Chem. Res.*, 1999, **32**, 397–406.
Drug delivery	P. Ghosh, G. Han, M. De, C. K. Kim and V. M. Rotello, Gold nanoparticles in delivery applications, *Adv. Drug Delivery Rev.*, 2008, **60**, 1307–1315.
Nano-biotechnology	C. M. Niemeyer, Nanoparticles, proteins, and nucleic acids: biotechnology meets materials science, *Angew. Chem., Int. Ed.*, 2001, **40**, 4128–4158.
Nanocages	S. E. Skrabalak, J. Chen, Y. Sun, X. Lu, L. Au, C. M. Cobley and Y. Xia, Gold Nanocages: Synthesis, properties, and applications, *Acc. Chem. Res.*, 2008, **41**, 1587–1595.
Nanochemistry	R. Sardar, A. M. Funston, P. Mulvaney and R. W. Murray, Gold nanoparticles: past, present, and future, *Langmuir*, 2009, **25**, 13840–13851.
Nanorods	J. Pérez-Juste, I. Pastoriza-Santos, L. M. Liz-Marzán and P. Mulvaney, Gold nanorods: synthesis, characterization and application, *Coord. Chem. Rev.*, 2005, **249**, 1870–1901. A. Alekseeva, V. Bogatyrev and B. Khlebtsov, A. Mel'nikov, L. Dykman and N. Khlebtsov, Gold nanorods: synthesis and optical properties, *Colloid. J.*, 2006, **68**, 661–678. X. Huang, S. Neretina and M. A. EI-Sayed, Gold nanorods: from synthesis and properties to biological and biomedical applications, *Adv. Mater.*, 2009, **21**, 4880–4910.
Nanorods in medicine	A. M. Alkilany, L. B. Thompson, S. P. Boulos, P. N. Sisco and C. J. Murphy, Gold nanorods: their potential for photothermal therapeutics and drug delivery, tempered by the complexity of their biological interactions, *Adv. Drug Delivery Rev.*, (in press), 2011.
Nanotechnology	M. C. Daniel and D. Astruc, Gold nanoparticles: assembly, supramolecular chemistry, quantum-size-related properties, and applications toward biology, catalysis, and nanotechnology, *Chem. Rev.*, 2004, **104**, 293–346.

Author Manuscript Author Manuscript Author Manuscript Author Manuscript

Topic	Reference
Pharmacokinetics	M. Longmire, P. L. Choyake and H. Kobayashi, Clearance properties of nano-sized particles and molecules as imaging agents: considerations and caveats, *Nanomedicine*, 2008, **3**, 703–717.
Photochemistry	L. Brus, Noble metal nanocrystals: plasmon electron transfer photochemistry and single-molecule Raman spectroscopy, *Acc. Chem. Res.*, 2008, **41**, 1742–1749.
Photophysics	S. Link and M. A. EI-Sayed, Shape and size dependence of radiative, non-radiative and photothermal properties of gold nanocrystals, *Int. Rev. Phys. Chem.*, 2000, **19**, 409–454. S. Eustis and M. A. Ei-Sayed, Why gold nanoparticles are more precious than pretty gold: noble metal surface plasmon resonance and its enhancement of the radiative and nonradiative properties of nanocrystals of different shapes, *Chem. Soc. Rev.*, 2006, **35**, 209–217. G. V. Hartland, Optical studies of dynamics in noble metal nanostructures, *Chem. Rev.*, 2011, **111**, 3858–3887.
Photothermal therapy	S. Lal, S. E. Clare and N. J. Halas, Nanoshell-enabled photothermal cancer therapy: impending clinical impact, *Acc. Chem. Rev.*, 2008, **41**, 1842–1851.
Plamonics	U. Kreibig and M. Vollmer, Optical properties of metal clusters, Springer, Berlin, 1995. C. F. Bohren and D. R. Huffman, Absorption and scattering of light by small particles, Wiley-VCH Verlag GmbH, Weinheim, 2007. K. L. Kelly, E. Coronado, L. L. Zhao and G. C. Schatz, The optical properties of metal nanoparticles: the influence of size, shape, and dielectric environment, *J. Phys. Chem. B.*, 2002, 668–677. H. Wang, D. W. Brandl, P. Nordlander and N. J. Halas, Plasmonic nanostructures: artificial molecules, *Acc. Chem. Res.*, 2006, **40**, 53–62. S. A. Maier, *Plasmonics: fundamentals and applications*, Springer Verlag, New York, 2007.
Purification and characterization	K. E. Sapsford, K. M. Tyner, B. J. Dair, J. R. Deschamps and I. L. Medintz, Analyzing nanomaterial bioconjugates: a review of current and emerging purification and characterization techniques, *Anal. Chem.*, 2011, **83**, 4453–4488.
Self-assembly	M. Grzelczak, J. Vermant, E. M. Furst and L. M. Liz-Marzán, Directed self-assembly of nanoparticles, *ACS Nano*, 2010, **4**, 3591–3605. L. M. Liz-Marzán, Tailoring surface plasmons through the morphology and assembly of metal nanoparticles, *Langmuir*, 2005, **22**, 32–41.
Surface functionalization	J. C. Love, L. A. Estroff, J. K. Kriebel, R. G. Nuzzo and G. M. Whitesides, Self-assembled monolayers of thiolates on metals as a form of nanotechnology, *Chem. Rev.*, 2005, **105**, 1103–1170.
Synthesis	M. Grzelczak, J. Perez-Juste, P. Mulvaney and L. M. Liz-Marzan, Shape control in gold nanoparticle synthesis, *Chem. Soc. Rev.*, 2008, **37**, 1783–1791.
Toxicology	N. Lewinski, V. Colvin and R. Drezek, Cytotoxicity of nanoparticles, *Small*, 2008, **4**, 26–49. A. Alkilany and C. Murphy, Toxicity and cellular uptake of gold nanoparticles; what we have learned so far?, *J. Nanopart. Res.*, 2010, **12**, 2313–2333.

Author Manuscript Author Manuscript Author Manuscript Author Manuscript

Table 2

Summary of synthetic approaches to obtain various gold nanostructures

Au nanostructure	Synthesis	Primary literature
Nanospheres	Citrate-mediated reduction	J. Turkevich, P. C. Stevenson and J. Hiller, *Discuss. Faraday Soc.*, 1951, **11**, 55–75. G. Frens, *Nature*, 1973, **241**, 20–22.
Nanoclusters	Alkanethiol/phosphine-stabilized reduction	G. Schmid, R. Pfeil, R. Boese, F. Bandermann, S. Meyer, G. H. M. Calis and J. W. A. van der Velden, *Chem. Ber.*, 1981, **114**, 3634–3642. M. Burst, M. Walker, D. Bethell, D. J. Schiffrin and R. Whyman, *J. Chem. Soc., Chem. Commun.*, 1994, **7**, 801–802.
Nanorods (colloidal)	Seeded growth (CTAB)	N. R. Jana, L. Gearheart, C. J. Murphy, *Adv. Mater.*, 2001, **13**, 1389. B. Nikoobakht, M. A. El-Sayed, *Chem. Mater.*, 2003, **15**, 1957. Y. Y. Yu, S. S. Chang, C. L. Lee, C. R. C. Wang, *J. Phys. Chem. B*, 1997, **101**, 6661.
Nanorods (electrochemical)	Template-directed electrochemical deposition	H. Masuda, H. Tanaka and N. Baba, *Chem. Lett.*, 1990, **4**, 621–622. C. R. Martin, *Adv. Mater.*, 1991, **3**, 457–459.
Striped nanorods (electrochemical)	Sequential template-directed electrochemical deposition	S. R. Nicewarner-Peña, R. G. Freeman, B. D. Reiss, L. He, D. J. Peña, I. D. Walton, R. Cromer, C. D. Keating and M. J. Natan, *Science*, 2001, **294**, 137–141. L. Qin, S. Park, L. Huang and C. A. Mirkin, *Science*, 2005, **309**, 113–115.
Nanoshells	Overgrowth of core-bound particles	S. J. Oldenburg, R. D. Averitt, S. L. Westcott and N. J. Halas, *Chem. Phys. Lett.*, 1998, **288**, 243–247.
Hollow nanospheres	Overgrowth of core-bound particles, core removal; galvanic displacement	Z. Liang, A. Susha and F. Caruso, *Chem. Mater.*, 2003, **15**, 3176–3183. H.-P. Liang, L.-J. Wan, C.-L. Bai and L. Jiang, *J. Phys. Chem. B*, 2005, **109**, 7795–7800.
Nanocages/frames	PVP-stabilized polyol, galvanic displacement	Y. Sun and Y. Xia, *Science*, 2002, **298**, 2176–2179. J. Chen, J. M. McLellan, A. Siekkinen, Y. Xiong, Z.-Y. Li and Y. Xia, *J. Am. Chem. Soc.*, 2006, **128**, 14776–14777.
Nanocubes/octahedra	PVP-stabilized polyol; seeded growth (CPC); seeded growth (CTAC)	F. Kim, S. Connor, H. Song, T. Kuykendall and P. Yang, *Angew. Chem., Int. Ed.*, 2004, **43**, 3673–3677. W. Niu, S. Zheng, D. Wang, X. Liu, H. Li, S. Han, J. Chen, Z. Tang and G. Xu, *J. Am. Chem. Soc.*, 2008, **131**, 697–703. J. Zhang, M. R. Langille, M. L. Personick, K. Zhang, S. Li and C. A. Mirkin, *J. Am. Chem. Soc.*, 2010, **132**, 14012–14014.
Icosahedra/tetrahedra	PVP-stabilized polyol; seeded growth (CTAC)	F. Kim, S. Connor, H. Song, T. Kuykendall and P. Yang, *Angew. Chem., Int. Ed.*, 2004, **43**, 3673–3677. J. Zhang, M. R. Langille, M. L. Personick, K. Zhang, S. Li, S. Han, J. Chen, Z. Tang and G. Xu, *J. Am. Chem. Soc.*, 2008, **131**, 697–703. J. Zhang, M. R. Langille, M. L. Personick, K. Zhang, S. Li and C. A. Mirkin, *J. Am. Chem. Soc.*, 2010, **132**, 14012–14014.
Nanoprisms	Biosynthesis; seeded growth (CTAB)	S. Shankar, A. Rai, B. Ankamwar, A. Singh, A. Ahmad and M. Sastry, *Nat. Mater.*, 2004, **3**, 482–488.

Author Manuscript

Author Manuscript

Author Manuscript

Author Manuscript

Au nanostructure	Synthesis	Primary literature
		J. E. Millstone, S. Park, K. L. Shuford, L. Qin, G. C. Schatz and C. A. Mirkin, *J. Am. Chem. Soc.*, 2005, **127**, 5312–5313.
Tetrahexahedra/elongated tetrahexahedra	Seeded growth (CTAB)	T. Ming, W. Feng, Q. Tang, F. Wang, L. Sun, J. Wang and C. Yan, *J. Am. Chem. Soc.*, 2009, **131**, 16350–16351.
Obtuse triangular bipyramids	Seeded growth (CTAC)	M. L. Personick, M. R. Langille, J. Zhang, N. Harris, G. C. Schatz and C. A. Mirkin, *J. Am. Chem. Soc.*, 2011, **133**, 6170–6173.
Rhombic dodecahedra/obtuse triangular bipyramids	Seeded growth (CPC); seeded growth (CTAC)	W. Niu, S. Zheng, D. Wang, X. Liu, H. Li, S. Han, J. Chen, Z. Tang and G. Xu, *J. Am. Chem. Soc.*, 2008, **131**, 697–703. M. L. Personick, M. R. Langille, J. Zhang, N. Harris, G. C. Schatz and C. A. Mirkin, *J. Am. Chem. Soc.*, 2011, **133**, 6170–6173.
Trisoctahedra	Ascorbate-mediated, CTAC-stabilized reduction	Y. Ma, Q. Kuang, Z. Jiang, Z. Xie, R. Huang and L. Zheng, *Angew. Chem., Int. Ed.*, 2008, **47**, 8901–8904.
Nanosphere lithograph	Nanosphere self-assembly, vapor-phase deposition, nanosphere removal	J. C. Hulteen and R. P. Van Duyne, *J. Vac. Sci. Technol. A*, 1995, **13**, 1553–1558.
Dip-pen lithograph	Vapor-phase deposition, AFM-patterned SAM, chemical etching	H. Zhang, Z. Li and C. A. Mirkin, *Adv. Mater.*, 2002, **14**, 1472–1474. H. Zhang and C. A. Mirkin, *Chem. Mater.*, 2004, **16**, 1480–1484.
Nanoskived pattern	Vapor-phase deposition on topologically-defined polymer, ultramicrotome, polymer removal	Q. Xu, R. M. Rioux and G. M. Whitesides, *ACS Nano*, 2007, **1**, 215–227. Q. Xu, R. M. Rioux, M. D. Dickey and G. M. Whitesides, *Acc. Chem. Res.*, 2008, **41**, 1566–1577.
STEPS pattern	Directional vapor-phase deposition on topologically-defined polymer, electrochemical deposition of conducting polymer, secondary	P. Kim, A. K. Epstein, M. Khan, L. D. Zarzar, D. J. Lipomi, G. M. Whitesides and J. Aizenberg, *Nano Lett.*, 2011, ASAP.
Nanocrescents	Nanosphere template, shadow-mask vapor-phase deposition, template removal and dissolution	Y. Lu, G. K. Liu, J. Kim, Y. X. Meija and L. P. Lee, *Nano Lett.*, 2005, **5**, 119–124.
Nanopyramids	Photoresist pattern on Si, Cr vapor-phase deposition/liftoff, Au vapor-phase deposition, Au film removal, Cr etch, Si etch	J. Lee, W. Hasan, C. L. Stender and T. W. Odom, *Acc. Chem. Res.*, 2008, **41**, 1762–1771.

CTAB, cetyl trimethylammonium bromide; PVP, poly(vinylpyrrolidone); CPC, cetylpyridinium chloride; CTAC, cetyl trimethylammonium chloride; AFM, atomic force microscopy; SAM, self-assembled monolayer; STEPS, structural transformation by electrodeposition on patterned substrates.

Author Manuscript Author Manuscript Author Manuscript Author Manuscript

Chem Soc Rev. Author manuscript; available in PMC 2018 March 29.

Table 3

Summary of *in vivo* photothermal studies using various gold nanoparticles

Gold nanoparticle class	Particle size/nm	Targeting ligand	Animal model: cancer type	Admin, route	Laser (λ, nm)	Laser power/W cm^{-2}	Exposure time/min	Results	Ref.
Nanorods	AR = 4	n/a; passive targeting with chitosan on the surface	Mice: squamous carcinoma (SCC7) tumors	i.v.	808	41.5	4	20% of the injected dose accumulated in the tumor. Complete resorption of the tumor was achieved.	368
	33.7 ± 3.5 × 9.1 ± 1.4	n/a; passive targeting with the PEGylated surface	Mice: squamous carcinoma (SCC7) tumors	i.v.	810	3.82	1	Second generation photosensitizer molecules were complexed to the surface of gold nanorods for dual therapy (photodynamic and plasmonic photothermal therapies). Dual therapy resulted in 95% reduction in tumor growth. Temperature at the tumor tissue reached 65 °C.	369
	50 × 12	n/a; passive targeting with the PEGylated surface	Mice: squamous cell carcinoma tumor	i.v. and direct	808	1.7–1.9 (i.v.); 0.9–1.1 (direct)	10	Resorption of >57% of tumors treated with direct injection of nanoparticles to the tumor site *versus* 25% of the intravenously-treated tumors.	119
	13 × 47	n/a; passive targeting with the PEGylated surface	Mice: MDA-MB-435 human tumors	i.v.	810	2	5	Circulation $t_{1/2}$ = 17 h. 7% of the injected dose in the	123

Author Manuscript Author Manuscript Author Manuscript Author Manuscript

Gold nanoparticle class	Particle size/nm	Targeting ligand	Animal model: cancer type	Admin, route	Laser (λ, nm)	Laser power/W cm^{-2}	Exposure time/min	Results	Ref.
								tumor site. Temperature at the tumor tissue reached 70 °C. Single i.v. injection of gold nanorods coupled with laser irradiation eliminated all the induced tumor in mice.	
Gold/silica nanoshells	150	n/a; passive targeting with the PEGylated surface	Dogs: brain tumor	i.v.	808	3.5	3	Temperature at the tumor tissue reached 56.8 °C	364
	130	n/a; passive targeting with the PEGylated surface	Mice: murine colon carcinoma cells	i.v.	808	4	3	All treated animals were tumor-free without toxicity for more than 90 days after treatment.	352
	110 ± 11	n/a; passive targeting with the PEGylated surface	Mice: canine TVT cancer cells	i.v.	820	4	<6	Average maximum temperature at the tumor site reached ~70 °C. Irradiated tumor exhibited tissue damage	356
Nanocages	48.0 ± 3.5	n/a; passive targeting with the PEGylated surface	Athymic nude mice: U87MG glioma xenografts	i.v.	808	0.7	10	Temperature at the tumor tissue reached 55 °C	371
Gold/gold sulfide nanoshells	45 nm	n/a; passive targeting with the PEGylated surface	BALBc mice: murine colon carcinoma cells	i.v.	808	4	3	80% of tested mice survived tumor-free. Temperature at the tumor tissue reached 61 °C	370
Hollow nanospheres	415 ± 2.3	α-melanocyte-stimulating hormone analog	Mice: B16/F10 melanoma tumor	i.v.	808	0.5	1	Nanoparticles were uptaken specifically by melanoma	373

Author Manuscript Author Manuscript Author Manuscript Author Manuscript

Gold nanoparticle class	Particle size/nm	Targeting ligand	Animal model: cancer type	Admin, route	Laser (λ, nm)	Laser power/W cm^{-2}	Exposure time/min	Results	Ref.
		and polyethylene glycol						cells.12.9 K of the injected dose per organ weight, in the tumor site.	